Aspects of finite temperature field theories in

AdS/CFT

by

Mauro Brigante

Submitted to the Department of Physics
in partial fulfillment of the requirements for the degree of

Doctor of Philosophy in Physics

at the

MASSACHUSETTS INSTITUTE OF TECHNOLOGY

June 2008

Author ..../.

<div style="text-align:right">

Department of Physics
May 23, 2008

</div>

Certified by..

<div style="text-align:right">

Hong Liu
Assistant Professor of Physics
Thesis Supervisor

</div>

Accepted by.....................................

<div style="text-align:right">

Thomas J. Greytak

</div>

Professor and Associate Department Head for Education
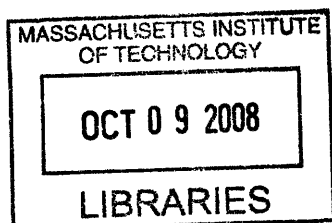
Aspects of finite temperature field theories in AdS/CFT

by

Mauro Brigante

Submitted to the Department of Physics
on May 23, 2008, in partial fulfillment of the
requirements for the degree of
Doctor of Philosophy in Physics

Abstract

In this dissertation I study some properties of field theories at finite temperature using the AdS/CFT correspondence.

I present a general proof of an "inheritance principle" satisfied by a weakly coupled $SU(N)$ (or $U(N)$) gauge theory with adjoint matter on a class of compact manifolds (like S^3). In the large N limit, finite temperature correlation functions of gauge invariant single-trace operators in the low temperature phase are related to those at zero temperature by summing over images of each operator in the Euclidean time direction. As a consequence, various non-renormalization theorems of $\mathcal{N} = 4$ Super-Yang-Mills theory on S^3 survive at finite temperature.

I use the factorization of the worldsheet to isolate the Hagedorn divergences at all orders in the genus expansion and to show that the Hagedorn divergences can be re-summed by introducing double scaling limits. This allows one to extract the effective potential for the thermal scalar. For a string theory in an asymptotic anti-de Sitter (AdS) spacetime, the same behavior should arise from the boundary Yang-Mills theory. Introducing "vortex" contributions for the boundary theory at finite temperature I will show that this is indeed the case and that Yang-Mills Feynman diagrams with vortices can be identified with contributions from boundaries of moduli space on the string theory side.

Finally, I consider the shear viscosity to entropy density ratio in conformal field theories dual to Einstein gravity with curvature square corrections. For generic curvature square corrections I show that the conjectured viscosity bound can be violated. I present the calculation in three different methods in order to check consistency. Gauss-Bonnet gravity is also considered, for any value of the coupling. It is shown that a lower bound (lower than the KSS bound) on the shear viscosity to entropy density ratio is determined by causality in the boundary theory.

Thesis Supervisor: Hong Liu
Title: Assistant Professor of Physics

Acknowledgments

I would like to thank my advisor, Hong Liu, for his guidance in my research. I am grateful to Roman Jackiw and Barton Zwiebach for their support at various stages of my MIT adventure. I also acknowledge the people with whom I collaborated in my work, Guido Festuccia, Rob Myers, Stephen Shenker and Sho Yaida.

Many thanks to Guido, Antonello, Claudio, Massimo, Eleonora, Nicola and Alfredo for their friendship and for making me feel at home in Cambridge.

Of my many CTP friends, I am especially grateful to Rishi for the walks around the river and the many conversations about physics, life and goldfish memory. Qudsia, Onur, Chris have also been important friends with whom I shared much of the toil and satisfaction of the CTP.

I owe a lot to my friends Bonna, Fred, Joe, Alejandro, Laura, Zoe, Eric, Kerri and Ashley, for being a constant source of good stories as well as support.

Melissa contributed greatly to my work and to my life in the past two years. I am deeply grateful for her help and for her patience.

I would also like to thank my family for being always by my side in every decision, my incredible friends in Milan for listening and sharing and the Mediterranean sea for calling me home.

Contents

List of Figures

Chapter 1

Introduction

1.1 Overview

In this dissertation we study some properties of gauge theories with string theory duals, at finite temperature. The conjectured duality between conformal quantum field theories and string theory (of which gravity is the low energy, classical limit) has been a remarkable idea since it connects two apparently very different theories. Its importance was such as to motivate much research in the past decade. The conjecture relates field theories in $(d-1)$-dimensions with string theory in d-dimensional asymptotically Anti-de Sitter (AdS) spacetimes (times a compact manifold). Through the duality it is possible to describe the same physics phenomena using two different languages; since one of the two descriptions may be significantly simpler than the other, researchers have been able to gain insight on physics previously unaccessible.

In this dissertation we will study two different situations where the correspondence can be fruitfully used. In the first case (described in chapters 2, 3), we will analyze the critical behavior of string theory at the Hagedorn temperature. We will start from a quantum field theory with a $U(N)$ gauge group and fields in the adjoint representation on a class of compact manifolds. We will study properties of the partition function at finite temperature and we will analyze the critical behavior of the theory. We can then use the duality to obtain information about the behavior of string theory at the Hagedorn temperature from this analysis. In particular we will show a way to re-

sum the contributions of the most divergent diagrams in order to obtain an effective potential description (Eq. (1.7)) of the phase transition. We will do this in both the gauge theory and in the string theory. Along the way we will prove a general result (Eq. (1.10)) valid for this class of field theories at finite temperature in the large N limit. This result allows us to deduce information on correlation functions at finite temperature from the zero temperature results. We will call this result an "Inheritance principle".

In the second part of this dissertation, described in chapter 4, we will consider an example of the correspondence working in the opposite direction, studying the gravity side to calculate hydrodynamic properties of quantum field theories. The limit in which a strongly interacting field theory is described by hydrodynamics is accessible in the gravity approximation and this allows us to compute transport coefficients from the dual spacetime geometry. In chapter 4 we will compute the shear viscosity and the entropy density of a field theory when string motivated higher derivative corrections to the Einstein-Hilbert action are taken into account. We also argue that a recently conjectured universal bound (Eq. (1.12)) on the ratio between shear viscosity and entropy density may be violated when such corrections are present (Eq. (1.13)).

In the remainder of this introductory chapter, we will describe the main ideas which laid the foundations for this work, and we will state more precisely what the main original results of the thesis work are. Detailed derivations are left for the subsequent chapters.

1.2 The holographic principle and the *AdS/CFT*

One of the main tools which is used in this thesis is the conjectured correspondence between string theory in asymptotic *AdS* spacetimes (times a compact manifold) and conformal field theories having one spatial dimension less than the *AdS* space. The possibility of having a relation between a theory with gravity and a lower dimensional theory without gravity is an idea which was first proposed in the works by 't Hooft [76] and Susskind [73]. The idea is that gravity poses an upper limit to the amount

of degrees of freedom that can be contained in a bounded region of spacetime. This limit scales with the size of the boundary of the region and not with the size of the volume contained. This also implies that a field theory defined on the boundary of the region contains enough information to describe the whole gravitational theory in the inside. The heuristic argument in support of this bound can be traced back to the Bekenstein formula for the entropy of a black hole which states that, for a black hole of horizon area A_{BH}, the entropy is (G is the Newton constant)

$$S_{BH} = \frac{A_{BH}}{4G}.$$ (1.1)

This provides an upper bound on the entropy of a bounded region of space in theories containing gravity. The idea is that, given a spherical region of space with some value S for entropy, one can produce a black hole of the same size by adding more matter in a process which does not decrease the entropy. Therefore S can't be larger than S_{BH}. This argument can be made more precise [12]; the sense in which the correspondence between Anti-de Sitter (AdS) spaces and conformal field theories (CFT) is a holographic correspondence is explained in [74], and we'll review this argument shortly.

The duality between string theory and gauge theory was first proposed by Maldacena [51] and in [34, 79], in the context of type IIB string theory. In this original example of the correspondence, the field theory in question is the maximally supersymmetric $SU(N)$ gauge field theory in 4 dimensions. Since the maximal number of spinor supercharges one can have in four dimension is 4, this theory is denoted as $\mathcal{N} = 4$ super Yang-Mills (SYM). This theory is conformal and has also an $SU(4)_R$ additional global symmetry (R-symmetry) which rotates the various fields among themselves.

On the other hand one considers type IIB super-string theory on an $AdS_5 \times S^5$ background, where the S^5 and AdS_5 have the same size $L^4 = 4\pi g_s N (\alpha')^2$. N is determined by the flux of the type IIB 5-form through the S^5.

In its strongest form (the one which is widely believed to be correct), the corre-

spondence states that the two theories are equivalent when the coupling constants are related by $g_s = g_{YM}^2 = \lambda/N$.

Classical string theory on $AdS_5 \times S^5$ is obtained by fixing λ and taking $N \sim g_s^{-1} \to \infty$. This limit corresponds to having a 't Hooft expansion in the conformal field theory.

The classical supergravity limit is obtained on the string theory side when, in addition to $g_s \to 0$, the length of the string is negligible compared to the size of AdS. This corresponds to $\frac{L^4}{\alpha'^2} = 4\pi\lambda \gg 1$, i.e. when the conformal field theory is strongly coupled and therefore difficult to access via perturbative techniques.

Since we can perform calculations in the super-gravity approximation, we can obtain information on the strongly coupled regime of the conformal field theory and vice versa, from perturbative field theory calculations we can have information on string theory on the curved background. In this thesis we will show examples of both cases. The downside of the complementarity of regimes is that tests of the correspondence are also very difficult, since we can very often reliably compute physical quantities only in one of the two dual theories. A noteworthy exception to this argument is the case of quantities protected by non-renormalization theorems which are the same at both strong and weak coupling. In particular, using the superconformal symmetry of $\mathcal{N} = 4$ SYM theory, it is possible to show that the spectrum of chiral operators and some correlation functions are independent on the Yang-Mills coupling and are therefore the same both at zero and at very large coupling. Comparing the results obtained in the supergravity approximation with the results from field theory provided an important early test for the correspondence. There are also other correlation functions (of chiral primary operators) which are conjectured to be protected by some non-renormalization theorem, [49, 23]. In chapter 2 we will prove that even though the non-renormalization is a consequence of the superconformal symmetry, these properties are inherited by the finite temperature correlation functions at leading order in the large N expansion.

Let us review now the sense in which the AdS/CFT is related to the holographic principle, following [74] (see also [3] for a review). The core of the argument is that in

order to measure the number of degrees of freedom of the field theory, it is necessary to introduce a cut-off δ at high energy (UV). The number of degrees of freedom of $\mathcal{N} = 4$ SYM on a S^3 of radius 1 scales then according to the number of elementary cells (with size of order δ^3) one can fit in the sphere

$$S_{CFT} \sim N^2 \delta^{-3}.$$

(1.2)

In a set of coordinates for AdS where the metric is

$$ds^2 = L^2 \left(- \left(\frac{1 + r^2}{(1 - r^2)} \right)^2 dt^2 + \frac{4}{(1 - r^2)^2} (dr^2 + r^2 d\Omega^2) \right),$$

(1.3)

imposing a UV cut-off of order δ in the field theory is equivalent to imposing an infrared (IR) cut-off at $r = 1 - \delta$. Using the metric Eq. (1.3), the area of the surface at $r = 1 - \delta$ is (when we include the compact S^5),

$$S_{AdS} = \frac{V_{S^5} L^3}{4\delta^3 G} \sim L^8 \delta^{-3} \sim N^2 \delta^{-3}$$

(1.4)

We see therefore that the entropy of the dual field theory scales in the same way as the entropy of the AdS space, as expected from holography.

1.2.1 Large N expansion

Another way of understanding the correspondence is given by the large N expansion of a field theory, first developed by 't Hooft [75](for a review see also [21] and [3]).

Since this is the language we'll employ in the chapters 2 and 3, we will give here a short introduction to the main idea. Consider a field theory with a $U(N)$ gauge group. Let us consider a field in the adjoint, with lagrangian of the form

$$\mathcal{L} = \text{Tr}(\partial\phi_i)^2 + g_c \alpha_{ijk} \text{Tr}\phi_i\phi_j\phi_k + g_c^2 \beta_{ijkl} \text{Tr}\phi_i\phi_j\phi_k\phi_l,$$

(1.5)

where g_c is the gauge coupling constant and the indices i, j, k, l span some set of non-color indices. The traces act on the color indices which are suppressed. The choice

of the power of the coupling constant is consistent with the self-coupling of a gauge field as in the case of a pure Yang-Mills or for $SU(N)$ SYM. Re-scaling the fields by a factor of g_c, we can rewrite this lagrangian as

$$\mathcal{L} = \frac{1}{g_c^2} \left(\text{Tr}(\partial \phi)^2 + \text{Tr}\phi^3 + \text{Tr}\phi^4 \right).$$ (1.6)

The propagator for this theory will carry a factor of g_c^2 and each vertex a factor of g_c^{-2}. In a Feynman diagram, each closed loop amounts to taking a trace, and will therefore give a factor of order N. Considering the set of diagrams with no external legs, it is easy to check that the total contribution of a diagram with V vertices, L propagators and F loops is proportional to

$$N^F g_c^{2(L-V)} = (N g_c^2)^{L-V} N^{F-L+V} = N^{2-2g} (\lambda)^{L-V},$$

where in the second equality we defined the 't Hooft coupling $\lambda = N g_c^2$ and we wrote $F - L + V$ in terms of the genus of the diagram, defined as the genus of the surface of which the diagram is a triangulation. If we consider the limit in which λ is kept fixed and N is large, we can organize the diagrams in a perturbative series in $1/N$, where the power of N is determined by the genus of the diagram. The expansion in genus is analogous to the quantum expansion in string theory where the perturbative expansion is in terms of diagrams of different genus with weights g_s^{2g-2}. The understanding is then that the sum over all diagrams with a fixed genus in field theory is equivalent to string theory amplitudes on a world-sheet of the same genus. In chapter 2 we will show how this expansion need to be augmented on the field theory side to include new contributions ("vortex diagrams") in order to account correctly for the finite temperature.

Using these new elements, in chapter 2 we are able to identify the leading order divergence at the Hagedorn temperature $T = T_H$ and to re-sum the contributions from diagrams of every genus. This will allow us to describe the phase transition in terms of a simple effective potential so that the free energy at the Hagedorn transition

is

$$F_{sing} = \log \int d\phi d\phi^* \, e^{-m_\phi^2 \phi\phi^* - g_s^2 \lambda_4 (\phi\phi^*)^2}. \tag{1.7}$$

In chapter 3 we will then show how the procedure of identifying and re-summing the leading divergence is possible also in the string theory side, in a double scaling limit.

1.3 Finite temperature

In this thesis we study various properties of systems at finite temperature. In the first part of this work we will concentrate on calculating the partition function and $n-$point functions of single trace operators. The partition function at temperature $T = 1/\beta$ is,

$$Z_\beta = \sum_{\text{all states}} e^{-\beta E},$$

where E is the energy of the state. This quantity can be calculated by considering a path integral with Euclidean time, compactified on a circle of radius β. In the path integral language,

$$Z_\beta = \int \mathcal{D}\phi e^{-\int_0^\beta d\tau \mathcal{L}[\phi]}, \tag{1.8}$$

where $\mathcal{L}[\phi]$ represents the Euclidean time lagrangian as a functional of the fields $\phi(\tau, \vec{x})$. Correlation functions of operators at finite temperature in the Eucliden time formalism are calculated as

$$\langle \mathcal{O}_1, \ldots, \mathcal{O}_n \rangle_\beta = \frac{1}{Z_\beta} \int \mathcal{D}\phi \mathcal{O}_1 \ldots \mathcal{O}_n e^{-\int_0^\beta d\tau \mathcal{L}[\phi]}. \tag{1.9}$$

In the finite temperature theory, bosons satisfy periodic boundary conditions in the Euclidean time direction, whereas fermions satisfy anti-periodic boundary conditions. The difference in boundary conditions causes fermions and bosons to have a different mode expansion, thus breaking supersymmetry.

In chapter 2 of this dissertation we will show that at leading order in the large N expansion, for a $U(N)$ gauge field theory with fields in the adjoint on S^3 at a

temperature $T = \frac{1}{\beta} < T_c$, the n-point functions of single trace bosonic [1] operators satisfies,

$$G_\beta(\tau_1, \vec{e}_1, \ldots, \tau_n, \vec{e}_n) = \sum_{m_1,\ldots,m_n=-\infty}^{\infty} G_0(\tau_1 - m_1\beta, \vec{e}_1, \ldots, \tau_n - m_n\beta, \vec{e}_n) \qquad (1.10)$$

where τ and $\vec{e}$ are coordinates in the Euclidean time and on the S^3 respectively, and G_β and G_0 are the correlation functions at $T = \frac{1}{\beta} < T_c$ and $T = 0$ respectively. If the n-point function satisfies some non-renormalization theorem at zero temperature, Eq. (1.10) implies that the same property is inherited at finite temperature at leading order in $\frac{1}{N}$.

In the context of the AdS/CFT we can ask whether these field theories at finite temperature have a gravity dual. In this case one should consider the gravity solutions with the correct asymptotic behavior. The thermodynamic properties of Anti-de Sitter spaces have been first studied by Hawking and Page [37]. They showed that at a certain temperature T_{HP} there is a first order phase transition between two possible gravity solutions. For $T < T_{HP}$, the relevant gravity background is the so-called thermal AdS_{d+1}, while at $T > T_{HP}$ the gravity background is the AdS_{d+1} black hole solution. This phase transition has been interpreted as a de-confinement phase transition for the dual field theory in [80]. The dual field theory is defined on the compact manifold $S^1 \times S^{d-1}$ and therefore the phase transition is sharp only in the large N limit. The partition function and the de-confinement phase transition for free $SU(N)$ gauge theories on compact manifolds have been studied more recently also by Aharony at al. in ([4, 5, 72]). Our discussion on properties of correlation functions at finite temperature in chapter 2 will use some of the formalism developed in these papers.

In the language of the last paragraph, Eq. (1.10) can be interpreted as suggesting that the manifold on which the dual string theory is defined at $T < T_H$ is the same manifold of the zero temperature theory, but with the Euclidean time direction compactified with period β. This is analogous to the thermal AdS described above, but

---

[1]For more details and for the extension to the case with fermions, see Eq. (2.4)

20

this description is now valid when the string length is comparable to the *AdS* scale.

1.4 Hydrodynamic properties of gauge theories

As mentioned in the previous section, we are able to calculate the partition function for free fields at zero or small 't Hooft coupling using perturbative methods. The gauge-gravity duality gives also a way to compute the free energy at infinite 't Hooft coupling using the gravity dual. For the case of $\mathcal{N} = 4$ *SYM*, where the gravity dual is well known, one can verify that the entropy calculated for free fields is comparable to the result at infinite coupling,

$$S_{\lambda=\infty \mathcal{N}=4\mathrm{SYM}} = \frac{\pi^2}{2}N^2T^3V_{S^3} = \left(\frac{3}{4}\right)S_{\lambda=0\mathcal{N}=4\mathrm{SYM}} = \left(\frac{3}{4}\right) \times \frac{2}{3}\pi^2 N^2 T^3 V_{S^3}. \quad (1.11)$$

The $\lambda = \infty$ result we quoted above is the Bekenstein entropy from the supergravity background. There are other thermodynamic properties of strongly coupled field theories which are calculable when the gravity dual is known. In particular, it is widely expected that the behavior of field theories at long distances and low frequencies should be described by hydrodynamics (for details see [62, 42]).

Hydrodynamics determines the form of correlation functions of the stress-energy tensor and of conserved currents as a function of a few parameters such as the shear viscosity η, the bulk viscosity ζ and the speed of sound c_s. The gravity description gives a description compatible with these constraints, and allows us to calculate the value of transport coefficients for strongly coupled field theories.

A striking feature of all the theories with a gravity dual is that, in all examples at hand, the ratio of shear viscosity over entropy density is found to be equal to [61, 46]

$$\frac{\eta}{s} = \frac{1}{4\pi}. \quad (1.12)$$

This result was proven to be a general result for all field theories with gravity dual in [17] and was conjectured to be a universal lower bound for all materials in [45].

On the other hand, we expect gravity to be just a zeroth order approximation

with modifications due to finite length of strings and to non-zero string coupling. The first type of corrections can be organized in a perturbative expansion, with terms containing higher derivatives suppressed by powers of l_s/L, where l_s is the length of the string and L is the *AdS* scale. The details of the perturbation will depend on the details of the compactification of string theory. It may be asked what happens to the lower bound Eq. (1.12) when higher order corrections to Einstein-Hilbert gravity are taken into account. The first α' correction to the IIB supergravity calculations result Eq. (1.11) has been calculated in literature [35, 57, 18, 9] and was found to be positive, therefore not violating the bound.

In chapter 4 we consider the lowest order higher derivative corrections to the Einstein-Hilbert action with arbitrary coefficients. We consider the background describing an AdS_5 black hole and we calculate the shear viscosity and the entropy density. We compute the shear viscosity using three different method as a check of consistency. We also show that the bound Eq. (1.12) is generically corrected and becomes,

$$\frac{\eta}{s} = \frac{1}{4\pi}[1 - 4\lambda_g + \mathcal{O}(\lambda_g^2)], \qquad (1.13)$$

where λ_g is the coefficient of the Riemann tensor squared term and has arbitrary sign. For positive λ_g the bound is manifestly violated.

We then concentrate on the particular case of Gauss-Bonnet gravity which is technically less involved and we look for inconsistencies in the region of parameter space where the bound is violated. In Gauss-Bonnet gravity the terms $\mathcal{O}(\lambda_g^2)$ in Eq. (1.13) vanish, and the result Eq. (1.13) is correct for any value of the Gauss-Bonnet coupling λ_g. We find that this theory violates causality in a region of parameter space where

$$\frac{\eta}{s} \leq \frac{1}{4\pi}\frac{16}{25}. \qquad (1.14)$$

It seems therefore that the bound may be violated by a consistent gravitational theory once higher derivative corrections are taken into account and it may therefore not be a universal bound on the properties of matter. The question whether this gravitational theory with higher derivative correction can arise as a consistent truncation of string

theory is still open.

Experimentally, there are indication that a strongly coupled quark-gluon plasma (QGP) has been produced during gold-gold collisions at RHIC. Experimental data suggests that the hydrodynamic approximation may be relevant for this plasma and that the ratio of shear viscosity over entropy density is very small, of the same order of magnitude of Eq. (1.12).

Calculating hydrodynamics properties of field theories in the regime relevant for experiments is difficult using the usual techniques of perturbative field theory or of lattice QCD (even though recent progress in this direction has been made by [53]). The *AdS/CFT* on the other hand gives us a setting where some of the computations can be performed. Even though the gravity dual of QCD is not known we can improve our understanding of it by using the results obtained for strongly coupled plasmas in theories with a gravity dual. We'll give more details on this and a more complete bibliography in chapter 4.

The results described in this dissertation have been published in the papers [13] and [14] written in collaboration with Guido Festuccia and Hong Liu, and in the papers [15] and [16] written in collaboration with Hong Liu, Robert Myers, Stephen Shenker and Sho Yaida.

Chapter 2

Large N field theory at finite temperature

2.1 Outline

In this chapter we consider a class of gauge theories with fields in the adjoint of a $U(N)$ gauge group on a class of compact manifolds, in the large N limit. In section 2.2 we consider their general properties and we show that the partition function and correlation functions can be obtained by integrals over Wilson lines U. In section 2.3 we concentrate on correlation functions in the low temperature phase. We show that, at leading order in N, correlation functions at $0 < T < T_H$ can be obtained from the result at zero temperature by introducing images in Euclidean time for each operator. This is valid for every value of the gauge coupling constant. Consequences of this property, which we call the "Inheritance Principle" are then described in section 2.4. In the remainder of the chapter we go beyond the leading order and we consider the expansion at all orders in $1/N$ for the partition function in the low temperature phase. At finite temperature new elements, which we call "vortex diagrams," need to be considered. Carefully analyzing this new diagrammatic expansion we are able to analyze and extract the leading divergence of the partition function at temperature T_H. We conclude the chapter by stating that the behavior close to the critical temperature can be described as the critical behavior of a scalar field. The relevance of

this fact in terms of string theory is analyzed in chapter 3.

Parts of this chapter have been published in [13, 14].

2.2 Free Yang-Mills theory on S^3

In this section we discuss some general aspects of free gauge theories with adjoint matter on S^3 at finite temperature. We will assume that the theory under consideration has a vector field A_μ and a number of scalar and fermionic fields[1] all in the adjoint representation of $SU(N)$. The discussion should also be valid for other simply-connected compact manifolds. We use the Euclidean time formalism with time direction τ compactified with a period $\beta = \frac{1}{T}$. Spacetime indices are denoted by $\mu = (\tau, i)$ with i along directions on S^3.

The theory on S^3 can be written as a $(0+1)$-dimensional (Euclidean) quantum mechanical system by expanding all fields in terms of spherical harmonics on S^3. Matter scalar and fermionic fields can be expanded in terms of scalar and spinor harmonics respectively. For the gauge field, it is convenient to use the Coulomb gauge $\nabla_i A^i = 0$, where ∇ denotes the covariant derivative on S^3. In this gauge, A_i can be expanded in terms of transverse vector harmonics, A_τ and the Fadeev-Popov ghost c can be expanded in terms of scalar harmonics. At quadratic level, the resulting action has the form

$$S_0 = N\text{Tr} \int d\tau \left[\left(\frac{1}{2}(D_\tau M_a)^2 - \frac{1}{2}\omega_a^2 M_a^2 \right) + \xi_a^\dagger (D_\tau + \tilde{\omega}_a)\xi_a + \frac{1}{2}m_a^2 v_a^2 + m_a^2 \bar{c}_a c_a \right] \quad (2.1)$$

where we have grouped all harmonic modes into three groups:

1. Bosonic modes M_a with nontrivial kinetic terms. Note that in the Coulomb gauge, the harmonic modes of the dynamical gauge fields have the same $(0 + 1)$-dimensional action as those from matter scalar fields. We thus use M_a to collectively denote harmonic modes coming from both the gauge field A_i and matter scalar fields.

---

[1]We also assume that the scalar fields are conformally coupled.

2. Fermionic modes ξ_a with nontrivial kinetic terms.

3. v_a and c_a are from nonzero modes of A_τ and the Fadeev-Popov ghost c, which have no kinetic terms.

The explicit expressions of various $(0+1)$-dimensional masses $\omega_a, \tilde{\omega}_a, m_a$ can in principle be obtained from properties of various spherical harmonics and will not be used below. In Eq. (2.1), following [4] we separated the zero mode $\alpha(\tau)$ of A_τ on S^3 from the higher harmonics and combine it with ∂_τ to form the covariant derivative D_τ of the $(0+1)$-dimensional theory, with

$$D_\tau M_a = \partial_\tau M_a - i[\alpha, M_a], \qquad D_\tau \xi_a = \partial_\tau \xi_a - i[\alpha, \xi_a] .$$

$\alpha(\tau)$ plays the role of the Lagrange multiplier which imposes the Gauss law on physical states. In the free theory limit the ghost modes c_a do not play a role and v_a only give rise to contact terms (i.e. terms proportional to delta functions in the time direction) in correlation functions[2]. Also note that M_a, ξ_a satisfy periodic and anti-periodic boundary conditions respectively

$$M_a(\tau + \beta) = M_a(\tau), \qquad \xi_a(\tau + \beta) = -\xi_a(\tau) . \tag{2.2}$$

Upon harmonic expansion, correlation functions of gauge invariant operators in the four-dimensional theory reduce to sums of those of the one-dimensional theory Eq. (2.1). More explicitly, a four-dimensional operator $\mathcal{O}(\tau, e)$ can be expanded as

$$\mathcal{O}(\tau, e) = \sum_i f_i^{(\mathcal{O})}(e) Q_i(\tau) \tag{2.3}$$

where e denotes a point on S^3 and Q_i are operators formed from M_a, ξ_a, v_a and their time derivatives. The functions $f_i^{(\mathcal{O})}(e)$ are given by products of various spherical harmonics. A generic n-point function in the four-dimensional theory can be written

---

[2]Also note that since v_a, c_a do not have kinetic terms, at free theory level they only contribute to the partition function by an irrelevant temperature-independent overall factor.

27

as:

$$\langle \mathcal{O}_1(\tau_1, e_1)\mathcal{O}_2(\tau_2, e_2)\cdots\mathcal{O}_n(\tau_n, e_n)\rangle =$$
$$= \sum_{i_1,\cdots,i_n} f_{i_1}^{\mathcal{O}_1}(e_1)\cdots f_{i_n}^{\mathcal{O}_n}(e_n)\,\langle Q_{i_1}(\tau_1)Q_{i_2}(\tau_2)\cdots Q_{i_n}(\tau_n)\rangle \tag{2.4}$$

where $\langle\cdots\rangle$ on the right hand side denotes correlation functions in the 1-dimensional theory Eq. (2.1). Note that Eq. (2.4) applies to all temperatures.

The theory Eq. (2.1) has a residue gauge symmetry

$$M_a \to \Omega M_a \Omega^\dagger,$$
$$\xi_a \to \Omega \xi_a \Omega^\dagger \tag{2.5}$$
$$\alpha \to \Omega\alpha\Omega^\dagger + i\Omega\partial_\tau\Omega^\dagger \ .$$

At zero temperature, the τ direction is uncompact. One can use the gauge symmetry Eq. (2.5) to set $\alpha = 0$. Correlation functions of the theory Eq. (2.1) can be obtained from the propagators of M_a, ξ_a by Wick contractions. Note that[3]

$$\langle M_{ij}^a(\tau)\, M_{kl}^b(0)\rangle_0 = \tfrac{1}{N}G_s(\tau; \omega_a)\delta_{ab}\delta_{il}\delta_{kj}$$
$$\langle \xi_{ij}^a(\tau)\, \xi_{kl}^b(0)\rangle_0 = \tfrac{1}{N}G_f(\tau; \tilde{\omega}_a)\delta_{ab}\delta_{il}\delta_{kj} \tag{2.6}$$

where

$$G_s(\tau; \omega) = \frac{1}{2\omega}e^{-\omega|\tau|}, \qquad G_f(\tau; \omega) = (-\partial_\tau + \omega)G_s(\tau; \omega) \ . \tag{2.7}$$

and i, j, k, l denote $SU(N)$ indices.

At finite temperature, one can again use a gauge transformation to set $\alpha(\tau)$ to zero. The gauge transformation, however, modifies the boundary conditions from Eq. (2.2) to

$$M_a(\tau + \beta) = UM_aU^\dagger, \qquad \xi_a(\tau + \beta) = -U\xi_aU^\dagger \ . \tag{2.8}$$

The unitary matrix U can be understood as the Wilson line of α wound around the τ direction, which cannot be gauged away. It follows that the path integral for Eq. (2.1)

---

[3]We use $\langle\cdots\rangle_0$ and $\langle\cdots\rangle_\beta$ to denote the correlation functions of Eq. (2.1) at zero and finite temperature respectively.

at finite T can be written as

$$\langle\cdots\rangle_\beta = \frac{1}{Z(\beta)} \int dU \int DM(\tau)D\xi(\tau) \cdots e^{-S_0[M_a,\xi_a;\alpha=0]} \tag{2.9}$$

with M_a, ξ_a satisfying boundary conditions Eq. (2.8) and Z the partition function.

Since the action Eq. (2.1) has only quadratic dependence on M_a and ξ_a, the functional integrals over M_a and ξ_a in Eq. (2.9) can be carried out straightforwardly, reducing Eq. (2.9) to a matrix integral over U. For example, the partition function can be written as

$$Z_0(\beta) = \int dU \, e^{I_0(U)} \tag{2.10}$$

where $I_0(U)$ was computed in [72, 4]

$$S_{eff}(U) = \sum_{n=1}^{\infty} \frac{1}{n} V_n(\beta) \mathrm{Tr} U^n \mathrm{Tr} U^{-n} \tag{2.11}$$

with

$$V_n(\beta) = z_s(n\beta) + (-1)^{n+1} z_f(n\beta), \qquad z_s(\beta) = \sum_a e^{-\beta\omega_a}, \qquad z_f(\beta) = \sum_a e^{-\beta\tilde{\omega}_a} . \tag{2.12}$$

Similarly, correlation functions at finite temperature are obtained by first performing Wick contractions and then evaluating the matrix integral for U. With boundary conditions Eq. (2.8), the contractions of M_a and ξ_a become

$$\underbrace{M_{ij}^a(\tau) \, M_{kl}^b(0)} = \frac{\delta_{ab}}{N} \sum_{m=-\infty}^{\infty} G_s(\tau - m\beta; \omega_a) U_{il}^{-m} U_{kj}^m$$

$$\underbrace{\xi_{ij}^a(\tau) \, \xi_{kl}^b(0)} = \frac{\delta_{ab}}{N} \sum_{m=-\infty}^{\infty} (-1)^m G_f(\tau - m\beta; \tilde{\omega}_a) U_{il}^{-m} U_{kj}^m . \tag{2.13}$$

Eq. (2.13) are obtained from Eq. (2.6) by summing over images in τ-direction and can be checked to satisfy Eq. (2.8). As an example, let us consider the planar expression of one- and two-point functions of a normal-ordered operator $Q = \mathrm{Tr} M^4$, with M

29

being one of the M_a in Eq. (2.1). One finds that

$$\langle \text{Tr} M^4 \rangle_\beta \;\; = \tfrac{2}{N^2} \sum_{m \neq 0, n \neq 0} G_s(-m\beta) G_s(-n\beta) \, \langle \text{Tr} U^m \text{Tr} U^n \text{Tr} U^{-m-n} \rangle_U$$

$$(2.14)$$

and the connected part of the two-point function is

$$\langle \text{Tr} M^4(\tau) \text{Tr} M^4(0) \rangle_\beta =$$

$$= \tfrac{4}{N^4} \sum_{m,n,p,q} G_s(\tau - m\beta) G_s(\tau - n\beta) G_s(\tau - p\beta) G_s(\tau - q\beta) \times$$

$$\times \langle \text{Tr} U^{q-m} \text{Tr} U^{m-n} \text{Tr} U^{n-p} \text{Tr} U^{p-q} \rangle_U +$$

$$+ \tfrac{16}{N^4} \sum_{m,n \neq 0,p,q} G_s(-m\beta) G_s(-n\beta) G_s(\tau - p\beta) G_s(\tau - q\beta) \times$$

$$\times \langle \text{Tr} U^m \text{Tr} U^n \left(\text{Tr} U^{-m-p+q} \text{Tr} U^{-n+p-q} + \text{Tr} U^{-m-p-n+q} \text{Tr} U^{p-q} \right) \rangle_U$$

$$(2.15)$$

In Eqs. (2.14)-(2.15) all sums are from $-\infty$ to $+\infty$ and

$$\langle \cdots \rangle_U = \frac{1}{Z} \int dU \, \cdots \, e^{S_{eff}(U)} \tag{2.16}$$

with Z given by Eq. (2.10). We conclude this section by noting some features of Eq. (2.14)-(Eq. (2.15)):

1. Since the operators are normal-ordered, the zero temperature contributions to the self-contractions (corresponding to $m, n = 0$) are not considered. In general, the one-point function is not zero at finite T because of the sum over images; this is clear from Eq. (2.14).

2. The first term of Eq. (2.15) arises from contractions in which all M's of the first operator contract with those of the second operator. The second term of Eq. (2.15) contains partial self-contractions[4], i.e. two of M's in $\text{Tr} M^4$ contract within the operator. The non-vanishing of self-contractions is again due to the sum over nonzero images.

---

[4] Full self-contractions correspond to disconnected contributions.

2.3 Correlation functions in the low temperature phase

It was found in [72, 4] that Eq. (2.1) has a first order phase transition at a temperature T_c in the $N = \infty$ limit. $\text{Tr}U^n$ can be considered as order parameters of the phase transition. In the low temperature phase, one has

$$\langle \text{Tr}U^n \rangle_U \approx N\delta_{n,0} + O(1/N) \tag{2.17}$$

while for $T > T_c$, $\text{Tr}U^n, n \neq 0$ develop nonzero expectation values. It follows from Eq. (2.17) that in the low temperature phase, to leading order in $1/N$ expansion

$$\langle \text{Tr}U^{n_1}\text{Tr}U^{n_2}\cdots \text{Tr}U^{n_k} \rangle_U \approx \langle \text{Tr}U^{n_1} \rangle_U \langle \text{Tr}U^{n_2} \rangle_U \cdots \langle \text{Tr}U^{n_k} \rangle_U$$
$$\approx N^k \delta_{n_1,0} \cdots \delta_{n_k,0} \tag{2.18}$$

where in the second line we have used the standard factorization property at large N.

We now look at the implications of Eq. (2.18) on correlation functions. Applying Eq. (2.18) to Eq. (2.14) and Eq. (2.15), one finds

$$\langle \text{Tr}M^4 \rangle_\beta = 0 + O(1/N)$$
$$\langle \text{Tr}M^4(\tau)\text{Tr}M^4(0) \rangle_\beta = 4\sum_m G_s^4(\tau - m\beta) + O(1/N^2)$$
$$= \sum_m \langle \text{Tr}M^4(\tau - m\beta)\text{Tr}M^4(0) \rangle_0 \tag{2.19}$$

Note that the second term of Eq. (2.15) due to partial self-contractions vanishes and the finite-temperature correlators are related to the zero-temperature ones by adding the images for the whole operator.

The conclusion is not special to Eq. (2.19) and can be generalized to any correlation functions of single-trace (normal-ordered) operators in the large N limit. Now consider a generic n-point function for some single-trace operators. At zero temper-

ature, the contribution of a typical contraction can be written in a form

$$\frac{1}{N^{n-2+2h}} \prod_{i<j=1}^{n} \prod_{p=1}^{I_{ij}} G_s^{(p)}(\tau_{ij}), \qquad \tau_{ij} = \tau_i - \tau_j \qquad (2.20)$$

where i, j enumerate the vertices, I_{ij} is the number of propagators between vertices i, j, $G^{(p)}(\tau_{ij})$ is the p-th propagator between vertices i and j, and h is the genus of the diagram. At finite temperature, one uses Eq. (2.13) to add images for each propagator and finds the contribution of the same diagram is given by

$$\frac{1}{N^I} \left(\prod_{i<j=1}^{n} \prod_{p=1}^{I_{ij}} \sum_{m_{ij}^{(p)}=-\infty}^{\infty} \right) \left(\prod_{i<j=1}^{n} \prod_{p=1}^{I_{ij}} G_s^{(p)} \left(\tau_{ij} - m_{ij}^{(p)}\beta \right) \right) \langle \mathrm{Tr} U^{s_1} \mathrm{Tr} U^{s_2} \cdots \rangle_U \quad (2.21)$$

where $m_{ij}^{(p)}$ label the images of $G^{(p)}(\tau_{ij})$. When involving contractions of fermions, one replaces $G_s^{(p)} \left(\tau_{ij} - m_{ij}^{(p)}\beta \right)$ by $(-1)^{m_{ij}^{(p)}} G_f^{(p)} \left(\tau_{ij} - m_{ij}^{(p)}\beta \right)$ for the relevant p's. The powers $s_1, s_2, \cdots$ in the last factor of Eq. (2.21) can be found as follows. To each propagator in the diagram we assign a direction, which can be chosen arbitrarily and similarly an orientation can be chosen for each face. For each face A in the diagram, we have a factor $\mathrm{Tr} U^{s_A}$, with s_A given by

$$s_A = \sum_{\partial A} (\pm) m_{ij}^{(p)}, \qquad A = 1, 2, \cdots F \qquad (2.22)$$

where the sum ∂A is over the propagators bounding the face A and F denotes the number of faces of the diagram. In Eq. (2.22) the plus (minus) sign is taken if the direction of the corresponding propagator is the same as (opposite to) that of the face. s_A has a precise mathematical meaning: it is the number of times that the propagators bounding a face A wrap the Euclidean time circle. We will thus call s_A the vortex number for the face A. To illustrate more explicitly how Eq. (2.21) works, we give some examples in section 2.5.1

In the low temperature phase, at leading order in $1/N$ expansion, due to equation
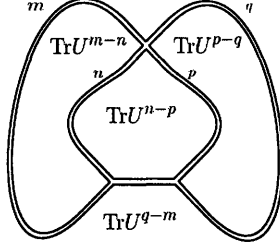
Figure 2-1: An example of a double-line diagram at finite temperature. Each propagator carries a winding number (or image number), which should be summed over. Due to the presence of U-factors in Eq. (2.13), associated with each face one finds a factor of $\mathrm{tr}U^{s_A}$, instead of a factor N as is the case at zero temperature.

Eq. (2.18) one has constraints on $m_{ij}^{(p)}$ associated with each face

$$s_A = \sum_{\partial A}(\pm)m_{ij}^{(p)} = 0, \qquad A = 1, 2, \cdots F . \tag{2.23}$$

Note that not all equations in Eq. (2.23) are independent. The sum of all the equations gives identically zero. One can also check that this is the only relation between the equations, thus giving rise to $F - 1$ constraints on $m_{ij}^{(p)}$'s. For a given diagram, the number I of propagators, the number F of faces and the number n of vertices[5] satisfy the relation $F + n - I = 2 - 2h$, where h is the genus of the diagram. It then follows that the number of independent sums over images is $K = I - (F - 1) = n - 1 + 2h$.

2.3.1 The planar case

For *planar* diagrams ($h = 0$), we have the number of independent sums over images given by

$$K = n - 1 \tag{2.24}$$

i.e. one less than the number of vertices. Also for any loop L in a planar diagram, one has[6]

$$\sum_{\partial L} \pm m_{ij}^{(p)} = 0 \tag{2.25}$$

---

[5]Note that since we are considering the free theory, the number of vertices coincides with the number of operators in the correlation functions.

[6]The following equation also applies to contractible loops in a non-planar diagram.

where one sums over the image numbers associated with each propagator that the loop contains with the relative signs given by the relative directions of the propagators. Eq. (2.25) implies that all propagators connecting the same two vertices should have the same images, i.e. $m_{ij}^{(p)} = m_{ij}$ (up to a sign), which are independent of p. Furthermore, this also implies that one can write

$$m_{ij} = m_i - m_j \ . \tag{2.26}$$

In other words, the sums over images for each propagator reduce to the sums over images for each operator. We thus find that Eq. (2.21) becomes (for $h = 0$)

$$\frac{1}{N^{n-2}} \sum_{m_1, \cdots m_n = -\infty}^{\infty} \prod_{i<j=1}^{n} \prod_{p=1}^{I_{ij}} G_s^{(p)} \left((\tau_i - m_i \beta) - (\tau_j - m_j \beta) \right) \ . \tag{2.27}$$

In the above we considered contractions between different operators. As we commented at the end of section 2.2, at finite temperature generically self-contractions do not vanish despite the normal ordering. One can readily convinces himself using the arguments above that all *planar* self-contractions reduce to those at zero temperature and thus are canceled by normal ordering. For example, for one-point functions, $n = 1$, from Eq. (2.24) there is no sum of images. Thus the finite-temperature results are the same as those of zero-temperature, which are zero due to normal ordering.

When the operators contain fermions, we replace G_s by G_f in appropriate places and multiply Eq. (2.27) by a factor

$$\prod_{i<j=1}^{n} (-1)^{m_{ij} I_{ij}^{(f)}} \tag{2.28}$$

where $I_{ij}^{(f)}$ is the number of fermionic propagators between vertices i, j. Using Eq. (2.26), we have

$$(-1)^{\sum_{i<j} m_{ij} I_{ij}^{(f)}} = (-1)^{\sum_{i,j} m_i I_{ij}^{(f)}} = (-1)^{\sum_i m_i \epsilon_i} \tag{2.29}$$

where $\epsilon_i = 0(1)$ if the i-th operator contains even (odd) number of fermions.

Since Eq. (2.27) and Eq. (2.29) do not depend on the specific structure of the

diagram, we conclude that to leading order in $1/N$ expansion the full correlation function should satisfy

$$G_\beta(\tau_1, \cdots \tau_n) = \sum_{m_1, m_2, \cdots m_n = -\infty}^{\infty} (-1)^{m_i \epsilon_i} G_0(\tau_1 - m_1 \beta, \cdots \tau_n - m_n \beta) \ . \qquad (2.30)$$

Note that Eq. (2.30) applies also to the correlation functions in the four dimensional theory since the harmonic expansion is independent of the temperature.

2.3.2 Including interactions

In the sections above we have focused on the free theory limit. We will now present arguments that Eq. (2.30) remains true order by order in the expansion over a small 't Hooft coupling λ. In addition to Eq. (2.1) the action also contains cubic and quartic terms which can be written as

$$S_{int} = N \int_0^\beta d\tau \ \left(\lambda^{\frac{1}{2}} \sum_\alpha b_\alpha \mathcal{L}_{3\alpha} + \lambda \sum_\alpha d_\alpha \mathcal{L}_{4\alpha} \right) \qquad (2.31)$$

where $\mathcal{L}_{3\alpha}$ and $\mathcal{L}_{4\alpha}$ are single-trace operators made from ξ_a, M_a, v_a, c_a and their time derivatives. b_α and d_α are numerical constants arising from the harmonic expansion. Again the precise form of the action will not be important for our discussion below. The corrections to free theory correlation functions can be obtained by expanding the exponential of Eq. (2.31) in the path integral. For example, a typical term will have the form

$$\int_0^\beta d\tau_{n+1} \cdots \int_0^\beta d\tau_{n+k} \ \langle \mathcal{O}_1(\tau_1) \cdots \mathcal{O}_n(\tau_n) \mathcal{L}_{3\alpha_1}(\tau_{n+1}) \cdots \mathcal{L}_{4\alpha_k}(\tau_{n+k}) \rangle_{\beta,0} \qquad (2.32)$$

where to avoid causing confusion we used $\langle \cdots \rangle_{\beta,0}$ to denote the correlation function at zero coupling and finite temperature. Using Eq. (2.30), Eq. (2.32) can be written

as[7]

$$\sum_{m_1, \cdots m_n} \int_{-\infty}^{\infty} d\tau_{n+1} \cdots \int_{-\infty}^{\infty} d\tau_{n+k}$$

$$\langle \mathcal{O}_1(\tau_1 - m_1\beta) \cdots \mathcal{O}_n(\tau_n - m_n\beta) \, \mathcal{L}_{3\alpha_1}(\tau_{n+1}) \cdots \mathcal{L}_{4\alpha_k}(\tau_{n+k}) \rangle_{0,0} \qquad (2.33)$$

where $\langle \cdots \rangle_{0,0}$ denotes correlation function at zero coupling and zero temperature and we have extended the integration ranges for $\tau_{n+1}, \cdots \tau_{n+k}$ into $(-\infty, +\infty)$ using the sums over the images of these variables. Eq. (2.33) shows that Eq. (2.30) can be extended to include corrections in λ.

2.4   The Inheritance Principle - Consequences of Eq. (2.30)

Eq. (2.30) implies that properties of correlation functions of the theory at zero temperature can be inherited at finite temperature in the large N limit. For example, for those correlation functions which are independent of the 't Hooft coupling in the large N limit at zero temperature, the statement remains true at finite temperature. For $\mathcal{N} = 4$ Super-Yang-Mills theory (SYM) on S^3, which was the main motivation of our study, it was conjectured in [49] that two- and three-point functions of chiral operators are nonrenormalized from weak to strong coupling[8]. The conjecture, if true, will also hold for $\mathcal{N} = 4$ SYM theory at finite temperature despite the fact that the conformal and supersymmetries are broken. Eq. (2.30) also suggests that, at leading order in $1/N$ expansion, the one-point functions of all gauge invariant operators (including the stress tensor) at finite temperature are zero. Eq. (2.30), while surprising from a gauge theory point of view, has a simple interpretation in terms of string theory dual. Suppose the gauge theory under consideration has a string theory dual described by some sigma-model M at zero temperature and some other sigma-model M' at finite temperature. The correlation functions in gauge theory to leading order in the $1/N$

---

[7]Note $\mathcal{L}_{3\alpha}$ and $\mathcal{L}_{4\alpha}$ also contain ghosts c_a whose contractions are temperature independent and so will not affect our results in the last section.

[8]See also [24, 40, 29, 31] for further evidence.

expansion should be mapped to sphere amplitudes of some vertex operators in the M or M' theory. Eq. (2.30) follows immediately if we postulate that M' is identical to M except that the target space time coordinate is compactified to have a period β. To see this, it is more transparent to write Eq. (2.30) in momentum space. Fourier transforming τ_i to ω_i in Eq. (2.30) we find that

$$G_\beta(\omega_1, \cdots, \omega_n) = G_0(\omega_1, \cdots, \omega_n), \qquad (2.34)$$

with all ω_i to be quantized in multiples of $\frac{2\pi}{\beta}$. Thus in momentum space to leading order in large N, finite temperature correlation functions are simply obtained by those at zero temperature by restricting to quantized momenta. From the string theory point of view, this is the familiar inheritance principle for tree-level amplitudes.

We note that given a perturbative string theory, it is not *a priori* obvious that the theory at finite temperature is described by the same target space with time direction periodically identified[9]. For perturbative string theory in flat space at a temperature below the Hagedorn temperature, this can be checked by explicit computation of the free energy at one-loop [59]. Equation Eq. (2.30) provides evidences that this should be the case for string theories dual to the class of gauge theories we are considering at a temperature $T < T_c$.

For $\mathcal{N} = 4$ SYM theory on S^3, the result matches well with that from the AdS/CFT correspondence [51, 34, 79].

When the curvature radius of the anti-de Sitter (AdS) spacetime is much larger than the string and Planck scales (which is dual to the YM theory at large 't Hooft coupling) the correspondence implies that IIB string in $AdS_5 \times S_5$ at $T < T_c$ is described by compactifying the time direction (so-called thermal AdS) [79, 80].

The result from the weakly coupled side suggests that this description can be extrapolated to weak coupling[10].

We conclude this section by some remarks:

---

[9]A counter example is IIB string in $AdS_5 \times S_5$ at a temperature above the Hawking-Page temperature. Also in curved spacetime this implies one has to choose a particular time slicing of the spacetime.

[10]Also note that it is likely that $AdS_5 \times S_5$ is an exact string background [52, 43, 10].

1. The inheritance principle Eq. (2.30) no longer holds beyond the planar level. For non-planar diagrams, it is possible to have images running along the non-contractible loops of the diagram. These may be interpreted in string theory side as winding modes for higher genus diagrams. We'll study in more details these diagrams in the remainder of this chapter.

2. In the high temperature (deconfined) phase, where $\text{Tr}U^n$ generically are non-vanishing at leading order, Eq. (2.30) no longer holds, as can be seen from the example of Eq. (2.15). This suggests that in the deconfined phase M' should be more complicated. In the case of $\mathcal{N} = 4$ SYM theory at strong coupling, the string dual is given by an AdS Schwarzschild black hole [79, 80]. It could also be possible that the deconfined phase of the class of gauge theories we are considering describe some kind of stringy black holes [72, 4].

We finally note that the argument of the section is but an example of how the inheritance property for the sphere amplitude in an orbifold string theory can have a non trivial realization in the dual gauge theory.

2.5 Yang-Mills Theory on S^3 beyond the planar level

In this section we will resume our discussion of the matrix model, considering contributions beyond the planar level in the partition function. In the large N limit, at zero temperature, the free energy of the matrix model in Eq. (2.1) can be organized in terms of the topology of Feynman diagrams

$$\log Z = \sum_{h=0}^{\infty} N^{2(1-h)} f_h(\lambda) \tag{2.35}$$

where $f_0(\lambda)$ is the sum of connected planar Feynman diagrams, and $f_1(\lambda)$ is the sum of connected non-planar diagrams which can be put on a torus, and so on. As mentioned in the introduction, Eq. (2.35) resembles the perturbative expansion of

a string theory, with $1/N$ identified with the closed string coupling g_s and $f_h(\lambda)$ identified with contributions from world-sheets of genus-h.

In the next few subsections, we discuss the large N expansion of Eq. (2.1) at finite temperature, and we see new ingredients arise. We find new contributions associated with Feynman diagrams with vortices, which can be identified with degenerate limits of a string world-sheet. In the next chapter we'll then show how this behavior is connected to the Hagedorn behavior in string theory.

In section 2.2 we showed that the free theory partition function reduces to an integral over the matrices U,

$$Z_0(\beta) = \int dU \; e^{I_0(U)} \tag{2.36}$$

with $I_0(U)$ given by

$$I_0(U) = \sum_{n=1}^{\infty} \frac{1}{n} V_n(\beta) \mathrm{Tr} U^n \mathrm{Tr} U^{-n}. \tag{2.37}$$

When the temperature T is small, this can be evaluated in the large N limit as [72, 4]

$$Z_0(\beta) = C \prod_{n=1}^{\infty} \frac{n}{1 - V_n(\beta)} + O(1/N^2) \tag{2.38}$$

where C is an N-independent constant factor. $Z_0(\beta)$ becomes divergent if some $V_n(\beta)$ are equal to 1. From Eq. (2.12) one can check that $V_1(\beta) > V_n(\beta)$ for $n > 1$ and that $V_1(\beta)$ is a monotonically increasing function of T, with $V_1(\beta = \infty) = 0$ and $V_1(\beta = 0) > 1$. Thus as one increases T from zero there exists a T_H at which $V_1(T_H) = 1$ and Z_0 becomes divergent. Eq. (2.38) only applies to $T < T_H$.

The partition function Eq. (2.36) and more generally matrix integrals in Eq. (2.21) can be evaluated to all orders in a $1/N^2$ expansion. In appendix A we prove that, *up to corrections non-perturbative in N*, the matrix integrals can be evaluated by treating each $\mathrm{Tr} U^n$ as an independent integration variable. More explicitly,

$$\langle \cdots \rangle_U = \frac{1}{Z_0(\beta)} \int dU \; \cdots \; e^{I_0(U)} \tag{2.39}$$

can be evaluated by replacing

$$\frac{1}{N}\mathrm{Tr}U^n \rightarrow \phi_n, \qquad \frac{1}{N}\mathrm{Tr}U^{-n} \rightarrow \phi_{-n} = \phi_n^*, \qquad \phi_0 = 1 , \qquad (2.40)$$

i.e.

$$\langle \frac{1}{N}\mathrm{Tr}U^{s_1}\frac{1}{N}\mathrm{Tr}U^{s_2}\cdots\frac{1}{N}\mathrm{Tr}U^{s_F}\rangle_U =$$
$$= \frac{1}{Z_0}\int_{-\infty}^{\infty}\left(\prod_{i=1}^{\infty}d\phi_i d\phi_i^*\right)\phi_{s_1}\cdots\phi_{s_F}\,\exp\left(-N^2\sum_{n=1}^{\infty}v_n(\beta)\phi_n\phi_n^*\right) +$$
$$+ \text{ nonperturbative in } N \qquad (2.41)$$

where

$$v_n(\beta) = \frac{1 - V_n(\beta)}{n} . \qquad (2.42)$$

From Eq. (2.41),

$$\langle \frac{1}{N}\mathrm{Tr}U^{s_1}\frac{1}{N}\mathrm{Tr}U^{s_2}\cdots\frac{1}{N}\mathrm{Tr}U^{s_F}\rangle_U =$$
$$= \prod_{i=1}^{F}\delta_{s_i,0} + \frac{1}{N^2}\sum_{i<j=1}^{F}\left(\frac{1}{v_{|s_i|}(\beta)}\delta_{s_i+s_j,0}\prod_{k=1\,k\neq i,j}^{F}\delta_{s_k,0}\right) +$$
$$+ O(N^{-4}) + \text{nonperturbative in } N \qquad (2.43)$$

where order $1/N^2$ terms are obtained by contractions of one pair of ϕ_{s_i}'s, order $1/N^4$ terms are obtained by contracting two pairs of ϕ's, and so forth. Each contraction brings a factor of $\frac{1}{N^2 v_{s_i}(\beta)}$. Perturbative corrections in $1/N^2$ terminate at order $1/N^F$ (or $1/N^{F-1}$) for F even (odd). For example, there is no other perturbative correction in $1/N^2$ for the partition function Eq. (2.38), and for $F = 2$,

$$\langle \frac{1}{N}\mathrm{tr}U^n\frac{1}{N}\mathrm{tr}U^m\rangle = \delta_{n,0}\delta_{m,0} + \frac{1}{N^2}\frac{1}{v_{|n|}(\beta)}\delta_{m+n,0} + \text{nonperturbative corrections} \qquad (2.44)$$

To summarize, combining Eq. (2.21) and Eq. (2.43) we find that for a correlation function of gauge invariant operators, there are two sources of $1/N^2$ corrections:

1. From the genus of the diagram as indicated by the power of $1/N$ in Eq. (2.21).
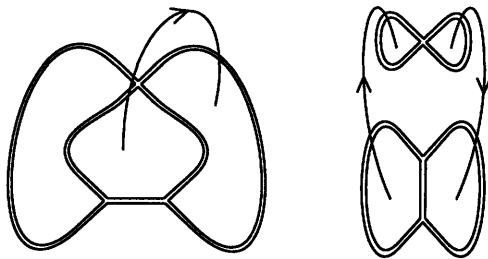
Figure 2-2: Examples of double-line diagrams with nonzero vortices. Each thin line (vortex propagator) represents a contraction in Eq. (2.43). Compare the left diagram to Fig. 2-1. Diagrams which are disconnected at zero temperature can be connected through vortex propagators as in the right diagram.

This follows from the standard large N counting.

2. From the $1/N^2$ corrections of the matrix integral Eq. (2.43). The leading order term in Eq. (2.43) imposes the constraint that for any face A of the diagram the vortex number s_A should be zero. The next order corresponds to having nonzero vortex numbers in two of the faces, say the faces A and B with $s_A s_B \neq 0$ and $s_A + s_B = 0$. Below, we will refer to those diagrams with nonzero vortex numbers as containing vortices, in anticipation of their interpretation from the string worldsheet which we will discuss in the next chapter[11]. From remarks below Eq. (2.22), if a face A of a Feynman diagram contains a vortex with vortex number s_A, then the propagators bounding the face wrap around the Euclidean time circle s_A times. At finite temperature, due to the presence of vortices, planar diagrams also contain higher order $1/N^2$ corrections.

It will be convenient to represents the vortex contributions diagrammatically: we represent each contraction in Eq. (2.43) by an oriented line between two surfaces which have the opposite vortex numbers. The orientation of a line is that it exists (enters) the surface if its vortex number is positive (negative). We associate a factor $1/N$ for each vortex and a factor $1/v_n(\beta)$ to a line (vortex propagator) connecting two surfaces with vortex number $\pm n$. See Fig. 2-2 for some examples of such diagrams. Note that a diagram with otherwise disconnected parts connected by vortex lines

---

[11]See also the discussion of [33] in the context of $c = 1$ matrix models.

41
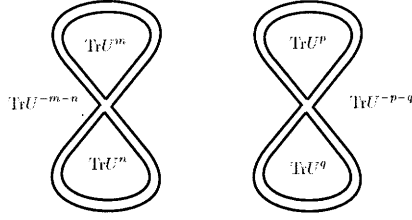
Figure 2-3: Planar disconnected contributions to $\langle \mathrm{Tr}M^4(\tau)\mathrm{Tr}M^4(0)\rangle$

should be considered as connected, as in the right diagram of Fig. 2-2. In computing a correlation function one should sum over all possible vortex contributions.

To summarize this subsection, in computing correlation functions at finite temperature, one should consider not only Feynman diagrams which appear at zero temperature, but also diagrams with nonzero vortices. Explicit examples are given in the next subsection.

2.5.1   Examples of Eq. (2.21)

In this subsection we give some explicit examples on the use of equation Eq. (2.21) for calculating correlation functions between single trace operators. For definiteness we consider only bosonic operators, but the procedure is analogous for operators involving fermions. Let us consider again the following simple example

$$\langle N\mathrm{Tr}M^4(\tau)N\mathrm{Tr}M^4(0)\rangle \tag{2.45}$$

where M can be any of the bosonic modes in Eq. (2.1). The calculation of Eq. (2.45) amounts to drawing all possible double line diagrams. For example the disconnected planar contribution is given in Fig. 2-3. From Eq. (2.13), each propagator carries an image number (or winding number), which should be summed over. Each face A carries a factor $\mathrm{tr}U^{s_A}$. s_A is determined by choosing a direction for the propagators, and an orientation for the face, as explained below Eq. (2.22). Fig. 2-3 therefore

42
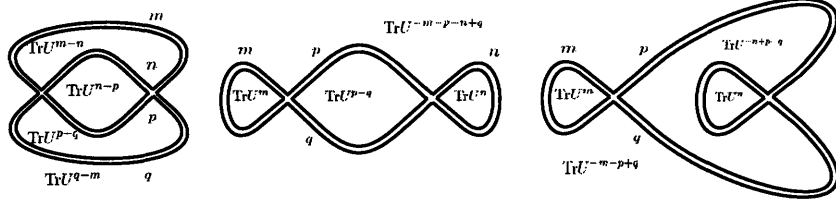
Figure 2-4: Planar connected contributions to $\langle \mathrm{Tr}M^4(\tau)\mathrm{Tr}M^4(0)\rangle$
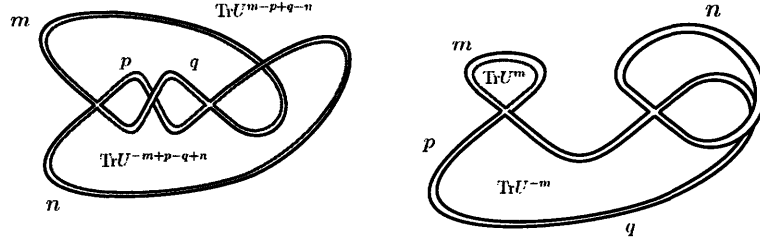
Figure 2-5: Some non-planar (torus) connected contributions to $\langle \mathrm{Tr}M^4(\tau)\mathrm{Tr}M^4(0)\rangle$. For visualization purpose, the edge of one of the faces is drawn in red.

gives a contribution of the form

$$
\frac{4}{N^2} \sum_{m,n,p,q=-\infty}^{\infty} G_s(-m\beta)G_s(-n\beta)G_s(-p\beta)G_s(-q\beta)\times
$$
$$
\times \langle \mathrm{Tr}U^m\mathrm{Tr}U^n\mathrm{Tr}U^{-m-n}\mathrm{Tr}U^p\mathrm{Tr}U^q\mathrm{Tr}U^{-p-q}\rangle_U. \tag{2.46}
$$

The connected planar contributions are given in Fig. 2-4 with, for example, the first diagram given by

$$
\langle \mathrm{Tr}M^4(\tau)\mathrm{Tr}M^4(0)\rangle_{\text{planar connected}} =
$$
$$
= \frac{4}{N^2} \sum_{m,n,p,q=-\infty}^{\infty} G_s(\tau - m\beta)G_s(\tau - n\beta)G_s(\tau - p\beta)G_s(\tau - q\beta)\times
$$
$$
\times \langle \mathrm{Tr}U^{m-n}\mathrm{Tr}U^{n-p}\mathrm{Tr}U^{p-q}\mathrm{Tr}U^{q-m}\rangle_U \tag{2.47}
$$

In Fig. 2-5 we have also plotted some connected non-planar diagrams, with the first diagram given by

$$
\frac{4}{N^2} \sum_{m,n,p,q=-\infty}^{\infty} G_s(\tau - m\beta)G_s(\tau - n\beta)G_s(\tau - p\beta)G_s(\tau - q\beta)\times
$$

43
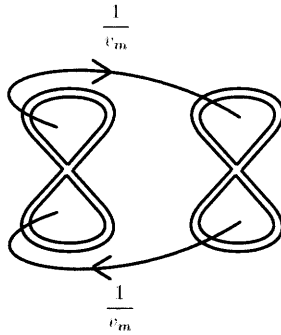
Figure 2-6: Connected vortex diagram from disconnected double line diagram

$$\times \langle \mathrm{Tr} U^{m-p+q-n} \mathrm{Tr} U^{-m+p-q+n} \rangle_U \qquad (2.48)$$

Now let us consider the evaluation of the expectation values of traces of U in Eq. (2.46)-(2.48) using Eq. (2.43). At leading order in the large N expansion the expectation values give N^F, where F is the number of traces, times some product of Kronecker delta enforcing all exponents to be zero. In this case we recover the results of section 2.2. Higher order corrections in $1/N$ can be described graphically by inserting pairs of vortices on different faces of the diagrams and connecting them with the propagator $\frac{1}{v_b(\beta)}$. One should sum over all the possible ways of inserting pairs of vortices. Note that each vortex insertion gives a factor of $1/N$. Diagrams with disconnected parts connected by vortex propagators should be considered as connected as in Fig. 2-6. Note that in terms of large N counting Fig. 2-6 is of the same order as those in Fig. 2-5 with no vortices.

2.6 Free energy in interacting theory and vortex diagrams

We now consider the Euclidean partition function of the interacting theory. Below Eq. (2.38) we identified T_H as the temperature at which Z_0 becomes divergent. Our purpose is now to identify T_H and the critical behavior near T_H to all orders in the $1/N^2$ expansion.

44

In perturbation theory, the partition function can be evaluated by expanding the interaction terms in the exponent of the path integral

$$Z(\beta, \lambda) = Z_0(\beta) \sum_{n=0}^{\infty} \frac{(-1)^n}{n!} \int_0^\beta \prod_{i=1}^n d\tau_i \, \langle V(\tau_1) \cdots V(\tau_n) \rangle_{0,\beta} \qquad (2.49)$$

In Eq. (2.49), $\langle \cdots \rangle_{0,\beta}$ denotes free theory correlation functions and recall that V is given by a sum of single trace operators of the form $N\mathrm{tr}(\cdots)$. The free energy can be obtained from

$$\log Z = \log Z_0 + \sum_{n=0}^{\infty} \frac{(-1)^n}{n!} \int_0^\beta \prod_{i=1}^n d\tau_i \, \langle V(\tau_1) \cdots V(\tau_n) \rangle_{0,\beta,connected} \qquad (2.50)$$

i.e. one sums only over the connected diagrams. The discussion in the last subsection for free theory correlation functions can now be directly carried over to $\log Z$. In particular, there are two sources of $1/N^2$ corrections: from the non-planar structure and from vortices. We can expand $\log Z$ in $1/N^2$ as

$$\log Z(\beta) = \sum_{n=0}^{\infty} N^{2-2n} \mathcal{Z}_n(\beta) = N^2 \mathcal{Z}_0(\beta) + \mathcal{Z}_1(\beta) + \frac{1}{N^2} \mathcal{Z}_2(\beta) + \cdots \qquad (2.51)$$

where $\mathcal{Z}_0$ corresponds to the sum over connected planar diagrams with no vortices, while $\mathcal{Z}_1$ contains the sum of connected genus-1 non-planar diagrams with no vortices *and* planar diagrams with one pair of vortices, and so on. Recall that each vortex carries a factor $1/N$ and they always come in pairs. Also as remarked at the end of the last subsection, a diagram with otherwise disconnected parts connected by vortex propagators is connected.

To elucidate the structure of $\mathcal{Z}_g$, we introduce a new set of "vortex diagrams", by generalizing the diagrammatical rules introduced below Fig. 2-2:

1. Denote $Q^{(h,n)}$ as the sum of connected Feynman diagrams with genus h and with n vortices. In terms of large N counting, $Q^{(h,n)}$ is of order N^{2-2h-n}, as we associate a factor $1/N$ with each vortex. Each vortex is labeled by a vortex

45

$$\frac{1}{v_b(\beta)} \qquad\qquad Q^{(0,2)} \qquad\qquad Q^{(1,3)}$$
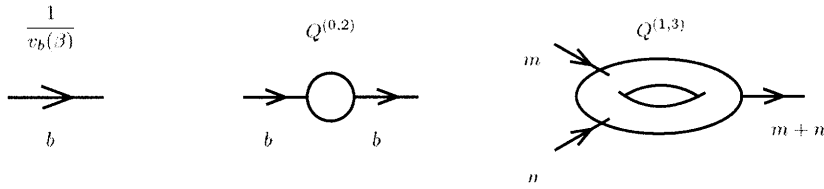
Figure 2-7: The propagators and vertices for vortex diagrams. The vertices $Q^{(h,n)}$ of a vortex diagram have n legs, each of which is labelled by a vortex number. The sign of the vortex number is positive (negative) if the corresponding leg exists (enters) the vertex. The total vortex number of a vertex is zero. We show $Q^{(0,2)}$, $Q^{(1,3)}$ in the figure as illustrations.

number and the total vortex number carried by $Q^{(h,n)}$ is zero[12]. Diagrammatically, $Q^{(h,n)}$ are represented as vertices with n oriented legs. The leg exits the vertex if the corresponding vortex number is positive.

2. Vortex diagrams are then constructed following the usual rules with $Q^{(h,n)}$ as fundamental vertices and $1/v_b(\beta), b > 0$ as propagators. Note that b is the vortex number carried by a propagator and v_b was defined in Eq. (2.42).

3. The combinatoric rules are the same as standard Feynman diagram. In particular, if there are m identical vertices $Q^{(h,n)}$ in a diagram, there is a factor $1/m!$, which comes from the fact that disconnected diagrams are obtained from connected ones by exponentiation.

Using the above diagrammatical rules, we now enumerate the contributions to $\mathcal{Z}_g$. See Fig. 2-7 for illustrations of propagators and vertices for vortex diagrams.

Let us first look at $\mathcal{Z}_0$, which is given by the sum of all planar diagrams without vortex. In section 4 of section 2.3.1 it was shown that $\mathcal{Z}_0$ is identical to the corresponding expression at zero temperature and thus is temperature-independent[13]. Since the free energy $-\beta F$ is defined by subtracting the zero-temperature contribution (which is the vacuum energy) from Eq. (2.51), we conclude that the planar contribution to

---

[12]This follows from the discussion below Eq. (2.22).

[13]$\mathcal{Z}_0$ is a special case of the discussion in section 4 of section 2.3.1 with no external operator insertions.

46
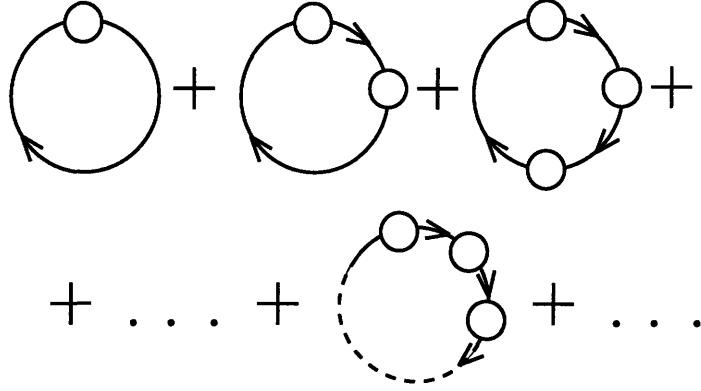
Figure 2-8: Vortex diagrams contributing to $\mathcal{Z}_1^{(3)}$.

the free energy is identically zero[14].

We now look at $\mathcal{Z}_1$, which contains three contributions: (i) genus-1 contribution in free theory coming from the first term in Eq. (2.50); (ii) sum of genus-1 Feynman diagrams with no vortices; (iii) planar diagrams with vortices. The first contribution $\mathcal{Z}_1^{(1)}$ is given by the logarithm of Eq. (2.38). The second contribution $\mathcal{Z}_1^{(2)}$ is given by $Q^{(1,0)}$. To find the third contribution $\mathcal{Z}_1^{(3)}$, let us denote $Q_b^{(0,2)}$ the sum of all planar connected diagrams with two vortices of winding $\pm b$. Graphically, it can be represented by a sphere with an arrow pointing in and an arrow pointing out, each carrying vortex number b, as in the second diagram of Fig. 2-7. Using $Q_b^{(0,2)}$, $\mathcal{Z}_1^{(3)}$ is obtained by summing the vortex diagrams in Eq. (2-8). The combinatoric factor for a diagram with m vertices is $1/m$ following from the cyclic symmetry and we find that

$$\mathcal{Z}_1^{(3)} = \sum_{b=1}^{\infty} \sum_{m=1}^{\infty} \frac{1}{m} \left(\frac{Q_b^{(0,2)}(\lambda, \beta)}{v_b(\beta)} \right)^m = -\sum_{b=1}^{\infty} \log \left(1 - \frac{Q_b^{(0,2)}(\lambda, \beta)}{v_b(\beta)} \right) . \tag{2.52}$$

Adding all three contributions together we find that

$$\mathcal{Z}_1 = \mathcal{Z}_1^{(1)} + \mathcal{Z}_1^{(2)} + \mathcal{Z}_1^{(3)} =$$
$$= Q^{1,0}(\beta, \lambda) - \sum_{b=1}^{\infty} \left(\log \left(1 - \frac{Q_b^{(0,2)}(\lambda, \beta)}{v_b(\beta)} \right) + \log v_b(\beta) \right) =$$

[14]as is the case for a string theory below the Hagedorn temperature.

47
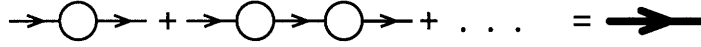
Figure 2-9: The dark thick line represents the re-summed propagator $\mathcal{G}_b = \frac{1}{v_b - Q_b^{(0,2)}}$.
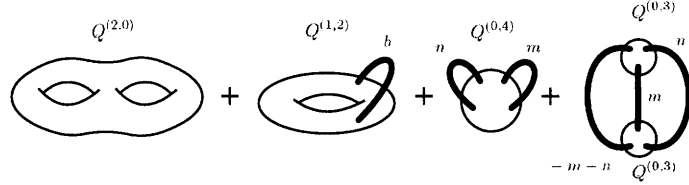
Figure 2-10: Vortex diagrams contributing to $\mathcal{Z}_2$. All this diagrams have genus $h = 2$ if we consider the re-summed propagator as adding an extra handle to the diagrams

$$= Q^{1,0}(\beta, \lambda) - \sum_{b=1}^{\infty} \log \left(v_b(\beta) - Q_b^{(0,2)}(\lambda, \beta) \right) . \tag{2.53}$$

It should be clear from the above discussion of $\mathcal{Z}_1^{(3)}$ that $Q_b^{(0,2)}$ should not really be treated as a vertex. Rather all $Q_b^{(0,2)}$ should be re-summed along with the propagators $\frac{1}{v_b(\beta)}$ to obtain a "re-summed propagator" for each vortex number

$$\mathcal{G}_b(\beta) = \sum_{n=1}^{\infty} \frac{1}{v_b^n(\beta)} (Q_b^{(0,2)})^n = \frac{1}{v_b - Q_b^{(0,2)}} \tag{2.54}$$

as shown diagrammatically in Fig. 2-9. Note that Eq. (2.53) can be rewritten in terms of $\mathcal{G}_b$ as

$$\mathcal{Z}_1 = Q^{1,0}(\beta, \lambda) + \sum_{b=1}^{\infty} \log \mathcal{G}_b(\beta) . \tag{2.55}$$

In the vortex diagrams for $\mathcal{Z}_g$ with $g \geq 2$, only re-summed propagators $\mathcal{G}_b$ appear. As an example, the vortex diagrams contributing to $\mathcal{Z}_2$ are shown in Fig. 2-10. Higher order diagrams contributing to general $\mathcal{Z}_g$ can be similarly constructed.

2.6.1 Critical behavior and the effective action

Now let us examine the critical behavior of Eq. (2.51) by increasing the temperature from zero.

48

In free theory, as reviewed after equation Eq. (2.38), there is a critical temperature given by equation $V_1(\beta_H) = 1$ at which the free energy diverges as $\log Z_0 \approx -\log(\beta - \beta_H)$. Note that there is *only* a one-loop divergence since all perturbative corrections in $1/N$ to Eq. (2.38) vanish.

In the interacting theory the effective vertices $Q^{(h,n)}$ should be regular at any temperature since they involve only sums of products of Eq. (2.7) and their images. The divergences of $\mathcal{Z}_n$ then can only occur when the re-summed propagator $\mathcal{G}_b(\beta)$ Eq. (2.54) become divergent, which happens when

$$v_b(\beta) = Q_b^{(0,2)}(\lambda, \beta), \qquad \text{i.e.} \qquad \frac{1 - V_b(\beta)}{b} = Q_b^{(0,2)}(\lambda, \beta), \qquad b = 1, 2 \cdots . \qquad (2.56)$$

If we again assume that Eq. (2.56) is first satisfied for $b = 1$ as one decreases β from infinity[15], the critical temperature in the interacting theory is determined by

$$V_1(\beta_H(\lambda)) = 1 - Q_1^{(0,2)}(\lambda, \beta_H(\lambda)) \qquad (2.57)$$

with the most divergent term in $\mathcal{Z}_1$ given by (see 2.53)

$$\mathcal{Z}_1 \approx -\log(\beta - \beta_H(\lambda)) + \text{finite}, \qquad \beta \sim \beta_H(\lambda) . \qquad (2.58)$$

The most divergent contribution to $\mathcal{Z}_n$ can be obtained counting the maximal number of divergent propagators at T_H. We will now prove that the most divergent contribution to $\mathcal{Z}_n$ as $\beta \to \beta_H$ is given by

$$\frac{1}{(\beta - \beta_H)^{2(n-1)}} . \qquad (2.59)$$

Denote $V^{(p,q)}$ as the number of $Q^{(p,q)}$ in a diagram. Then the total number of re-

---

[15]which should be the case for λ small since $Q_b^{(0,2)}$ starts at order $O(\lambda)$. For large λ, in principle this does not appear to be guaranteed from the gauge theory point of view. However, from string theory it appears always to be the case that the lowest winding modes become massless first.

summed propagators and the genus g of the diagram can be written as

$$2L = \sum_{p,q} qV^{(p,q)}, \qquad g = 1 + \sum_{p,q} \left(\frac{q}{2} + p - 1\right) V^{(p,q)} . \tag{2.60}$$

The second equation of Eq. (2.60) can be obtained by thinking of each vortex propagator as adding a "handle" to the diagram and therefore increasing the genus by one. Then the total genus will depend on the genus of the various "blobs" in the diagram (p) and on the various "handles" connecting them (q). It is also convenient to introduce

$$V = \sum_{p,q} V^{(p,q)}, \qquad g_a = \sum_{p,q} pV^{(p,q)}, \tag{2.61}$$

where V is the total number of vertices, g_a is the apparent genus of the diagram (i.e. the sum of the genus of each vertex). Equations Eq. (2.60) and Eq. (2.61) lead to

$$L - (V - 1) = g - g_a . \tag{2.62}$$

Since vortex numbers carried by propagators have to be conserved at each vertex, Eq. (2.62) implies that the total number of independent vortices in a diagram is $g - g_a$. The maximal number of independent vortices among different degenerate limits is then g, in which cases each vertex has the topology of a sphere.

From Eq. (2.60) and Eq. (2.61), we also have

$$V = \frac{1}{2}L - \frac{1}{4}\sum_{p,q}(q - 4)V^{(p,q)} \tag{2.63}$$

and Eq. (2.63) and Eq. (2.62) lead to

$$L = 2(g - 1) - \sum_{p,q}(2p + \frac{q}{2} - 2)V^{(p,q)}. \tag{2.64}$$

Eq. (2.64) implies that the maximal number of re-summed propagators is indeed $3g - 3$, obtained when only $Q^{(0,3)}$ appear in a diagram. However, it is impossible to have all $3g - 3$ propagators to be divergent at the same time, i.e. to have all vortex

numbers to be ± 1, since by vortex number conservation if the vortex numbers of two of the propagators coming out of a 3-point vertex are ± 1, then the third one can only be ± 2.

Since at least one of the propagators going out of a 3-point vertex must have vortex number $|b| \neq 1$, if our purpose is to find the *maximum* number of propagators that can have $b = \pm 1$, one can ignore such a propagator. This implies we only need to consider those diagrams in which every vertex has at least four insertions, i.e. $m \geq 4$. Ignoring $V^{(0,3)}$ for the purpose of finding the leading divergence, equation Eq. (2.64) implies that

$$L \leq 2(g - 1) \tag{2.65}$$

where the equality holds when

$$V^{(0,4)} \neq 0, \qquad \text{otherwise } V^{(p,q)} = 0 \ . \tag{2.66}$$

Thus we have proven that the most divergent term is of the form Eq. (2.59).

Furthermore, since the construction of vortex diagrams follows the standard combinatoric rules of Feynman diagrams, we find that the most divergent pieces at each $1/N^{2h}$ order is precisely given by the expansion of

$$
\begin{aligned}
F_{sing} &= \log \int d\phi d\phi^* \, e^{-m_\phi^2 \phi\phi^* - \frac{\lambda_4}{N^2}(\phi\phi^*)^2} \\
&= -\log(\beta - \beta_H) - 2\frac{\lambda_4}{m_\phi^4 N^2} + 10\frac{\lambda_4^2}{N^4 m_\phi^8} + \cdots
\end{aligned}
\tag{2.67}
$$

with ϕ is a c-number. with the identification

$$m_\phi^2 = v_1(\beta) - Q_1^{(0,2)}(\lambda, \beta), \qquad \frac{\lambda_4}{N^2} = Q_{1,1,-1,-1}^{(0,4)} + \frac{1}{v_2(\beta) - Q_2^{(0,2)}} Q_{1,1,-2}^{(0,3)} Q_{-1,-1,2}^{(0,3)} \tag{2.68}$$

where the subscripts in $Q^{(h,n)}$ denote the vortex numbers for each leg. Notice that the four point coupling constant λ_4 will indeed contain a pair of $Q^{(0,3)}$ connected by a propagator regular at β_H. Eq. (2.68) is exactly the behavior of a complex scalar field with mass m_ϕ in $0 + 1$-dimensions. It is important to emphasize that our discussion

above should also apply to strong coupling. $Q^{(n,m)}(\lambda)$, which are the basic building blocks of the vortex diagrams, can be defined non-perturbatively as follows. Since at each genus the number of Feynman diagrams grows with loops only as a power, we expect that $Q^{(n,m)}(\lambda)$ should have a finite radius of convergence in the complex λ plane. Once one obtains $Q^{(n,m)}(\lambda)$ near the origin, one can analytically continue them to strong coupling.

2.7   Summary and outlook

In this chapter we studied the large N expansion of a generic field theory with fields in the adjoint representation at some finite temperature $T < T_H$. We proved an "inheritance principle" satisfied by correlation function at planar level. We also considered sub-leading corrections to correlation functions and to the partition function and we showed that at finite temperature new ingredients arise. The large N expansion contains corrections due to the usual genus expansion and corrections due to sub-leading order contributions in the integrals over Wilson lines U. Close to the critical temperature T_H we can identify the diagrams contributing to the leading divergence. We then argued, from the diagrammatical expansion, that the leading divergence close to T_H can be re-summed and expressed in terms of a simple integral Eq. (2.67), similar in structure to a scalar $\lambda\phi^4$ theory. In the next chapter we are going to analyze the critical behavior of string theory close to the Hagedorn transition, and we are going to find the string theory interpretation of the results in this chapter.

Chapter 3

String theory amplitudes, Hagedorn transition and tachion potential

3.1 Outline

Since the early days of string theory, it was observed that the free string spectrum has a density of states which grows exponentially with energy, and that the partition function $Z = e^{-\beta H}$ of a free string gas at a temperature $T = \frac{1}{\beta}$ would diverge when T is greater than some critical value T_H [36, 39, 30]. The Hagedorn divergence occurs for all known (super)string theories with spacetime dimensions greater than two. The physical meaning of the critical temperature T_H and of the divergence has been a source of much discussion since then.

In the late eighties, a few important observations were made which suggested that the Hagedorn divergence signals a phase transition, analogous to the deconfinement transition in QCD [67, 44, 56, 7]. At the Hagedorn temperature T_H the lowest winding modes (with winding ± 1) around the periodic Euclidean time direction become marginal operators in the world-sheet conformal field theory [67, 44, 56]. Sathiapalan and Kogan [67, 44] argued that above the Hagedorn temperature, the winding modes

would condense in a fashion similar to the Kosterlitz-Thouless transition in the $X - Y$ model and the world-sheet theory will flow to a new infrared fixed point. From the spacetime point of view, these winding modes (with winding ± 1) correspond to a complex scalar field ϕ living in one fewer spacetime dimension (i.e. not including Euclidean time). Near the Hagedorn temperature, the spacetime effective potential for ϕ can be written in a form

$$V = m_\phi^2(\beta)\phi^*\phi + \lambda_4 g_s^2(\phi^*\phi)^2 + \lambda_6 g_s^4(\phi^*\phi)^3 + \cdots , \qquad m_\phi^2(\beta) \propto T_H - T . \qquad (3.1)$$

If λ_4 is positive (negative), the phase transition would be second order (first order). In [7] Atick and Witten argued that for a string theory in asymptotic flat spacetime the transition should be first order [1] (i.e. $\lambda_4 < 0$) due to the coupling of the thermal scalar to the dilaton.

The purpose of this chapter is to point out a relation between Hagedorn divergences and the effective potential Eq. (3.1). While the one-loop Hagedorn divergence has been extensively discussed in the past (see e.g. [81, 58] for reviews), Hagedorn divergences from higher genus amplitudes have been investigated rather little. In this chapter we use a factorization argument to extract Hagedorn divergences for higher genus amplitudes. We show that they can be re-summed by introducing various double scaling limits, which smooth the divergences. The double scaling limits also allow one to extract the effective potential Eq. (3.1) to arbitrary high orders. That a double scaling limits might exist for higher genus Hagedorn divergences was speculated earlier in [50] and further discussed in [6] in a toy model motivated from AdS/CFT.

Our discussion further highlights that Hagedorn divergences signal a breakdown of string perturbation theory due to appearance of massless modes and do not imply a limiting temperature for string theory [67, 44, 7].

The discussion of this chapter will be rather general, e.g. applicable to string theories in asymptotic anti-de Sitter (AdS) spacetime. The AdS/CFT correspondence then implies that the critical Hagedorn behavior from high genera and the relation

---

[1]That the transition is of first order can also be argued from the non-perturbative instability of the thermal flat spacetime discovered in [32].

with the effective potential should also arise from Yang-Mills theories.

In the previous chapter we showed that the free energy of Yang-Mills theory contains "vortex" contributions at finite temperature. In this chapter we show that Yang-Mills Feynman diagrams with vortices can be identified with contributions from the boundary of the moduli space on the string theory side.

The plan of the chapter is as follows. In section 3.2.1 we first review the one-loop result and discuss the physical set-up of our calculation. We then extract the critical Hagedorn behavior from higher genus amplitudes and show that one can find terms in Eq. (3.1) by defining suitable double scaling limits. In section 3.3 we turn to the comparison with Yang-Mills theory. We conclude in section 3.3 with a discussion of some physical implications.

Parts of this chapter have been published in [13].

3.2 High-loop Hagedorn divergences in perturbative string theory

3.2.1 Review of one-loop divergence and set-up

Consider a string theory consisting of a compact CFT times $\mathbf{R}^{1,d}$. The one-loop free energy of the system at a finite temperature can be computed by the torus path integral with a target space in which the Euclidean time direction is compactified with period $\beta = \frac{1}{T}$ and with anti-periodic boundary condition for spacetime fermions [59]. The Hagedorn singularity appears when the lowest modes with winding ± 1 around the compactified time direction become massless [56, 67, 44]. More explicitly, the mass square can be written as

$$m_\phi^2(\beta) = \left(\frac{\beta}{2\pi\alpha'}\right)^2 - c_0 \equiv \left(\frac{\beta}{2\pi\alpha'}\right)^2 - \left(\frac{\beta_H}{2\pi\alpha'}\right)^2 \tag{3.2}$$

where the first term is the winding contribution and c_0 is the zero point energy of the string (in the winding sector). The second equality of Eq. (3.2) should be considered as

a definition of the Hagedorn temperature. From Eq. (3.2), $m_\phi^2(\beta) \to 0$ as $\beta \to \beta_H$ and becomes tachyonic when $\beta < \beta_H$. In spacetime, the winding ± 1 modes correspond to a complex scalar field ϕ living in one fewer spacetime dimension (i.e. spatial part of the spacetime), which is often called the thermal scalar in the literature. We will follow this terminology below. We will also collectively call modes with general winding numbers (and no internal excitations) winding tachyons. Equation Eq. (3.2) applies to both bosonic and superstring theories with possibly different c_0 for different theories.

The critical behavior of the one-loop free energy F_1 as $\beta \to \beta_H$ is controlled by that of the thermal scalar

$$F_1 = -2 \times \frac{1}{2} \log(-\nabla^2 + m_\phi^2(\beta)) + F_{finite}, \qquad \beta \to \beta_H \qquad (3.3)$$

where ∇^2 is the Laplacian on the *spatial* manifold. If the gap of ∇^2 along the compact CFT directions is bigger than $m_\phi^2(\beta)$, the singular part of Eq. (3.3) can be further written as

$$F_1 \quad \propto -\int \frac{d^d k}{(2\pi)^d} \log(k^2 + m_\phi^2(\beta)) + \cdots$$
$$\propto \begin{cases} (m_\phi^2(\beta))^{\frac{d}{2}} & d \quad \text{odd} \\ (m_\phi^2(\beta))^{\frac{d}{2}} \log m_\phi^2(\beta) & d \quad \text{even} \end{cases} \qquad (3.4)$$

F_1 has a branch point singularity at $m_\phi^2(\beta) = 0$ for all d. In particular, for $d = 0$ it is logarithmically *divergent* as $\beta \to \beta_H$

$$F_1 = -\log(\beta - \beta_H) + \text{finite} . \qquad (3.5)$$

The above discussion should also apply to a static curved spacetime, for example in *AdS* spacetime, even though an explicit computation of the one-loop free energy is often not possible. For an *AdS* spacetime, since the Laplacian has a mass gap, we expect the free energy for a thermal gas of *AdS* strings should behave as Eq. (3.5) when the Hagedorn temperature is approached (see e.g. [48] for further discussion).

In this paper we will focus our discussion on $d = 0$ or more generally those space-times (including *AdS*) in which Eq. (3.5) is satisfied, for the following reasons:

1. The thermal ensemble cannot be defined in an uncompact asymptotically flat spacetime due to Jeans instability. To make the canonical ensemble well defined, an Infrared (IR) cutoff is needed. One particularly convenient (and well-defined) IR regulator is to introduce a small negative cosmological constant[2]. For our discussion below the precise nature of such a regulator will not be important as far as it makes the thermal ensemble well defined. Such IR regulators introduce a gap in the Laplacian ∇^2, which will be kept fixed in the limit $T \to T_H$ and thus will be greater than m_ϕ^2 when the temperature is sufficiently close to T_H.

2. The Hagedorn singularity is sharpest at $d = 0$. While the free energy is singular at $\beta = \beta_H$ for all dimensions, it is divergent only for $d = 0$.

The logarithmic divergence of Eq. (3.5) at $\beta \to \beta_H$ implies that the string perturbation theory breaks down *before* $\beta = \beta_H$ is reached. Thus it is not sufficient to consider only the one-loop contribution to the free energy and higher genus contributions could be important. Below we will show that as $\beta \to \beta_H$, it is necessary to re-sum the string perturbation theory to all orders. We will then show that one can extract the spacetime effective action for the thermal scalar from the re-summed series and that the divergences are smoothed out.

When λ_4 in Eq. (3.1) is negative, i.e. when the transition is first order, there exists a lower temperature $T_c < T_H$, at which the thermal gas of strings becomes metastable. At a temperature $T_c < T < T_H$, the thermal gas is still perturbatively stable. Here we are interested in probing the critical behavior in

---

[2]In an asymptotic *AdS* spacetime it is possible to define a canonical ensemble in the presence of gravity, as discovered by Hawking and Page [37]. Hawking and Page also found that the system undergoes a first order phase transition at a temperature T_{HP} from a thermal gas in *AdS* to a stable black hole. Treating an *AdS* spacetime with a small cosmological constant as an IR regularization of the flat spacetime, it is natural to identify the first order phase transition argued by [7] with the Hawking-Page transition. Note that the flat space limit, which corresponds to keeping g_s small, but fixed and taking the curvature radius of *AdS* to infinity, is rather subtle. In this limit the stable black hole phase in *AdS* disappears and the Jeans instability should develop at a certain point.
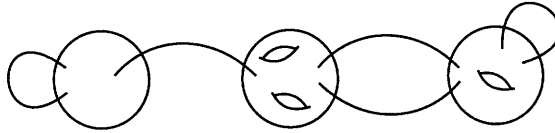
Figure 3-1: An example of a degenerate genus-6 Riemann surface. Each blob represents a surface of certain genus and thin lines connecting blobs represent pinched cycles.
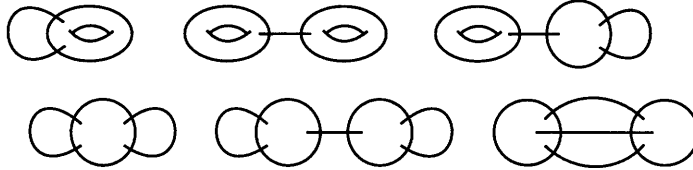
Figure 3-2: Degenerate limits of a genus-2 Riemann surface. Notice that the 2nd, 3rd and 5th diagrams here did not appear in Figure 2-10, since they contain propagators which have zero windings

the metastable phase (or superheated phase) as $T \to T_H$ from below.

3.2.2 Higher loop divergences

We now examine higher loop divergences as $\beta \to \beta_H$. For simplicity we will restrict our discussion to bosonic strings. We expect the conclusion to hold for superstring theories as well.

The genus-g contribution F_g to the free energy is obtained by integrating the single string partition function on a genus-g surface over the moduli space $\mathcal{M}_g$ of such surfaces. The potentially divergent contributions to F_g arise from the integration near the boundary of the moduli space.

The boundary Δ_g of $\mathcal{M}_g$ is where a Riemann surface degenerates, which can be described by pinching cycles on the surface (for reviews see e.g. [25, 8, 58]). There are two types of basic degenerations depending on whether the pinched cycle is homologous to zero or not. If the pinched cycle is homologous to zero, a surface of genus g degenerates into two surfaces of genus g_1 and g_2 ($g = g_1 + g_2$) which are joined together at a point. If the pinched cycle is not homologous to zero, a genus g surface

58

degenerates into a surface of genus $g - 1$ with two points glued together. One can pinch more than one cycle at the same time as far as they do not intersect with each other. On a genus g surface, the maximal number of non-intersecting closed geodesics is $3g - 3$, so one can pinch at most $3g - 3$ cycles at the same time. See Fig. 3-1 and Fig. 3-2 for examples of degenerate limits.

Let us now examine the contribution to F_g from boundaries of moduli space. The pinching of a Riemann surface can be described in terms of cutting open the path integral on the surface. The pinching is a local operation and so is cutting the path integral (other than possible constraints from the zero mode integration). We follow the standard procedure as described in [58]. One has

$$\langle 1 \rangle_g = \sum_i q^{h_i} \bar{q}^{\bar{h}_i} \langle \mathcal{A}_i(z_1) \rangle_{g_1} \langle \mathcal{A}_i(z_2) \rangle_{g_2} \tag{3.6}$$

and

$$\langle 1 \rangle_g = \sum_i q^{h_i} \bar{q}^{\bar{h}_i} \langle \mathcal{A}_i(z_1) \mathcal{A}_i(z_2) \rangle_{g-1} \tag{3.7}$$

for the two types of basic degenerations, where $\langle \cdots \rangle_g$ denote world-sheet correlation functions on a genus g surface and i sums over a complete set of intermediate states. q can be considered as the complex coordinate transverse to the boundary with $q \to 0$ corresponding to the degeneration limit. Integration of Eq. (3.6) and Eq. (3.7) near $q \to 0$ yields the propagator

$$G = \sum_i \frac{8\pi}{\alpha'(-\nabla^2 + m_i^2)} \ . \tag{3.8}$$

The contribution to the free energy from boundaries of moduli space can be extracted from diagrams like the ones in Fig. 3-1 and Fig. 3-2. One can treat blobs (representing surfaces of certain genus with some insertions) as effective vertices and thin lines (pinched cycles) as propagators. For $\beta \to \beta_H$ and assuming that the spatial Laplacian operator $-\nabla^2$ has a gap, then the propagator Eq. (3.8) for a pinched cycle
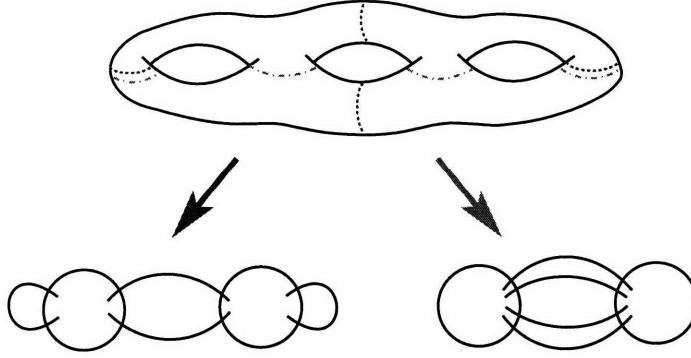
Figure 3-3: Two possible degenerate limits of a genus-3 Riemann surface which give rise to most divergent contributions. Each propagator has the thermal scalar running through it.

is potentially dominated by that of the thermal scalar[3],

$$G \approx \frac{8\pi}{\alpha' m_\phi^2(\beta)} + \text{finite} \propto \frac{1}{\beta - \beta_H} + \cdots , \quad \beta \to \beta_H \tag{3.9}$$

Since one can pinch at most $3g - 3$ cycles at the same time, naively we may conclude from Eq. (3.9) that F_g diverges as $\frac{1}{(\beta-\beta_H)^{3g-3}}$ for $g \geq 2$ as $\beta \to \beta_H$. However, there are global constraints due to winding number conservation at each blob of Fig. 3-1 and Fig. 3-2. As a result, not all propagators can have the nearly-massless thermal scalar propagating through them. Using exactly the same discussion as in section 2.6.1, we can show that the most divergent terms at genus g are proportional to

$$\frac{1}{(\beta - \beta_H)^{2g-2}} \qquad g \geq 2 , \tag{3.10}$$

and happens when only $V^{(0,4)} \neq 0$, where $V^{(g,m)}$ is the number of vertices with genus g and m insertions.

See Fig. 3-3 for degenerations which give rise to the most divergent contributions

---

[3]Note that it is not immediately obvious that the thermal scalar (or other winding modes along the Euclidean time direction) appears in the intermediate states from the point of view of calculating the free energy of a finite temperature string gas, since they do not correspond to spacetime physical states. Indeed in the one-loop calculation, they appear only after a modular transformation. However, it is clear that they should appear in the intermediate states from the point of view that we are working with a string theory compactified on a circle with anti-periodic boundary condition for fermions.

at genus 3.

To summarize, the most divergent contributions at each genus have the following diagrammatic structure:

1. Each vertex has the topology of a sphere and has four winding tachyon operator insertions with winding numbers $1, 1, -1, -1$ respectively. The total number of vertices in a genus g diagram is $g - 1$. The path integral over each vertex gives rise to an effective coupling

$$g_s^2 \tilde{\lambda}_4 = \langle \mathcal{V}_{+1}(0) \mathcal{V}_{+1}(1) \mathcal{V}_{-1}(\infty) \int d^2 z \, \mathcal{V}_{-1}(z) \rangle_{S^2} \qquad (3.11)$$

Note that at $\beta = \beta_H$, the vertex operators $\mathcal{V}_{\pm 1}$ for the thermal scalar are marginal and Eq. (3.11) is well defined. Also $\tilde{\lambda}_4$ is g_s-independent.

2. The propagators are given by that of the winding tachyon 3.9. The total number of propagators is $2(g - 1)$.

Thus vortex diagrams correspond to a specific decomposition of the boundary of the moduli space and can be considered as defining an effective string field theory for the winding tachyon modes. Thus the most divergent contribution to the free energy at genus-$(n + 1)$ has the form

$$a_n g_s^{2n} \tilde{\lambda}_4^n \left(\frac{8\pi}{\alpha' m_\phi^2(\beta)} \right)^{2n} \propto \frac{g_s^{2n}}{(\beta - \beta_H)^{2n}} \qquad (3.12)$$

where a_n is a combinatoric numerical factor depending on the specific geometric structure of boundaries of moduli space. Determining these numerical factors from direct world-sheet computation is a rather complicated mathematical question, which goes beyond the scope of this paper. Below we will determine them using an indirect argument. By now readers may have recognized the resemblance of vortex diagrams with the diagrams in Fig. 3-1 and in Fig. 3-2. Indeed it is natural to identify vortex diagram contributions in the gauge theory with contributions from degenerate limits of string world-sheets in the corresponding string theory. For example, diagrams

in Fig. 2-10 can be identified with various degenerate limits (Fig. 3-2) of genus two Riemann surfaces. In particular, vortices in gauge theory vortex diagrams can be identified with insertions of winding tachyon modes in the world-sheet. On the world-sheet if one follows a closed contour around the vertex operator of a winding tachyon mode of winding number b, the Euclidean time circle is traversed b times. Similarly, as discussed in the previous chapter, if a face of a Feynman diagram contains a vortex with vortex number b, the propagators bounding the face wrap around the Euclidean time circle b times.

A more careful comparison between vortex diagrams for $\mathcal{Z}_g$ and degenerate limits of a genus-g surface (e.g. between Fig. 2-10 and Fig. 3-2) also show some important differences:

1. Notice that the 2nd, 3rd and 5th diagrams in Fig. 3-2 do not appear in Fig. 2-10. These diagrams are distinguished in that some propagators are forced to have zero winding due to winding number conservation. One can convince oneself that this feature persists to all orders. Thus YM vortex diagrams do not correspond to the full contributions from degenerate limits of a Riemann surface. All propagators in the YM vortex diagrams carry nonzero windings.

2. Various degenerate limits of a Riemann surface do not follow the standard Feynman rules and cannot be treated as Feynman diagrams. For example, the third diagram of Fig. 3-2 can be obtained as a degenerate limit of the first diagram and the fifth as a limit of the fourth, etc. In contrast, the vortex diagrams we constructed in Yang-Mills theory do follow standard Feynman rules. In particular, different diagrams in Fig. 2-10 do not overlap.

3.2.3 Double scaling limits and the effective thermal scalar action

In the last subsection we showed that the leading order Hagedorn divergences at all loop orders can be written as

$$F_{sing} = -\log(\beta - \beta_H) + a_1 \frac{\lambda_4 g_s^2}{m_\phi^4} + \cdots + a_n \left(\frac{g_s^2 \lambda_4}{m_\phi^4}\right)^n + \cdots \tag{3.13}$$

with

$$\lambda_4 = \tilde{\lambda}_4 \left(\frac{8\pi}{\alpha'}\right)^2, \qquad m_\phi^2 \approx \frac{\beta_H}{2\pi^2 \alpha'}(\beta - \beta_H) . \tag{3.14}$$

Equation Eq. (3.13) suggests a double scaling limit

$$\beta - \beta_H \to 0, \qquad g_s \to 0, \qquad \frac{\beta - \beta_H}{g_s} = \text{finite} \tag{3.15}$$

in which case all higher order terms in the series become equally important and we need to be re-summed.

How do we interpret the free energy F obtained by re-summing the series? A clue comes from the structure of the degenerate diagrams summarized at the end of the last subsection, which resemble the Feynman diagrams of a $|\phi|^4$ theory (see e.g. Fig. 3-3). Indeed the free energy of a $|\phi|^4$ theory gives an asymptotic expansion which is precisely of the form Eq. (3.13) with specific values for the numerical coefficients a_n. Given that string theory should reduce to a field theory in the low energy limit, and that here we are essentially isolating an effective theory for the nearly-massless thermal scalar, it is natural to conjecture that Eq. (3.13) can be written as

$$\begin{aligned} F_{sing} &= \log \int d\phi d\phi^* \, e^{-m_\phi^2 \phi \phi^* - g_s^2 \lambda_4 (\phi \phi^*)^2} \\ &= -\log(\beta - \beta_H) - 2\frac{g_s^2 \lambda_4}{m_\phi^4} + 10\frac{g_s^4 \lambda_4^2}{m_\phi^8} + \cdots \end{aligned} \tag{3.16}$$

with ϕ is a c-number. Equation Eq. (3.2.3) determines a_n to all orders uniquely and

implies the following effective potential for the thermal scalar

$$V = m_\phi^2 \phi\phi^* + \lambda_4 g_s^2 (\phi\phi^*)^2 + \cdots . \tag{3.17}$$

In the past chapter we showed that the effective action Eq. (3.17) and Eq. (3.2.3) arises from the critical behavior of Yang-Mills theories near the Hagedorn temperature. The discussion in this chapter has used only fundamental properties of string theory amplitudes, and we expect it to apply also to string theory on *AdS* background. Using *AdS/CFT* the field theory calculation would serve as a proof of Eq. (3.2.3) for string theories in an asymptotic *AdS* spacetime. Furthermore, since the factors a_n in Eq. (3.12) and Eq. (3.13) depend only on the mathematical structure of the moduli space of Riemann surfaces and not on the specific string theory, the Yang-Mills theory results serve as an indirect proof of Eq. (3.2.3).

It is clear from equation Eq. (3.2.3) that Hagedorn divergences at each genus order in Eq. (3.13) simply signal breakdown of the asymptotic expansion in g_s due to that ϕ becomes massless. The $m_\phi \to 0$ limit is apparently smooth in the re-summed integral expression Eq. (3.2.3). When λ_4 is positive, i.e. when the transition is second order, the integral Eq. (3.2.3) is finite and non-perturbatively defined. For negative (or zero) λ_4, i.e. when the transition is first order, the integral Eq. (2.67) is not defined non-perturbatively and higher order terms in the effective potential are needed. In either cases the $m_\phi \to 0$ limit is well-defined.

Eq. (3.2.3) implies that $a_n \sim n!$ for n large. This is in contrast with the $(2n)!$ growth of the asymptotic behavior for the full free energy. Here we are only looking at contributions from boundaries of moduli space, which accounts for the slower growth.

Here we have been focusing on the lowest spacetime mode[4] of the thermal scalar, which gives the most divergent contribution to the free energy. This explains the finite-dimensional integral in Eq. (3.2.3). From general covariance it seems natural

---

[4]Recall that we assume that the Laplacian of the spacetime manifold has a mass gap.

to generalize Eq. (3.17) to include derivatives

$$S = \int d^d x \sqrt{g} \left(|\partial \phi|^2 + m_\phi^2 \phi \phi^* + \lambda_4 g_s^2 (\phi \phi^*)^2 + \cdots \right) . \tag{3.18}$$

where $d^d x$ integrates over the spatial directions[5].

Let us now consider the generalization of the above double scaling argument to extract higher orders terms in Eq. (3.17). From equation Eq. (2.60) the leading contribution of a generic degenerate surface to the free energy can be written in the form

$$\frac{g_s^{2g-2}}{(\beta - \beta_H)^L} = \frac{g_s^{\sum_{n,k} V^{(n,2k)}(2n+2k-2)}}{(\beta - \beta_H)^{\sum_{n,k} k V^{(n,2k)}}} \tag{3.19}$$

where in writing down Eq. (3.19) we have assumed that all propagators in a degenerate diagram carry winding numbers[6] ± 1 and that each vertex contains an even number of insertions $m = 2k, k = 2, 3, \cdots$, due to winding number conservation. Now consider the double scaling limit

$$\frac{(\beta - \beta_H)}{g_s^a} = \text{finite}, \qquad g_s \to 0 \tag{3.20}$$

under which Eq. (3.19) is proportional to g_s^K with K given by

$$K = \sum_{n=0}^{\infty} \sum_{k=2}^{\infty} V^{(n,2k)}(2n + 2k - 2 - ka) . \tag{3.21}$$

For $a < 1$, we always have $K > 0$ for any choice of $V^{(n,2k)}$. At $a = 1$, we get $K = 0$ for diagrams with $V^{(0,4)} \neq 0$ only while $K > 0$ for all other diagrams. In the double scaling limit Eq. (3.20) only the contributions of diagrams with $K = 0$ survive. These are the most divergent contributions we isolated in Eq. (3.13) and lead to the effective action Eq. (3.17). Now let us set by hand $\lambda_4 = 0$, then in Eq. (3.21), $V^{(0,4)} = 0$. The

---

[5]Note that for an *AdS* with a small negative cosmological constant, Eq. (3.18) applies to regions in the interior of the spacetime, since in *AdS* g_{tt} component of the metric is nontrivial and the thermal scalar always has a large mass near the boundary.

[6]If there is a propagator carrying a winding number other than ± 1, we can treat the two vertices connected by this propagator as a single effective vertex. Keeping doing this we obtain a degenerate diagram whose propagators only carry winding numbers ± 1.

most divergent contributions in the remaining diagrams are isolated by taking $a = \frac{4}{3}$, at which $K = 0$ for diagrams with $V^{0,6} \neq 0$ only and $K > 0$ for all the rest. In other words now the most divergent contributions to the free energy can be written as

$$F = -\log(\beta - \beta_H) + \frac{c_1 g_s^2}{(\beta - \beta_H)^{\frac{3}{2}}} + \cdots + \frac{c_n g_s^{2n}}{(\beta - \beta_H)^{\frac{3n}{2}}} + \cdots \qquad (3.22)$$

which implies the effective potential

$$V = m_\phi^2 \phi\phi^* + \lambda_6(\phi\phi^*)^3 + \cdots \qquad (3.23)$$

where λ_6 is related to the genus-0 six-point function of the vertex operators for the thermal scalar on the world-sheet. Now restoring λ_4 and combining Eq. (2.67) and Eq. (3.23) we would conclude that the effective potential can be written as

$$V = m_\phi^2 \phi\phi^* + \lambda_4(\phi\phi^*)^2 + \lambda_6(\phi\phi^*)^3 + \cdots \qquad (3.24)$$

The same procedure can then be repeated to the next order by first setting λ_4 and λ_6 to zero and then extracting the most divergent terms in the remaining diagrams. One can continue this to arbitrary orders in $(\phi\phi^*)^n$ and we find the effective potential[7]

$$V = m_\phi^2 \phi\phi^* + \sum_{k=2}^{\infty} \lambda_{2k} g_s^{2k-2}(\phi\phi^*)^k + \cdots \qquad (3.25)$$

The λ_{2k} term is obtained by setting all vertices with $m < 2k$ to zero and performing the scaling $\beta - \beta_H \sim g_s^{2(1-\frac{1}{k})}$, i.e. $a = 2(1 - \frac{1}{k})$ in Eq. (3.20).

Finally let us consider how to define various $\lambda_6, \lambda_8, \cdots$ from string amplitudes. Recall that λ_4 can be obtained from Eq. (3.11) and Eq. (3.14). Naively one might want to define λ_{2k} for $k = 3, 4, \cdots$ by the *tree-level* amplitudes of k winding 1 and k winding -1 modes. However, from factorization argument, these amplitudes are

---

[7]Note that the procedure is not well adapted to re-sum divergences due to vertices with genus $n \geq 1$. From Eq. (3.21), to have $K = 0$ for $n = 1$, we need $a = 2$, in which case all genus 1 vertices with arbitrary number of insertions contribute equally. To have $K = 0$ for $n > 1$, we need $a > 2$, then from Eq. (3.21), diagrams with large k become more dominant regardless of the value of n.

divergent at $m_\phi^2 = 0$. The divergences come from diagrams containing lower order vertices $\lambda_{2k'}$ with $k' < k$ and ϕ in the internal propagators, which can be found from standard Feynman diagrams for the action $m_\phi^2 \phi \phi^* + \sum_{k'=2}^{k-1} \lambda_{2k} g_s^{2k-2} (\phi \phi^*)^k$. λ_{2k} is thus given by the sphere amplitude of k winding 1 and k winding -1 modes with the divergent parts subtracted.

3.3 Comparison with the gauge theory expansion and comments

As we mentioned above our discussion should also apply to type IIB string theory in $AdS_5 \times S_5$ or other string theories in asymptotic AdS spacetime. In an AdS spacetime with curvature radius R much bigger than the string and Planck lengths, there is a first order Hawking-Page transition at temperature $T_{HP} \sim \frac{1}{R}$ much below the Hagedorn temperature $T_H \sim \frac{1}{\sqrt{\alpha'}}$ at which the thermal string gas in AdS becomes perturbatively unstable [37]. The discussion of the last section describes what happens if one stays in the superheated thermal AdS phase above the Hawking-Page temperature all the way to the Hagedorn temperature. From the critical behavior at the Hagedorn temperature one can then map out the potential for the thermal scalar.

Hawking and Page's semi-classical discussion applies to IIB string theory in AdS with a cosmological constant small compared to the string scale and to the Planck scale, which corresponds to $\mathcal{N} = 4$ super-Yang-Mills theory on S^3 at strong 't Hooft coupling [51]. At zero and weak 't Hooft coupling, which is dual to a small AdS, thermodynamics of $\mathcal{N} = 4$ SYM theory on S^3 has been discussed in [72, 4]. In the free theory limit the Hagedorn and Hawking-Page temperatures coincide. At weak coupling it is not yet clear whether the transition is of first or second order [4].

To summarize, in this chapter we extracted the Hagedorn divergences to all string loop orders and showed that they can be re-summed. The re-summed amplitudes have the form of an integral over the potential Eq. (3.1) for the thermal scalar and smooth the divergences. We presented arguments both from a world-sheet approach and from

Yang-Mills theories using *AdS/CFT*. In the double scaling limits Eq. (3.20), world-sheets with arbitrary number of thermal scalar insertions become equally important, which is consistent with the expectation that the thermal scalar will condense and the spacetime background will shift.

The fact that one can obtain the thermal scalar potential to arbitrary higher orders by analyzing the local divergences in the thermal string phase is interesting. The potential would enable one to find other possible phases of the theory. The results also give an unambiguous prescription for computing the potential for the thermal scalar near the Hagedorn temperature from string amplitudes. The relation we found between vortex diagrams in Yang-Mills theory at finite temperature and degenerate limits of world-sheet Riemann surfaces is rather intriguing and worth investigating further.

Chapter 4

Viscosity bound and causality violation

4.1 Outline

The *AdS/CFT* correspondence [51, 34, 79, 80] has yielded many important insights into the dynamics of strongly coupled gauge theories. Among numerous results obtained so far, one of the most striking is the universality of the ratio of the shear viscosity η to the entropy density s [61, 46, 17, 45]

$$\frac{\eta}{s} = \frac{1}{4\pi} \tag{4.1}$$

for all gauge theories with an Einstein gravity dual in the limit $N \to \infty$ and $\lambda \to \infty$. Here, N is the number of colors and λ is the 't Hooft coupling. It was further conjectured in [45] that Eq. (4.1) is a universal lower bound (the KSS bound) for all materials. So far, all known substances including water and liquid helium satisfy the bound. The systems coming closest to the bound include the quark-gluon plasma created at RHIC[1] [77, 65, 71, 64, 27] and certain cold atomic gases in the unitarity limit (see e.g. [68]).

---

[1] η/s for pure gluon QCD slightly above the deconfinement temperature has also been calculated on the lattice recently [53] and is about 30% larger than Eq. (4.1). See also [66].

Now, as stated above, the ratio Eq. (4.1) was obtained for a class of gauge theories whose holographic duals are dictated by classical Einstein gravity (coupled to matter). More generally, string theory (or any quantum theory of gravity) contains higher derivative corrections from stringy or quantum effects, inclusion of which will modify the ratio. In terms of gauge theories, such modifications correspond to $1/\lambda$ or $1/N$ corrections. As a concrete example, let us take $\mathcal{N} = 4$ super-Yang-Mills theory, whose dual corresponds to type IIB string theory on $AdS_5 \times S^5$. The leading order correction in $1/\lambda$ arises from stringy corrections to the low-energy effective action of type IIB supergravity, schematically of the form $\alpha'^3 R^4$. The correction to η/s due to such a term was calculated in [18, 9]. It was found that the correction is positive, consistent with the conjectured bound.

In this chapter, instead of limiting ourselves to specific known string theory corrections, we explore the modification of η/s due to generic higher derivative terms in the holographic gravity dual. The reason is partly pragmatic: other than in a few maximally supersymmetric circumstances, very little is known about forms of higher derivative corrections generated in string theory. Given the vastness of the string landscape [26], one expects that generic corrections do occur. Restricting to the gravity sector in AdS_5, the leading order higher derivative corrections can be written as[2]

$$ I = \frac{1}{16\pi G_N} \int d^5x \, \sqrt{-g} \left(R - 2\Lambda + L^2 \left(\alpha_1 R^2 + \alpha_2 R_{\mu\nu} R^{\mu\nu} + \alpha_3 R^{\mu\nu\rho\sigma} R_{\mu\nu\rho\sigma} \right) \right) \; . \quad (4.2) $$

where $\Lambda = -\frac{6}{L^2}$ and for now we assume that $\alpha_i \sim \frac{\alpha'}{L^2} \ll 1$. Other terms with additional derivatives or factors of R are naturally suppressed by higher powers of $\frac{\alpha'}{L^2}$. String loop (quantum) corrections can also generate such terms, but they are suppressed by powers of g_s and we will consistently neglect them by taking $g_s \to 0$ limit.[3] To lowest order in α_i the correction to η/s will be a linear combination of α_i's, and the viscosity bound is then violated for one side of the half plane. Specifically,

---

[2]Our conventions are those of [20].

[3]Note that to calculate g_s corrections, all the light fields must be taken into account. In addition, the calculation of η/s could be more subtle once we begin to include quantum effects.

we will find

$$\frac{\eta}{s} = \frac{1}{4\pi}\left(1 - 8\alpha_3\right) + O(\alpha_i^2) \tag{4.3}$$

and hence the bound is violated for $\alpha_3 > 0$. Note that the above expression is independent of α_1 and α_2. This can be inferred from a field redefinition argument (see section 4.2.3).

How do we interpret these violations? Possible scenarios are:

1. The bound can be violated. For example, this scenario would be realized if one explicitly finds a well-defined string theory on AdS_5 which generates a stringy correction with $\alpha_3 > 0$.

2. The bound is correct (for example, if one can prove it using a field theoretical method), and a bulk gravity theory with $\alpha_3 > 0$ cannot have a well-defined boundary CFT dual.

   (a) The bulk theory is manifestly inconsistent as an effective theory. For example, it could violate bulk causality or unitarity.

   (b) It is impossible to generate such a low-energy effective classical action from a consistent quantum theory of gravity. In modern language we say that the theory lies in the swampland of string theory.

Any of these alternatives, if realized, is interesting. Needless to say, possibility 1 would be interesting. While there is clear evidence that for QCD η/s is bounded from above, recent analyses of η/s from RHIC data [65, 71, 64, 27] are important steps toward being able to bound it from below. This further motivates to investigate the universality of the KSS bound in holographic models.

Possibility 2(a) should help clarify the physical origin of the bound by correlating bulk pathologies and the violation of the bound. Possibility 2(b) could provide powerful tools for constraining possible higher derivative corrections in the string landscape. Note that while there are some nice no-go theorems which rule out classes of non-gravitational effective field theories [1] (also see [2]), the generalization of the

71

arguments of [1] to gravitational theories is subtle and difficult. Thus, constraints from *AdS/CFT* based on the consistency of the boundary theory would be valuable.

In investigating the scenarios above, Gauss-Bonnet gravity will provide a useful model. Gauss-Bonnet gravity, defined by the classical action of the form [82]

$$I = \frac{1}{16\pi G_N} \int d^5x \sqrt{-g} \left[R - 2\Lambda + \frac{\lambda_{GB}}{2} L^2 (R^2 - 4R_{\mu\nu}R^{\mu\nu} + R_{\mu\nu\rho\sigma}R^{\mu\nu\rho\sigma}) \right] , \quad (4.4)$$

has many nice properties that are absent for theories with more general ratios of the α_i's. For example, expanding around flat Minkowski space, the metric fluctuations have exactly the same quadratic kinetic terms as those in Einstein gravity. All higher derivative terms cancel [82]. Similarly, expanding around the *AdS* black brane geometry, which will be the main focus of the paper, there are also only second derivatives on the metric fluctuations. Thus small metric fluctuations can be quantized for finite values of the parameter λ_{GB}.[4] Furthermore, crucial for our investigation is its remarkable feature of solvability: sets of exact solutions to the classical equation of motion have been obtained [11, 19] and the exact form of the Gibbons-Hawking surface term is known [55].

Given these nice features of Gauss-Bonnet gravity, we will venture outside the regime of the perturbatively-corrected Einstein gravity and study the theory with finite values of λ_{GB}. To physically motivate this, one could envision that somewhere in the string landscape λ_{GB} is large but all the other higher derivative corrections are small. One of the main results of the paper is a value of η/s for the *CFT* dual of Gauss-Bonnet gravity, *non-perturbative* in λ_{GB}:[5]

$$\frac{\eta}{s} = \frac{1}{4\pi} [1 - 4\lambda_{GB}]. \quad (4.5)$$

We emphasize that this is not just a linearly-corrected value. In particular, the viscosity bound is badly violated as $\lambda_{GB} \rightarrow \frac{1}{4}$. As we will discuss shortly, λ_{GB} is

---

[4]Generic theories in Eq. (4.2) contain four derivatives and a consistent quantization is not possible other than treating higher derivative terms as perturbations.

[5]We have also computed the value of η/s for Gauss-Bonnet gravity for any spacetime dimension D and the expression is given in Eq. (4.45).

bounded above by $\frac{1}{4}$ for the theory to have a boundary CFT, and η/s never decreases beyond $\frac{16}{25}\frac{1}{4\pi}$ without violating causality.

Given the result Eq. (4.5) for Gauss-Bonnet, if the possibility 2(a) were correct, we would expect that pathologies would become easier to discern in the limit where η/s is small. We will investigate this line of thought in section 4.6.

The plan of the chapter is as follows. In section 4.2, we review various properties of two-point correlation functions and outline the real-time AdS/CFT calculation of the shear viscosity. In section 4.3 we review the black brane geometry and the thermodynamic properties of this background. We then explicitly calculate the shear viscosity for Gauss-Bonnet theory in section 4.4 and section 4.5. In section 4.6, we seek possible pathologies associated with theories violating the viscosity bound. Various appendices are also part of this chapter. In appendix B we consider the black brane solution of Eq. (4.2) and we calculate its thermodynamic properties without doing the field redefinition. We also present an alternative calculation of the entropy density using a compact formula obtained by Wald [78]. In appendix D we present a calculation of the shear viscosity without doing the field redefinition, using the three methods outlined in section 4.2.

Parts of this chapter have been published in [15] and [16].

4.2 Shear viscosity in R^2 theories: preliminaries

4.2.1 Two-Point correlation functions and viscosity

Let us begin by collecting various properties of two-point correlation functions, following [62, 63, 47] (see also [70]). Consider retarded two-point correlation functions of the stress energy tensor $T_{\mu\nu}$ of a CFT in $3 + 1$-dimensional Minkowski space at a finite temperature T

$$G_{\mu\nu,\alpha\beta}(\omega, \vec{q}) = -i \int dt d\vec{x} e^{i\omega t - i\vec{q}\cdot\vec{x}} \theta(t) \langle [T_{\mu\nu}(t, \vec{x}), T_{\alpha\beta}(0, 0)] \rangle. \tag{4.6}$$

They describe linear responses of the system to small disturbances. It turns out that various components of Eq. (4.6) can be expressed in terms of three independent scalar functions. For example, if we take spatial momentum to be $\vec{q} = (0, 0, q)$, then

$$G_{12,12} = \frac{1}{2} G_3(\omega, q), \qquad G_{13,13} = \frac{1}{2} \frac{\omega^2}{\omega^2 - q^2} G_1(\omega, q), \qquad G_{33,33} = \frac{2}{3} \frac{\omega^4}{(\omega^2 - q^2)^2} G_2(\omega, q),$$

$$(4.7)$$

and so on. At $\vec{q} = 0$ all three function $G_{1,2,3}(\omega, 0)$ are equal to one another as a consequence of rotational symmetry.

When $\omega, |\vec{q}| \ll T$ one expects the CFT plasma to be described by hydrodynamics. The scalar functions $G_{1,2,3}$ encode the hydrodynamic behavior of shear, sound, and transverse modes, respectively. More explicitly, they have the following properties:

- G_1 has a simple diffusion pole at $\omega = -iDq^2$, where

$$D = \frac{\eta}{\epsilon + P} = \frac{1}{T} \frac{\eta}{s} \qquad (4.8)$$

with ϵ and s being the energy and entropy density, and P the pressure of the gauge theory plasma.

- G_2 has a simple pole at $\omega = \pm c_s q - i\Gamma_s q^2$, where c_s is the speed of sound and Γ_s is the sound damping constant, given by (for conformal theories)

$$\Gamma_s = \frac{2}{3T} \frac{\eta}{s} \qquad c_s = \frac{1}{\sqrt{3}} \qquad (4.9)$$

- η can also be obtained from $G_{1,2,3}$ at zero spatial momentum by the Kubo formula, e.g.,

$$\eta = \lim_{\omega \to 0} \frac{1}{\omega} \mathrm{Im} G_{12,12}(\omega, 0) \qquad (4.10)$$

Equations (4.8)–(4.10) provide three independent ways of extracting η/s. In the next subsection, we outline how to obtain retarded two-point functions within the framework of the real-time AdS/CFT correspondence.

4.2.2 *AdS/CFT* calculation of shear viscosity: outline

The stress tensor correlators for a boundary *CFT* described by Eq. (4.2) or Eq. (4.4), can be computed from gravity as follows. One first finds a black brane solution (i.e. a black hole whose horizon is $\mathbf{R}^3$) to the equations of motion of Eq. (4.2) or Eq. (4.4). Such a solution describes the boundary theory on $\mathbf{R}^{3,1}$ at a temperature T, which can be identified with the Hawking temperature of the black brane. The entropy and energy density of the boundary theory are given by the corresponding quantities of the black brane. The fluctuations of the boundary theory stress tensor are described in the gravity language by small metric fluctuations $h_{\mu\nu}$ around the black brane solution. In particular, after taking into account various symmetries and gauge degrees of freedom, the metric fluctuations can be combined into three independent scalar fields $\phi_a, a = 1, 2, 3$, which are dual to the three functions G_a of the boundary theory.

To find G_a, one could first work out the bulk two-point retarded function for ϕ_a and then take both points to the boundary of the black brane geometry. In practice it is often more convenient to use the prescription proposed in [69], which can be derived from the real-time *AdS/CFT* correspondence [38]. Let us briefly review it here:

1. Solve the linearized equation of motion for $\phi_a(r; k)$ with the following boundary conditions:

    (a) Impose the infalling boundary condition at the horizon. In other words, modes with time-like momenta should be falling into the horizon and modes with spacelike momenta should be regular.

    (b) Take r to be the radial direction of the black brane geometry with the boundary at $r = \infty$. Require

$$\phi_a(r; k)|_{r=\frac{1}{\epsilon}} = J_a(k), \qquad k = (\omega, q) \qquad (4.11)$$

where $\epsilon \to 0$ imposes an infrared cutoff near the infinity of the spacetime

and $J_a(k)$ is an infinitesimal boundary source for the bulk field $\phi_a(r; k)$.

2. Plug in the above solution into the action, expanded to quadratic order in $\phi_a(r; k)$. It will reduce to pure surface contribution. The prescription instructs us to pick up only the contribution from the boundary at $r = \frac{1}{\epsilon}$. The resulting action can be written as

$$S = -\frac{1}{2} \int \frac{d^4 k}{(2\pi)^4} \, J_a(-k) \mathcal{F}_a(k, r) J_a(k) \Big|_{r=\frac{1}{\epsilon}} . \qquad (4.12)$$

Finally the retarded function $G_a(k)$ in momentum space for the boundary field dual to ϕ_a is given by

$$G_a(k) = \lim_{\epsilon \to 0} \mathcal{F}_a(k, r) \Big|_{r=\frac{1}{\epsilon}} . \qquad (4.13)$$

Using the Kubo formula Eq. (4.10), we can get the shear viscosity by studying a mode ϕ_3 with $\vec{q} = 0$ in the low-frequency limit $\omega \to 0$. We will do so in the next section.

Alternatively, we can solve the linearized equations of motion in the shear and sound channels; using Eq. (4.8) or Eq. (4.9), we can then read off the viscosity and the sound velocity from the pole structure of the retarded two-point functions. In section 4.5 we will apply this procedure to calculate η/s.

The above prescriptions for computing retarded functions in *AdS/CFT* work well if the bulk scalar field has only two derivatives as in Gauss-Bonnet case Eq. (4.4). If the bulk action contains more than two derivatives, complications could arise even if one treats the higher derivative parts as perturbations. For example, one needs to add Gibbons-Hawking surface terms to ensure a well-defined variational problem. A systematic prescription for doing so is, however, not available at the moment beyond the linear order. Thus there are potential ambiguities in implementing Eq. (4.13).[6] Clearly these are important questions which should be explored more systematically. At the R^2 level, as we describe below in section 4.2.3, all of our calculations can be reduced to the Gauss-Bonnet case in which these potential complications do not arise.

---

[6]In [18], such additional terms do not appear to affect the calculation at the order under discussion there.

4.2.3 Field redefinitions in R^2 theories

We now show that to linear order in α_i, η/s for Eq. (4.2) is independent of α_1 and α_2. It is well known that to linear order in α_i, one can make a field redefinition to remove the R^2 and $R_{\mu\nu}R^{\mu\nu}$ term in Eq. (4.2). More explicitly, in Eq. (4.2) set $\alpha_3 = 0$ and take

$$g_{\mu\nu} = \tilde{g}_{\mu\nu} + \alpha_2 L^2 \tilde{R}_{\mu\nu} - \frac{L^2}{3}(\alpha_2 + 2\alpha_1)\tilde{g}_{\mu\nu}\tilde{R}, \qquad (4.14)$$

where $\tilde{R}$ denotes the Ricci scalar for $\tilde{g}_{\mu\nu}$ and so on. Then Eq. (4.2) becomes

$$I = \frac{1}{16\pi G_N}\int \sqrt{-\tilde{g}}((1+\mathcal{K})\tilde{R} - 2\Lambda) + O(\alpha^2) = \frac{1+\mathcal{K}}{16\pi G_N}\int \sqrt{-\tilde{g}}(\tilde{R} - 2\tilde{\Lambda}) + O(\alpha^2)$$

$$(4.15)$$

with

$$\mathcal{K} = \frac{2\Lambda L^2}{3}(5\alpha_1 + \alpha_2), \qquad \tilde{\Lambda} = \frac{\Lambda}{1+\mathcal{K}}. \qquad (4.16)$$

It follows from Eq. (4.14) that a background solution $g^{(0)}$ to Eq. (4.2) (with $\alpha_3 = 0$) is related to a solution $\tilde{g}^{(0)}$ to Eq. (4.15) by

$$ds_0^2 = A^2 \tilde{ds}_0^2, \qquad A = 1 - \frac{\mathcal{K}}{3}. \qquad (4.17)$$

The scaling in Eq. (4.17) does not change the background Hawking temperature. The diffusion pole Eq. (4.8)) calculated using Eq. (4.15) around $\tilde{g}^{(0)}$ then gives the standard result $D = \frac{1}{4\pi T}$ [62]. Thus we conclude that $\eta/s = \frac{1}{4\pi}$ for Eq. (4.2) with $\alpha_3 = 0$. Then to linear order in α_i, η/s can only depend on α_3. To find this dependence, it is convenient to work with the Gauss-Bonnet theory Eq. (4.4). Gauss-Bonnet gravity is not only much simpler than Eq. (4.2) with generic $\alpha_3 \neq 0$, but also contains only second derivative terms in the equations of motion for $h_{\mu\nu}$, making the extraction of boundary correlators unambiguous.

4.3 Black brane geometry and thermodynamics

Exact solutions and thermodynamic properties of black objects in Gauss-Bonnet gravity Eq. (4.4) were discussed in [19]. Here we summarize some features relevant for our discussion below. The black brane solution can be written as

$$ds^2 = -f(r)N_\sharp^2 dt^2 + \frac{1}{f(r)}dr^2 + \frac{r^2}{L^2}\left(\sum_{i=1}^{3} dx_i^2\right), \qquad (4.18)$$

where

$$f(r) = \frac{r^2}{L^2}\frac{1}{2\lambda_{GB}}\left[1 - \sqrt{1 - 4\lambda_{GB}\left(1 - \frac{r_+^4}{r^4}\right)}\right]. \qquad (4.19)$$

In Eq. (4.18), $N_\sharp$ is an arbitrary constant which specifies the speed of light of the boundary theory. Note that as $r \to \infty$,

$$f(r) \to \frac{r^2}{a^2 L^2}, \quad \text{with} \quad a^2 \equiv \frac{1}{2}\left(1 + \sqrt{1 - 4\lambda_{GB}}\right). \qquad (4.20)$$

It is straightforward to see that the *AdS* curvature scale of these geometries is aL.[7] If we choose $N_\sharp = a$, then the boundary speed of light is unity. However, we will leave it unspecified in the following. We assume that $\lambda_{GB} \leq \frac{1}{4}$. Beyond this point, Eq. (4.4) does not admit a vacuum *AdS* solution, and cannot have a boundary *CFT* dual. In passing, we note that while the curvature singularity occurs at $r = 0$ for $\lambda_{GB} \geq 0$, it shifts to $r = r_+\left(1 - \frac{1}{4\lambda_{GB}}\right)^{-\frac{1}{4}}$ for $\lambda_{GB} < 0$.

The horizon is located at $r = r_+$ and the Hawking temperature, entropy density, and energy density of the black brane are [8]

$$T(r_+) = \frac{1}{2\pi}[\frac{1}{\sqrt{g_{rr}}}\frac{d}{dr}\sqrt{g_{tt}}]|_{r=r_+} = N_\sharp\frac{1}{\pi}\frac{r_+}{L^2}. \qquad (4.21)$$

To get the free energy $F[T]$ of the macroscopic configuration Eq. (4.18), we note

---

[7]Here we note that the Gauss-Bonnet theory also admits another background with the curvature scale $\tilde{a}L$ where $\tilde{a}^2 = \frac{1}{2}\left(1 - \sqrt{1 - 4\lambda_{GB}}\right)$. Even though this remains an asymptotically *AdS* solution for $\lambda_{GB} > 0$, we do not consider it here because this background is unstable and contains ghosts [11].

[8]Note that for *planar* black branes in Gauss-Bonnet theory, the area law for entropy still holds [41]. This is not the case for more general higher-derivative-corrected black objects.

the following correspondence in the classical limit:

$$e^{-\frac{1}{T}F[T]} = Z[T] = e^{-I[T]}.$$

(4.22)

Here, $I[T]$ is the Euclidean action of the configuration with temperature T. Evaluating the Euclideanized bulk action for Gauss-Bonnet gravity Eq. (4.4) with the background metric Eq. (4.18), we find

$$
\begin{aligned}
I_{bulk}[T(r_+)] &= -\frac{1}{16\pi G_N} \times \\
&\times \int_{r_+}^{r_{max}} dr \int_0^{\frac{1}{T}} dt_E \int d^3x_i \sqrt{g_E}[R - 2\Lambda + c_{GB}(R^2 - 4R_{\mu\nu}R^{\mu\nu} + R_{\mu\nu\rho\sigma}R^{\mu\nu\rho\sigma})] = \\
&= \frac{V_3}{16\pi G_N} \frac{N_\sharp}{T} \frac{r_+^4}{\lambda_{GB}L^5} \left[\frac{r_{max}^4}{r_+^4} \left(12\lambda_{GB} - 5 + 5\sqrt{1-4\lambda_{GB}}\right) - 4\lambda_{GB} + \frac{2\lambda_{GB}}{\sqrt{1-4\lambda_{GB}}} \right].
\end{aligned}
$$

We regulate this result by subtracting the Euclidean action of the λ_{GB}-modified pure AdS space (obtained by setting $r_+ = 0$ in Eq. (4.18))

$$
I_{bulk}^{pure}[T'(T(r_+))] = \frac{1}{16\pi G_N} V_3 \frac{N_\sharp}{T'} \frac{r_+^4}{L^5} \frac{1}{\lambda_{GB}} \times \left[\frac{r_{max}^4}{r_+^4} \left(12\lambda_{GB} - 5 + 5\sqrt{1-4\lambda_{GB}}\right) \right]
$$

(4.23)

with $T'(T)$ chosen so that the geometries at $r = r_{max}$ agree [80]. Quantitatively,

$$
\frac{1}{T'} \sqrt{\frac{r_{max}^2}{2\lambda_{GB}L^2}\left(1 - \sqrt{1-4\lambda_{GB}}\right)} = \frac{1}{T} \sqrt{\frac{r_{max}^2}{L^2}\frac{1}{2\lambda_{GB}}\left(1 - \sqrt{1-4\lambda_{GB} + 4\lambda_{GB}\frac{r_+^4}{r_{max}^4}}\right)}.
$$

Then the free energy is,

$$
F[T] = T(I_{bulk}[T] - I_{bulk}^{pure}[T'(T)]) = -\frac{1}{4G_N}V_3(\pi LT)^3 \left(\frac{T}{4}\right)\frac{1}{N_\sharp^3}.
$$

(4.24)

The entropy density is then given by

$$
s[T] = \frac{1}{V_3}\left(-\frac{d}{dT}F[T]\right) = \frac{1}{4G_N}(\pi LT)^3 \frac{1}{N_\sharp^3} = \frac{1}{4G_N}\left(\frac{r_+}{L}\right)^3.
$$

(4.25)

If we fix the boundary theory temperature T and the speed of light to be unity

(taking $N_\sharp = a$), the entropy is a monotonically increasing function of λ_{GB}, reaching a maximum at $\lambda_{GB} = \frac{1}{4}$ and going to zero as $\lambda_{GB} \to -\infty$.

In appendix B,we will calculate the entropy density using Wald's entropy formula (for a recent work on the relation between these two approaches for calculating the entropy in *AdS* spaces, see [28]).

4.4 Shear viscosity for Gauss-Bonnet gravity in the scalar channel

In this section we compute the shear viscosity for Gauss-Bonnet gravity Eq. (4.4) non-perturbatively in λ_{GB}. Here, we follow the outline presented in the previous section, with the Kubo formula Eq. (4.10) in mind. In section 4.5, we extract η/s from the shear channel Eq. (4.8)) and the sound channel Eq. (4.9) (perturbatively in λ_{GB}). There we also find that the sound velocity remains at the conformal value $c_s^2 = \frac{1}{3}$ as it should. In the paper [15], a fourth method to calculate the shear-viscosity using the membrane paradigm [46] was also presented. All four methods give the same result.

4.4.1 Action and equation of motion for the scalar channel

To compute the shear viscosity, we now study small metric fluctuations $\phi = h^1_{\ 2}$ around the black brane background of the form

$$ds^2 = -f(r)N_\sharp^2 dt^2 + \frac{1}{f(r)}dr^2 + \frac{r^2}{L^2}\left(\sum_{i=1}^{3} dx_i^2 + 2\phi(t,\vec{x},r)dx_1 dx_2\right) . \quad (4.26)$$

We will take ϕ to be independent of x_1 and x_2 and write

$$\phi(t,\vec{x},r) = \int \frac{d\omega dq}{(2\pi)^2}\,\phi(r;k)\,e^{-i\omega t + iqx_3}, \quad k = (\omega,0,0,q), \quad \phi(r;-k) = \phi^*(r;k) . \quad (4.27)$$

For notational convenience, let us introduce

$$z = \frac{r}{r_+}, \quad \tilde{\omega} = \frac{L^2}{r_+}\omega, \quad \tilde{q} = \frac{L^2}{r_+}q, \quad \tilde{f} = \frac{L^2}{r_+^2}f = \frac{z^2}{2\lambda_{GB}}\left(1 - \sqrt{1 - 4\lambda_{GB} + \frac{4\lambda_{GB}}{z^4}}\right).$$

(4.28)

Then, at quadratic order, the action for ϕ can be written as

$$S = \int \frac{dk_1 dk_2}{(2\pi)^2} S(k_1, k_2) \quad \text{with}$$
$$S(k_1 = 0, k_2 = 0) = -\frac{1}{2}C \int dz \frac{d\omega dq}{(2\pi)^2}\left(K(\partial_z\phi)^2 - K_2\phi^2 + \partial_z(K_3\phi^2)\right) \quad (4.29)$$

where

$$C = \frac{1}{16\pi G_N}\left(\frac{N_{\sharp}r_+^4}{L^5}\right), \quad K = z^2\tilde{f}(z - \lambda_{GB}\partial_z\tilde{f}), \quad K_2 = K\frac{\tilde{\omega}^2}{N_{\sharp}^2\tilde{f}^2} - \tilde{q}^2 z\left(1 - \lambda_{GB}\partial_z^2\tilde{f}\right),$$

(4.30)

and ϕ^2 should be understood as a shorthand notation for $\phi(z;k)\phi(z,-k)$. Here, S is the sum of the bulk action Eq. (4.4) and the associated Gibbons-Hawking surface term [55]. The explicit expression for K_3 will not be important for our subsequent discussion.

The equation of motion following from Eq. (4.29) is[9]

$$K\phi'' + K'\phi' + K_2\phi = 0 , \quad (4.31)$$

where primes indicate partial derivatives with respect to z. Using the equation of motion, the action Eq. (4.29) reduces to the surface contributions as advertised in section 4.2.2,

$$S(k_1 = 0, k_2 = 0) = -\frac{1}{2}C \int \frac{d\omega dq}{(2\pi)^2}\left(K\phi'\phi + K_3\phi^2\right)|_{\text{surface}} . \quad (4.32)$$

The prescription described in section 4.2.2 instructs us to pick up the contribution from the boundary at $z \to \infty$. Here, the term proportional to K_3 will give rise to a

---

[9]An easy way to get the quadratic action Eq. (4.29) is to first obtain the linearized equation of motion and then read off K and K_2 from it.

real divergent contact term, which are discarded.

4.4.2   Low-frequency expansion and the viscosity

General solutions to the equation of motion Eq. (4.31) can be written as

$$\phi(z;k) = a_{in}(k)\phi_{in}(z;k) + a_{out}(k)\phi_{out}(z;k) \ , \tag{4.33}$$

where ϕ_{in} and ϕ_{out} satisfy infalling and outgoing boundary conditions at the horizon, respectively. They are complex conjugates of each other, and we normalize them by requiring them to approach 1 as $z \to \infty$. Then, the prescription of section 4.2.2 corresponds to setting

$$a_{in}(k) = J(k) \ , \qquad a_{out}(k) = 0 \ , \tag{4.34}$$

where $J(k)$ is an infinitesimal boundary source for the bulk field ϕ.

More explicitly, as $z \to 1$, various functions in Eq. (4.31) have the following behavior

$$\frac{K_2}{K} \approx \frac{\tilde{\omega}^2}{16N_\sharp^2(z-1)^2} + O((z-1)^{-1}) + O(\tilde{q}^2), \qquad \frac{K'}{K} = \frac{1}{z-1} + O(1) \ . \tag{4.35}$$

It follows that near the horizon $z = 1$, equation Eq. (4.31) can be solved by (for $\vec{q} = 0$)

$$\phi(z) \sim (z-1)^{\pm\frac{i\tilde{\omega}}{4N_\sharp}} \sim (z-1)^{\pm\frac{i\omega}{4\pi T}} \tag{4.36}$$

with the infalling boundary condition corresponding to the negative sign. To solve Eq. (4.31) in the small frequency limit, it is convenient to write

$$\phi_{in}(z;k) = e^{-i\frac{\tilde{\omega}}{4N_\sharp}\ln\frac{a^2 f}{z^2}} \left(1 - i\frac{\tilde{\omega}}{4N_\sharp}g_1(z) + O(\tilde{\omega}^2,\tilde{q}^2)\right) \ , \tag{4.37}$$

where we require $g_1(z)$ to be non-singular at the horizon $z = 1$. We show in Ap-

pendix C that g_1 is a non-singular function with the large z expansion

$$g_1(z) = \frac{4\lambda_{GB}}{\sqrt{1-4\lambda_{GB}}} \frac{a^2}{z^4} + O(z^{-8}) .$$ (4.38)

Therefore, with our boundary conditions Eq. (4.34), we find

$$\phi(z;k) = J(k) \left[1 + \frac{i\tilde{\omega}}{4N_\sharp} a^2 \sqrt{1-4\lambda_{GB}} \left(\frac{1}{z^4} + O(z^{-8}) \right) + O(\tilde{\omega}^2, \tilde{q}^2) \right] .$$ (4.39)

Plugging Eq. (4.39) into Eq. (4.32) and using the expressions for C and K in Eq. (4.30), the prescription described in section 4.2.2 gives

$$\text{Im} G_{12,12}(\omega, 0) = \omega \frac{1}{16\pi G_N} \left(\frac{r_+^3}{L^3} \right) (1 - 4\lambda_{GB}) + O(\omega^2).$$ (4.40)

Then, the Kubo formula Eq. (4.10) yields

$$\eta = \frac{1}{16\pi G_N} \left(\frac{r_+^3}{L^3} \right) (1 - 4\lambda_{GB})$$ (4.41)

Finally, taking the ratio of Eq. (4.41) and Eq. (4.25) we find that

$$\frac{\eta}{s} = \frac{1}{4\pi}(1 - 4\lambda_{GB})$$ (4.42)

This is *non-perturbative* in λ_{GB}. Especially, the linear correction is the only non-vanishing term.[10]

We now conclude this section with various remarks:

1. Based on the field redefinition argument presented in section 4.2.3, one finds from Eq. (4.42) that for Eq. (4.2),

$$\frac{\eta}{s} = \frac{1}{4\pi} (1 - 8\alpha_3) + O(\alpha_i^2)$$ (4.43)

   We have also performed an independent calculation of η/s (without using field redefinitions) for Eq. (4.2) using all three methods outlined in section 4.2.1 and

---

[10]It would be interesting to find an explanation for vanishing of higher order corrections.

confirmed Eq. (4.43). This calculation is summarized in appendix D.

2. The ratio η/s dips below the viscosity bound for $\lambda_{GB} > 0$ in Gauss-Bonnet gravity and for $\alpha_3 > 0$ in Eq. (4.2). In particular, the shear viscosity approaches zero as $\lambda_{GB} \to \frac{1}{4}$ for Gauss-Bonnet.

3. Fixing the temperature T and the boundary speed of light to be unity, as we take $\lambda_{GB} \to -\infty$, $\eta \sim (-\lambda_{GB})^{\frac{1}{4}} \to \infty$. In contrast the entropy density decreases as $s \sim (-\lambda_{GB})^{-\frac{3}{4}} \to 0$.

4. The shear viscosity of the boundary conformal field theory is associated with absorption of transverse modes by the black brane in the bulk. This is a natural picture since the shear viscosity measures the dissipation rate of those fluctuations: the quicker the black brane absorbs them, the higher the dissipation rate will be. For example, as $\lambda_{GB} \to -\infty$, η/s approaches infinity; this describes a situation where every bit of the black brane horizon devours the transverse fluctuations very quickly. In this limit the curvature singularity at $z = \left(1 - \frac{1}{4\lambda_{GB}}\right)^{-\frac{1}{4}}$ approaches the horizon and the tidal force near the horizon becomes strong. On the other hand, as $\lambda_{GB} \to \frac{1}{4}$, $\eta/s \to 0$ and the black brane very slowly absorbs transverse modes.

5. The calculation leading to Eq. (4.42) can be generalized to general D spacetime dimensions and one finds for $D \geq 4 + 1$[11]

$$\frac{\eta}{s} = \frac{1}{4\pi}\left[1 - 2\frac{(D-1)}{(D-3)}\lambda_{GB}\right] \ . \tag{4.45}$$

Here again λ_{GB} is bounded above by $\frac{1}{4}$. Thus for $D > 4 + 1$, η never approaches zero within Gauss-Bonnet theory. For $D = 3 + 1$ or $2 + 1$, in which case the Gauss-Bonnet term is topological, there is no correction to η/s.

---

[11]For general dimensions we use the convention

$$S = \frac{1}{16\pi G_N} \int d^D x \sqrt{-g} \left[R - 2\Lambda + \alpha_{GB} L^2(R^2 - 4R_{\mu\nu}R^{\mu\nu} + R_{\mu\nu\rho\sigma}R^{\mu\nu\rho\sigma})\right] \tag{4.44}$$

with $\Lambda = -\frac{(D-1)(D-2)}{2L^2}$ and $\lambda_{GB} = (D-3)(D-4)\alpha_{GB}$.

4.5 η/s for Gauss-Bonnet gravity in the shear and sound channels

In this section we present the calculation of the shear viscosity in the shear and sound channels, for Gauss-Bonnet gravity. This calculation is perturbative in λ_{GB}, and follows the techniques developed in [47].

As we outlined is section 4.2.2 we can combine the metric fluctuations into three independent scalar fields. In particular, if we consider a perturbation of the background metric of the form $h_{\mu\nu} = h_{\mu\nu}(r)e^{-i\omega t + iqx_3}$, with $\mu, \nu = t, r, x_1, x_2, x_3$, we can label various kinds of perturbations according to their transformations under the symmetry group of rotations in the $1 - 2$ plane. There are three types of decoupled excitations corresponding to spin 2 (scalar channel), spin 1 (shear channel) and spin 0 (sound channel). We presented in the section 4.4 the calculation in the scalar channel. Here we consider the other two channels.

4.5.1 Shear channel

The shear channel excitations involve $h_{t\alpha}$, $h_{r\alpha}$ and $h_{3\alpha}$ with $\alpha = 1, 2$. Choosing the radial gauge $h_{\mu r} = 0$, the shear channel equations can be reduced to a single equation for $Z(r) = qg^{11}h_{t1} + \omega g^{11}h_{31}$. At first order in λ_{GB}, $Z(r)$ satisfies the equation (below we use the notation introduced in Eq. (4.28))

$$
\begin{aligned}
0 = {}& Z''(z) + \frac{Z'(z)}{z}\left(\frac{5z^4 - 1}{z^4 - 1} + \frac{4\tilde{q}^2}{\tilde{q}^2(-z^4 + 1) + z^4\frac{\tilde{\omega}^2}{N_\sharp^2}}\right) + \\
& + Z(z)\left(\frac{\tilde{q}^2(-z^4 + 1) + z^4\frac{\tilde{\omega}^2}{N_\sharp^2}}{(z^4 - 1)^2}\right) + \\
& + \frac{\lambda_{GB}}{2}\left[Z'(z)\left(-\frac{8(2\tilde{q}^4(z^4 - 1)^2 + 4\tilde{q}^2z^4\frac{\tilde{\omega}^2}{N_\sharp^2} - 3z^8\frac{\tilde{\omega}^4}{N_\sharp^4})}{z^5(\tilde{q}^2(z^4 - 1) - z^4\frac{\tilde{\omega}^2}{N_\sharp^2})^2}\right) + \\
& + Z(z)\left(2\frac{\tilde{q}^2(z^4 + 3) - 2z^4\frac{\tilde{\omega}^2}{N_\sharp^2}}{z^4(z^4 - 1)}\right)\right].
\end{aligned}
\tag{4.46}
$$

Following a similar analysis to that at the beginning of section 4.4.2, we find that the solution to Eq. (4.46) which satisfies an infalling boundary condition at the horizon $z = 1$ can be written as

$$Z(z) = \left(1 - \frac{1}{z^4}\right)^{-i\frac{\tilde{\omega}}{4N_\sharp}} g(z) \tag{4.47}$$

where g is regular at $z = 1$. The exponent is fixed by an expansion in the near horizon limit. In order to find the hydrodynamical poles, it is enough to find $g(z)$ for small values of $\tilde{\omega}$ and $\tilde{q}$, which we will assume are of the same order. For this purpose, we introduce a scaled quantity $W = \frac{\tilde{\omega}}{\tilde{q}N_\sharp}$ and expand $g(z)$ as a power series of $\tilde{q}$. The solution can be readily found to be

$$g(z) = 1 + \frac{i\tilde{q}}{4W}\left(1 - \frac{1}{z^4}\right)\left[1 + \lambda_{GB}\left(3(W^2 - 1) - \frac{1}{z^4}\right)\right] + O(\tilde{q}^2, \lambda_{GB}^2) . \tag{4.48}$$

We thus find near infinity $Z(z)$ can be expanded in $1/z$ as

$$Z(z) \approx \mathcal{A} + \mathcal{B}z^{-4} + O(z^{-8}), \quad z \to \infty \tag{4.49}$$

where

$$\begin{aligned}
\mathcal{A} &= 1 + \frac{i\tilde{q}}{4W} + 3i\frac{\tilde{q}}{4W}\lambda_{GB}\left(W^2 - 1\right) + O(\tilde{q}^2) \\
&= 1 + \frac{iN_\sharp^2}{4\pi T}\left(1 - 3\lambda_{GB}\right)\frac{q^2}{\omega} + \frac{3i\lambda_{GB}\omega}{4\pi T} + \cdots \tag{4.50} \\
\mathcal{B} &= -\frac{i\tilde{q}}{4W} + i\frac{W\tilde{q}}{4} + i\frac{\lambda_{GB}\tilde{q}}{W}\left(\frac{1}{2} - 3\frac{W^2}{4}\right) + O(\tilde{q}^2) \\
&= \frac{i}{4\pi T}\frac{1 - 3\lambda_{GB}}{\omega}\left(\omega^2 - \frac{N_\sharp^2}{1 - \lambda_{GB}}q^2\right) + \cdots \tag{4.51}
\end{aligned}$$

Carrying out the procedure Eq. (4.11)–Eq. (4.13) one finds that

$$G_R(k) \propto \frac{\mathcal{B}}{\mathcal{A}} . \tag{4.52}$$

In particular one can show that the poles of $G_R(k)$ solely arise from zeros of $\mathcal{A}$.

The Dirichlet boundary condition corresponding to $\mathcal{A} = 0$ determines the hydro-dynamical pole as[12],

$$\omega = -iDq^2 + O(q^3), \qquad D = \frac{N_\sharp^2}{4\pi T}(1 - 3\lambda_{GB}) \tag{4.53}$$

Note that in the relation Eq. (4.8)) between the diffusion constant D and η/s, the boundary speed of light c has been set to unity (otherwise the right hand side should be multiplied by c^2). Choosing $N_\sharp^2 = a^2 \approx 1 - \lambda_{GB}$ (see (Eq. (4.20)) so that the boundary speed of light is unity, we find that

$$\frac{\eta}{s} = \frac{1}{4\pi}(1 - 4\lambda_{GB}) + O(\lambda_{GB}^2) . \tag{4.54}$$

4.5.2 Sound channel

The sound channel excitations involve $h_{tt}, h_{t3}, h_{33}, h_{11} + h_{22}, h_{rr}, h_{tr}, h_{r3}$. Choosing the radial gauge $h_{\mu r} = 0$, the sound channel equations can be reduced to a single equation for the variable [47]

$$Z_s(r) = \frac{4q}{\omega}g^{33}h_{t3} + 2g^{33}h_{33} - (g^{22}h_{22} + g^{11}h_{11})\left(1 - \frac{q^2}{\omega^2}\frac{\partial_r g_{tt}}{\partial_r g_{11}}\right) + 2\frac{q^2}{\omega^2}\frac{h_{tt}}{g_{11}} . \tag{4.55}$$

At first order in λ_{GB}, the equation for $Z_s(z)$ can be written as

$$0 = Z_s''(z) + Z_s'(z)\left(\frac{3\frac{\tilde{\omega}^2}{N_\sharp^2}z^4(1 - 5z^4) + \tilde{q}^2(9 - 16z^4 + 15z^8)}{z(-1 + z^4)(-3\frac{\tilde{\omega}^2}{N_\sharp^2}z^4 + \tilde{q}^2(-1 + 3z^4))}\right) + \tag{4.56}$$

$$+ Z_s(z)\left(\frac{-3\frac{\tilde{\omega}^4}{N_\sharp^4}z^{10} + 2\tilde{q}^2\frac{\tilde{\omega}^2}{N_\sharp^2}z^6(3z^4 - 2) - \tilde{q}^2(z^4 - 1)(\tilde{q}^2z^2(-1 + 3z^4) - 16)}{z^2(-1 + z^4)^2(-3\frac{\tilde{\omega}^2}{N_\sharp^2}z^4 + \tilde{q}^2(-1 + 3z^4))}\right) +$$

$$+ \lambda_{GB}\left[Z_s'(z)\left(\frac{4(27\frac{\tilde{\omega}^4}{N_\sharp^4}z^8 + 6\tilde{q}^2\tilde{\omega}^2z^4(z^4 - 11) + \tilde{q}^4(-11 + 66z^4 - 27z^8))}{z^5(-3\frac{\tilde{\omega}^2}{N_\sharp^2}z^4 + \tilde{q}^2(-1 + 3z^4))^2}\right) +\right.$$

$$+ \frac{Z_s(z)}{z^6(-1 + z^4)(-3\frac{\tilde{\omega}^2}{N_\sharp^2}z^4 + \tilde{q}^2(-1 + 3z^4))^2}\left(3\tilde{q}^2\frac{\tilde{\omega}^4}{N_\sharp^4}z^{10}(17 + 15z^4) - 18\frac{\tilde{\omega}^6}{N_\sharp^6}z^{14} +\right.$$

$$+ \tilde{q}^4(\tilde{q}^2(7 + z^4)(z - 3z^5)^2 + 32(4 - 23z^4 + 15z^8)) -$$

---

[12]We now need to assume $\omega \sim O(q^2)$.

$$- 4\frac{\tilde{q}^2\tilde{\omega}^2}{N_\sharp^2}z^4(-180 + 132z^4 + \tilde{q}^2z^2(-10 + 9z^4(3 + z^4))))\Big)\Big]$$

Again the solution satisfying the in-falling boundary condition at the horizon $z = 1$ can be written as

$$Z(z) = \left(1 - \frac{1}{z^4}\right)^{-i\frac{\tilde{\omega}}{4N_\sharp}} s(z) \qquad (4.57)$$

Defining as above the quantity $W = \frac{\tilde{\omega}}{\tilde{q}N_\sharp}$, and expanding $s(z)$ in $\tilde{q}$, we find that

$$s(z) = \frac{3W^2z^4 - (1 + z^4)}{(3W^2 - 2)z^4} - \lambda_{GB}\frac{-3 + 2z^4 + z^8}{z^8(3W^2 - 2)} +$$
$$+ i\tilde{q}\left[\frac{W(z^4 - 1)}{z^4(3W^2 - 2)} + \lambda_{GB}W\left(1 - \frac{1}{z^4}\right)\frac{(3(3W^2 - 5)z^4 - 7)}{4z^4(3W^2 - 2)}\right] + O(\tilde{q}^2) \quad (4.58)$$

The leading asymptotic behavior close to the boundary at infinity is

$$Z_s(z) = \mathcal{A}_s + \mathcal{B}_s z^{-4} + O(z^{-8}),$$

with

$$\mathcal{A}_s \propto q^2(1 + \lambda_{GB}) - \frac{i}{\pi T}q^2\omega\left(1 - \frac{15}{4}\lambda_{GB}\right) - \frac{3\omega^2}{N_\sharp^2} - \frac{i9\lambda_{GB}}{4\pi T}\frac{\omega^3}{N_\sharp^2} + \cdots \qquad (4.59)$$

Again, the hydrodynamical pole is found by setting $\mathcal{A}_s = 0$, leading to

$$\omega_{sound} = \pm c_s q - i\Gamma_s q^2 \qquad (4.60)$$

$$c_s = \frac{1}{\sqrt{3}}N_\sharp(1 + \frac{\lambda_{GB}}{2}) \qquad (4.61)$$

$$\Gamma_s = \frac{2}{3}\frac{N_\sharp^2}{4\pi T}(1 - 3\lambda_{GB}) \qquad (4.62)$$

By choosing the boundary speed of light to be unity, i.e. $N_\sharp = a \approx (1 - \frac{\lambda_{GB}}{2})$, we thus find that $c_s = \frac{1}{\sqrt{3}}$ and from Eq. (4.9)

$$\frac{\eta}{s} = \frac{1}{4\pi}(1 - 4\lambda_{GB}) + O(\lambda_{GB}^2) . \qquad (4.63)$$

88

in agreement with the results obtained from the scalar and shear channel.

4.6 Causality in bulk and on boundary

4.6.1 Graviton cone tipping

As a consequence of higher derivative terms in the gravity action, graviton wave packets in general do not propagate on the light-cone of a given background geometry. For example, when $\lambda_{GB} \neq 0$, the equation Eq. (4.31) for the propagation of a transverse graviton differs from that of a minimally coupled massless scalar field propagating in the same background geometry Eq. (4.18).

The equation of motion Eq. (4.31) can be written as

$$\tilde{g}_{eff}^{\mu\nu} \tilde{\nabla}_\mu \tilde{\nabla}_\nu \phi = 0 \qquad (4.64)$$

where $\tilde{\nabla}_\mu$ is a covariant derivative with respect to the effective geometry $\tilde{g}_{\mu\nu}^{eff} = \Omega^2 g_{\mu\nu}^{eff}$ given by

$$g_{\mu\nu}^{eff} dx^\mu dx^\nu = f(r) N_\sharp^2 \left(-dt^2 + \frac{1}{c_g^2} dx_3^2 \right) + \frac{1}{f(r)} dr^2 . \qquad (4.65)$$

Here, $\Omega^2 = \frac{K}{f} z (1 - \lambda_{GB} \tilde{f}'')$ and

$$c_g^2(z) = \frac{N_\sharp^2 \tilde{f}(z)}{z^2} \frac{1 - \lambda_{GB} \tilde{f}''(z)}{1 - \frac{\lambda_{GB} \tilde{f}'(z)}{z}} \equiv c_b^2(z) \frac{1 - \lambda \tilde{f}''(z)}{1 - \frac{\lambda \tilde{f}'(z)}{z}} \qquad (4.66)$$

can be interpreted as the local "speed of graviton" on a constant r-hypersurface. $c_b^2(z) \equiv \frac{N_\sharp^2 \tilde{f}(z)}{z^2}$ introduced in the second equality in Eq. (4.66) is the local speed of light as defined by the background metric Eq. (4.18). Thus the graviton cone in general does not coincide with the standard null cone or light cone defined by background metric.[13]

---

[13]Note that

$$\frac{c_g^2}{c_b^2} = \frac{1 - \lambda_{GB} \tilde{f}''}{1 - \frac{\lambda_{GB} \tilde{f}'}{z}} = \frac{1 - 4\lambda_{GB} + 12\frac{\lambda_{GB}}{z^4}}{1 - 4\lambda_{GB} + 4\frac{\lambda_{GB}}{z^4}} , \qquad (4.67)$$

and in particular the ratio is greater than 1 for $\lambda_{GB} > 0$. Note that bulk causality and the existence of a well posed Cauchy problem do not crucially depend on reference metric light-cones and such
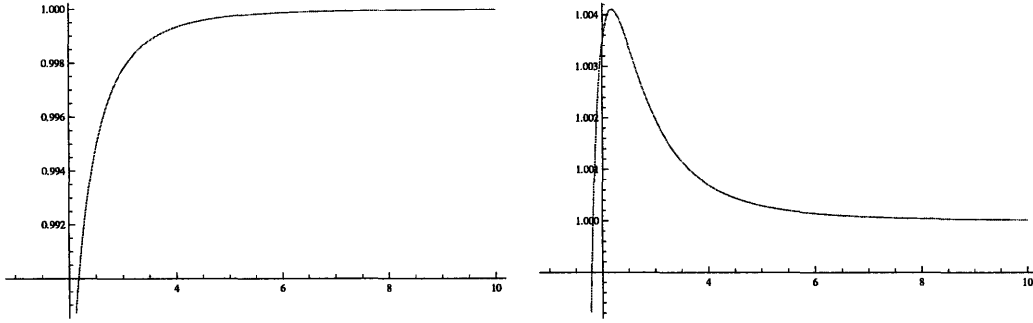
Figure 4-1: $c_g^2(z)$ (vertical axis) as a function of z (horizontal axis) for $\lambda_{GB} = 0.08$ (left panel) and $\lambda_{GB} = 0.1$ (right panel). For $\lambda_{GB} < \frac{9}{100}$, c_g^2 is a monotonically increasing function of z. When $\lambda_{GB} > \frac{9}{100}$, as one decreases z from infinity, c_g^2 increases from 1 to a maximum value at some $z > 1$ and then decreases to 0 as $z \to 1$ (horizon).

In the non-gravitational boundary theory there is an invariant notion of light-cone and causality. At a heuristic level, a graviton wave packet moving at speed $c_g(z)$ in the bulk should translate into disturbances of the stress tensor propagating with the same velocity in the boundary theory. It is thus instructive to compare c_g and c_b with the boundary speed of light, which we now set to unity by taking $N_\sharp = a$ (a was defined in Eq. (4.20)). At the boundary ($z = \infty$) one finds that $c_g(z) = c_b(z) = 1$. In the bulk, the background local speed of light c_b is always smaller than 1, which is related to the redshift of the black hole geometry. The local speed of graviton $c_g(z)$, however, can be greater than 1 for certain range of z if λ_{GB} is sufficiently large. To see this, we can examine the behavior of c_g^2 near $z = \infty$,

$$c_g^2(z) - 1 = \frac{b_1}{z^4} + O(z^{-8}), \quad z \to \infty, \qquad b_1(\lambda_{GB}) = -\frac{1 + \sqrt{1 - 4\lambda_{GB}} - 20\lambda_{GB}}{2(1 - 4\lambda_{GB})}.$$
(4.68)

$b_1(\lambda_{GB})$ becomes positive and thus c_g^2 increases above 1 if $\lambda_{GB} > \frac{9}{100}$. For such a λ_{GB}, as we decrease z from infinity, c_g^2 will increase from 1 to a maximum at some value of z and then decrease to zero at the horizon. See Fig. 4-1 for the plot of $c_g^2(z)$ as a function z for two values of λ_{GB}. When $\lambda_{GB} = \frac{9}{100}$ one finds that the next order term

tipping is not a definitive sign of causality problems. Also note that For $\lambda_{GB} < -\frac{1}{8}$, there exists a region outside the horizon where $c_g^2 < 0$. This is rather peculiar since there appears to be more than one time direction in the effective geometry. Since this is not correlated with the viscosity bound, we shall not explore it further in this paper.

90

in Eq. (4.68) is negative and thus c_g^2 does not go above 1. Also note that $\lambda_{GB} \to \frac{1}{4}$, $b_1(\lambda_{GB})$ goes to plus infinity.[14] Thus heuristically, in the boundary theory there is a potential for superluminal propagation of disturbances of the stress tensor. In the next sections, we will show that this indeed happens.

We now briefly comment on the status of the null energy condition in Gauss-Bonnet gravity. The easiest condition to check is the null energy condition on the λ_{GB}-corrected black brane spacetime: $R_{\mu\nu}l^\mu l^\nu \geq 0$ for all null vectors l^μ. Somewhat surprisingly we find that it is satisfied when the viscosity bound is violated ($\lambda_{GB} > 0$), and violated when the viscosity bound is satisfied ($\lambda_{GB} \leq 0$). However for gravitational theories with higher curvature terms this apparent violation is not a compelling signal of problems.

4.6.2 Causality violation and the KSS bound

In this section, we will argue that when $\lambda_{GB} > \frac{9}{100}$, the theory violates causality and is inconsistent. Thus, for (3+1)-dimensional CFT duals of (4+1)-dimensional Gauss-Bonnet gravity, consistency of the theory requires

$$\frac{\eta}{s} \geq \frac{16}{25}\left(\frac{1}{4\pi}\right). \tag{4.69}$$

This provides a concrete example in which a lower bound on η/s and the consistency of the theory are correlated. The 36% difference from the KSS bound is mysterious, and we discuss two obvious possibilities below.

From standard geometrical optics arguments [54], in the large momentum limit, a localized wave packet of a graviton should follow a null geodesic $x^\mu(s)$ in the effective graviton geometry Eq. (4.65). More explicitly, write the wave function

$$\phi(t, \vec{x}, r) = \int \frac{d\omega}{(2\pi)^2}\phi(r; \omega, q)e^{-i\omega t + iqx_3}$$

in Eq. (4.64) in the form $\phi = e^{i\Theta(t, r, x_3)}\phi_{en}(t, r, x_3)$ where Θ is a rapidly varying phase

---

[14]In fact coefficients of all higher order terms in $1/z$ expansion become divergent in this limit.
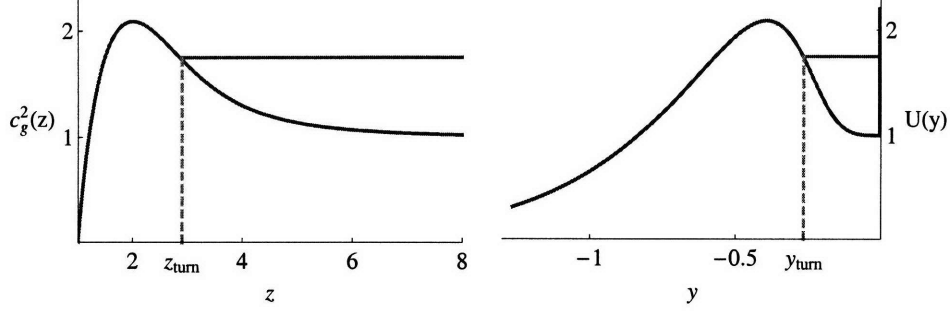
Figure 4-2: Left: $c_g^2(z)$ as a function of z for $\lambda_{GB} = 0.245$. c_g^2 has a maximum $c_{g,max}^2$ at z_{max}. As λ_{GB} is increased from $\lambda_{GB} = \frac{9}{100}$ to $\lambda_{GB} = \frac{1}{4}$, $c_{g,max}^2$ increases from 1 to 3. $c_g^2(z)$ also serves as the classical potential for the 1-d system Eq. (4.72). The horizontal line indicates the trajectory of a classical particle. Right: $U(y)$ (defined in Eq. (4.80)) as a function of y for $\lambda_{GB} = 0.245$.

and ϕ_{en} denotes a slowly varying envelope function. Inserting into Eq. (4.64), we find at leading order [15]

$$\frac{dx^\mu}{ds}\frac{dx^\nu}{ds}g_{\mu\nu}^{eff} = 0 \qquad (4.70)$$

with the identification $\frac{dx^\mu}{ds} \equiv g_{eff}^{\mu\nu}k_\nu \equiv g_{eff}^{\mu\nu}\nabla_\nu\Theta$. Given translational symmetries in the t and x_3 directions, we can interpret ω and q as conserved integrals of motion along the geodesic,

$$\omega = \left(\frac{dt}{ds}\right)fN_\sharp^2, \qquad q = \left(\frac{dx_3}{ds}\right)fN_\sharp^2\frac{1}{c_g^2} . \qquad (4.71)$$

Assuming $q \neq 0$ and rescaling the affine parameter as $\tilde{s} = qs/N_\sharp$, we get from Eq. (4.70) and Eq. (4.71)

$$\left(\frac{dr}{d\tilde{s}}\right)^2 = \alpha^2 - c_g^2, \quad \alpha \equiv \frac{\omega}{q}. \qquad (4.72)$$

This describes a one-dimensional particle of energy α^2 moving in a potential given by c_g^2. As is clear from Fig. 4-2, geodesics starting from the boundary can bounce back to the boundary, with a turning point $r_{turn}(\alpha)$ given by

$$\alpha^2 = c_g^2(r_{turn}) . \qquad (4.73)$$

---

[15]Any (non-singular) conformal factor multiplying $g_{\mu\nu}^{eff}$ will not matter for null geodesics since we can reparametrize affine parameters to get rid of it.

In contrast, for $\lambda_{GB} \leq \frac{9}{100}$, $c_g(z)$ is a monotonically increasing function of z and there is no bouncing geodesic. For a null bouncing geodesic starting and ending at the boundary, we then have

$$\Delta t(\alpha) = 2 \int_{r_{turn}(\alpha)}^{\infty} \frac{\dot{t}}{\dot{r}} dr = \frac{2}{N_\sharp} \int_{r_{turn}(\alpha)}^{\infty} \frac{\alpha}{f\sqrt{\alpha^2 - c_g^2}} dr, \qquad (4.74)$$

$$\Delta x_3(\alpha) = 2 \int_{r_{turn}(\alpha)}^{\infty} \frac{\dot{x}_3}{\dot{r}} dr = \frac{2}{N_\sharp} \int_{r_{turn}(\alpha)}^{\infty} \frac{c_g^2}{f\sqrt{\alpha^2 - c_g^2}} dr, \qquad (4.75)$$

where dots indicate derivatives with respect to $\tilde{s}$.

In the boundary CFT we have local operators which create bulk disturbances at infinity that propagate on graviton geodesics sufficiently deep inside the bulk ($r \lesssim \omega$) [60]. In particular, we expect causality violation in the boundary CFT if there exists a bouncing graviton geodesic with $\frac{\Delta x_3(\alpha)}{\Delta t(\alpha)} > 1$ [16]. Now, as $r_{turn} \to r_{max}$ ($\alpha \to c_{g,max}$), a geodesic hovers near r_{max} for a long time, propagating with a speed $c_{g,max}$ in x_3-direction. Indeed, the integrals in Eq. (4.74) and Eq. (4.75) are dominated by contributions near r_{max}. In such a limit, the ratio of the integrand in $\Delta x_3(\alpha)$ to that in $\Delta t(\alpha)$ near r_{max} is $c_{g,max}$. Thus, $\frac{\Delta x_3(\alpha)}{\Delta t(\alpha)} \to c_{g,max} > 1$, violating causality.

We will now show explicitly that the superluminal graviton propagation described above corresponds to superluminal propagation of metastable quasi-particles[17] in the boundary CFT with $\frac{\Delta x_3}{\Delta t}$ identified as the group velocity of the quasi-particles. For this purpose, we rewrite the full wave equation Eq. (4.64) in a Schrödinger form

$$-\partial_y^2 \psi + V(y)\psi = \tilde{\omega}^2 \psi \qquad (4.76)$$

---

[16]To be precise this only indicates the presence of a pole outside the boundary CFT light-cone in the time-ordered two-point function. To be complete, we need to show that the retarded two-point function does not vanish outside the light-cone.

[17]Quasi-particles in the boundary CFT correspond to poles in the retarded Green function which are sufficiently close to the real axis in the complex ω-plane. Such poles in turn correspond to solutions of the equation of motion Eq. (4.64) which are normalizable near the AdS boundary and in-falling at the horizon [69].
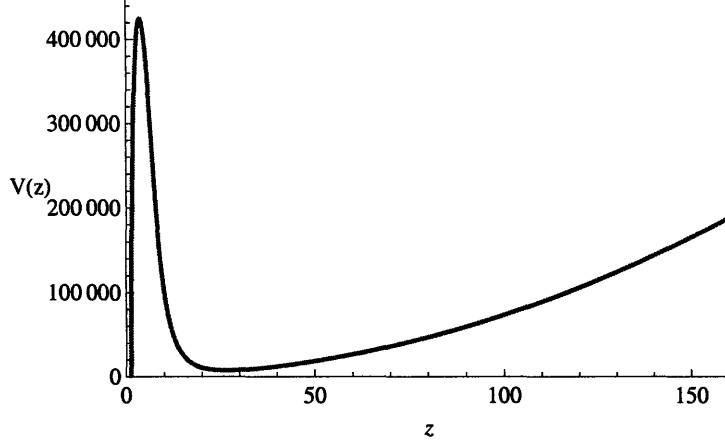
Figure 4-3: $V(z)$ as a function of z for $\lambda_{GB} = 0.2499$ and $\tilde{q} = 500$.

with ψ and y defined by

$$\frac{dy}{dz} = \frac{1}{N_\natural \tilde{f}(z)}, \qquad \psi = B\phi, \qquad B = \sqrt{\frac{K}{\tilde{f}}}, \qquad (4.77)$$

and

$$V(y) = \tilde{q}^2 c_g^2(z) + V_1, \qquad V_1(y) = \frac{N_\natural^2 \tilde{f}^2}{B}\left(B'' + \frac{\tilde{f}'}{\tilde{f}}B'\right). \qquad (4.78)$$

In the above primes denote derivatives with respect to z. Note that $y(z)$ is a mono-tonically increasing function of z with $y \to 0$ as $z \to \infty$ (boundary) and $y \to -\infty$ as $z \to 1$ (horizon). $c_g^2(z)$ is given by Eq. (4.66). V_1 is a monotonically increasing function of y (for $\lambda_{GB} > 0$) with $V_1(y = -\infty) = 0$ and $V_1 \sim y^{-2}$ as $y \to 0$.

Since c_g^2 is monotonically decreasing for $r > r_{max}$, for large enough $\tilde{q}$, $V(y)$ devel-ops a well and admits metastable states (see Fig. 4-3). The wave functions of such metastable states are normalizable at the AdS boundary and have an in-falling tail at the horizon, corresponding to quasi-particles in the boundary CFT

Now consider the limit $\tilde{q} \to \infty$. Since V_1 is independent of $\tilde{q}$, the dominant contribution to the potential is given by $\tilde{q}^2 c_g^2(z)$ except for a tiny region $y \gtrsim -\frac{1}{\tilde{q}}$. Thus in this limit, we can simply replace $V_1(y)$ by $V_1(y) = 0$ for all $y < 0$ and $V_1(0) = +\infty$. Equation (4.76) can then be written as

$$-\hbar^2 \partial_y^2 \psi + U(y)\psi = \alpha^2 \psi, \qquad \hbar \equiv \frac{1}{\tilde{q}} \to 0 \qquad (4.79)$$

94

where α was introduced in Eq. (4.72) and (see Fig. 4-2)

$$U(y) = \begin{cases} c_g^2(y) & y < 0 \\ +\infty & y = 0 \end{cases}. \qquad (4.80)$$

In the $\hbar \to 0$ limit, we can apply the WKB approximation. The leading WKB wave function $e^{i\Theta(t,r,x_3)}$ is just the rapidly varying phase of the geometric optics approximation. The real part of α^2 satisfies the Bohr-Sommerfeld quantization condition (with n some integer)

$$\tilde{q} \int_{y_{turn}}^{0} dy \sqrt{\alpha^2 - c_g^2(y)} = (n - \frac{1}{4})\pi \qquad (4.81)$$

The above equation determines ω as a function of q for each given n. Taking the derivative with respect to q on both sides of Eq. (4.81), we find that the group velocity of the quasi-particles is given by

$$v_g = \frac{d\omega}{dq} = \frac{\Delta x_3(\alpha)}{\Delta t(\alpha)} \qquad (4.82)$$

where $\Delta t(\alpha)$ and $\Delta x_3(\alpha)$ are given by Eq. (4.74) and Eq. (4.75) respectively. Thus as argued in the paragraph below Eq. (4.75), v_g approaches $c_{g,max} > 1$ as $\alpha \to c_{g,max}$, violating causality. In this limit the WKB wave function is strongly peaked near r_{max}, reflecting the long time the geodesic spends there. One can also estimate the imaginary part of α^2 (or ω), which has the form $e^{-h(\alpha)\tilde{q}}$ with $h(\alpha)$ given by the standard WKB formula. Thus in the $\tilde{q} \to \infty$ limit the quasi-particles become stable. Presumably local boundary operators that couple primarily to the long-lived quasi-particles can be constructed by following [60].

4.7 Summary

To summarize, we have argued that signals in the boundary theory propagate outside the light-cone. In a boosted frame disturbances will propagate backward in time. Since the boundary theory is non-gravitational, these are unambiguous signals of

causality violation and hence inconsistency.

Here we observe causality violation in the high momentum limit by looking at metastable states near the top of the potential. This is in agreement with the expectation that causality should be tied to the local, short-distance behavior of the theory. Also, a sharp transition from causal to acausal behavior as a function of λ_{GB} is possible because of the limiting procedure $\tilde{q} \to \infty$ needed in our argument. A more rigorous derivation of these phenomena using the full spectral function obtained from the Schrödinger operator would be desirable.

We argued that, for a (4+1)-dimensional Gauss-Bonnet gravity, causality requires $\lambda_{GB} \leq \frac{9}{100}$. Thus, consistency of this theory requires,

$$\frac{\eta}{s} \geq \frac{16}{25} \left(\frac{1}{4\pi} \right).$$

(4.83)

This still leaves rooms for a violation of the KSS bound. We see two possibilities.

First, it could be that Gauss-Bonnet theory with $\lambda_{GB} \leq \frac{9}{100}$ is consistent and appears as a classical limit of a consistent theory of quantum gravity, somewhere in the string landscape. Maybe this is how nature works and the KSS bound can be violated, at least by 36%.

Alternatively, it could be that there is a more subtle inconsistency in the theory within the window of $0 < \lambda_{GB} \leq \frac{9}{100}$. These issues deserve further investigation.

Appendix A

Proof of Eq. (2.41)

In this appendix we prove equation Eq. (2.41). In the next subsection we discuss some elementary aspects of $U(N)$ group integrals. We then proceed to evaluate Eq. (2.10). Equation Eq. (2.41) is proved in the end.

A.1 Group integrals over $U(N)$

Consider the following integral over the unitary group $U(N)$

$$I = \frac{1}{V_N} \int dU \prod_{i=1}^{k} (\text{Tr} U^{a_i})^{b_i} \prod_{j=1}^{s} (Tr U^{-c_j})^{d_j} \tag{A.1}$$

where a_i, b_i, c_i, d_i are positive integers and

$$D = \sum_{i=1}^{k} a_i b_i = \sum_{j=1}^{s} c_j d_j \ . \tag{A.2}$$

V_N is the volume of $U(N)$.

Products of traces of U can be expanded in terms of characters of irreducible representations of $U(N)$, which are in one to one correspondence with irreducible

representations of the symmetric group (see for example [22]),

$$\prod_{i=1}^{k}(\text{Tr}U^{a_i})^{b_i} = \sum_{\lambda} \chi_\lambda(a_i, b_i)\chi_\lambda(U) \tag{A.3}$$

where λ labels the irreducible representations of the symmetric group S_D. $\chi_\lambda(a_i, b_i)$ is the character of the conjugacy class[1] of S_D given by the set $\{(a_i, b_i)\}$ in the representation λ. $\chi_\lambda(U)$ is the character of U in the irreducible representation of $U(N)$ labeled by λ. Now by using the orthogonality property for characters we can write:

$$\begin{aligned} I &= \sum_{\lambda\lambda'} \chi_\lambda(a_i, b_i)\chi_{\lambda'}(c_i, d_i)\frac{1}{V_N} \int dU \chi_\lambda(U)\chi_{\lambda'}(U^\dagger) \\ &= \sum_{\lambda} \chi_\lambda(a_i, b_i)\chi_\lambda(c_i, d_i) \end{aligned} \tag{A.4}$$

The evaluation of Eq. (A.4) can be divided into the following two cases:

1. If $D \leq N$, then the sum over λ can be evaluated giving [22]

$$I = \delta_{\{(a_i,b_i)\},\{(c_i,d_i)\}} \sum_{\lambda} \chi_\lambda(a_i, b_i)^2 = \delta_{\{(a_i,b_i)\},\{(c_i,d_i)\}} \prod_{i=1}^{k} a_i^{b_i} b_i! \tag{A.5}$$

   where the completeness of characters of the symmetric group S_D enforces the sets $\{(a_i, b_i)\}$ and $\{(c_i, d_i)\}$ to define the same conjugacy class in S_D, i.e., to be the same apart from reordering. This means that the integral is zero for $D < N$ unless for any factor of $Tr[U^a]^b$ in the integrand there is a corresponding factor of $Tr[U^{-a}]^b$.

2. If $D > N$ one needs to restrict the sum over the irreducible representations λ to the representations where $\chi_\lambda(U) \neq 0$, that we will indicate formally as $\lambda < N$. In this case the result is more complicated and we do not have a closed form expression. For the case in which the sets $\{(a_i, b_i)\}$ and $\{(c_i, d_i)\}$ are equal up

---

[1]Recall that two elements of S_D are conjugate if and only if they consist of the same number of disjoint cycles of the same lengths. Denote the number of cycles of length a_i by b_i then a conjugacy class in S_D is given by a set of k couples $\{(a_i, b_i)\}$ $i = 1, ..k$ such that $\sum_{i=1}^{k} a_i b_i = D$.

to reordering one has

$$I = \sum_{\lambda < N} \chi_\lambda(a_i, b_i)^2 < \prod_{i=1}^{k} a_i{}^{b_i} b_i! \ . \tag{A.6}$$

A.2 Partition function integrals

We now consider the evaluation of the free theory partition function Eq. (2.10). To warm up let us consider the following integral

$$\frac{1}{V_N} \int dU \, e^{z_1 \text{Tr} U \text{Tr} U^\dagger} = \frac{1}{V_N} \int dU \sum_{p=0}^{\infty} \frac{1}{p!} (z_1 \text{Tr} U \text{Tr} U^\dagger)^p$$

$$= \sum_{p=0}^{N} z_1^p + O(z_1^N)$$

$$= \frac{1}{1 - z_1} + O(z_1^N) \ . \tag{A.7}$$

For $0 < z_1 < 1$ the corrections to the $N = \infty$ result are of order $O(z_1^N)$ and are therefore exponentially suppressed in N. In the more general case Eq. (2.10) (with $V_n(\beta) = z_n$) one can proceed exactly as above, writing

$$Z_0 = \frac{1}{V_N} \int dU \, e^{I_0(U)} = \frac{1}{V_N} \int dU \, \exp \left(\sum_{n=1}^{\infty} \frac{z_n}{n} \text{Tr} U^n \text{Tr} U^{\dagger n} \right)$$

$$= \frac{1}{V_N} \int dU \prod_{n=1}^{\infty} \left(\sum_{p_n=0}^{\infty} \frac{z_n^{p_n}}{p_n! \, n^{p_n}} (\text{Tr} U^n \text{Tr} U^{-n})^{p_n} \right)$$

$$= \prod_{n=1}^{\infty} \frac{1}{1 - z_n} - C(N) \tag{A.8}$$

where $C(N)$ is given by

$$C(N) = \left[\prod_{n=1}^{\infty} \left(\sum_{p_n=0}^{\infty} z_n^{p_n} \right) - \frac{1}{V_N} \int dU \prod_{n=1}^{\infty} \left(\sum_{p_n=0}^{\infty} \frac{z_n^{p_n}}{p_n! \, n^{p_n}} (\text{Tr} U^n \text{Tr} U^{-n})^{p_n} \right) \right]_{\sum_n n p_n > N}$$

$$< \left[\prod_{n=1}^{\infty} \left(\sum_{p_n=0}^{\infty} z_n^{p_n} \right) \right]_{\sum_n n p_n > N} \equiv D(N) \tag{A.9}$$

Note the the subscript in the above equation indicates that one should only sum over those p_n which satisfy $\sum_n np_n > N$. $D(N)$ can be estimated as follows. Consider the expansion

$$\prod_{n=1}^{\infty} \frac{1}{1 - z_n t^n} = \sum_{n=0}^{\infty} a_n(z_1, z_2, ...)t^n \tag{A.10}$$

where a_n are polynomials in the z_i with positive coefficients. Note that

$$D(N) = \sum_{n=N+1}^{\infty} a_n(z_1, z_2, ...) \ . \tag{A.11}$$

Define

$$z_* = \max(z_1, z_2^{\frac{1}{2}}, z_3^{\frac{1}{3}}, ..., z_n^{\frac{1}{n}}, ...) \tag{A.12}$$

Below T_H, we have $z_* < 1$. Then we have $0 < a_n(z_1, z_2, ...) < a_n(z_*, z_*^2, z_*^3, ...) = b_n z_*^n$ where the b_n's are the coefficients of the series of $\prod_{m=1}^{\infty} \frac{1}{1-z_*^m} = \sum_{n=0}^{\infty} b_n z_*^n$. This series has radius of convergence equal to 1 because the function has no singularities for $|z_*| < 1$. It then follows that for a given $\epsilon > 0$ there exists an $M(\epsilon)$ such that for $n > M(\epsilon)$ it is true that $b_n < (1 + \epsilon)^n$. Then for $\epsilon < \frac{1}{z_*} - 1$ and $N > M(\epsilon)$ the following holds:

$$C(N) < D(N) < \sum_{n=N+1}^{\infty} ((1 + \epsilon)z_*)^n = \frac{((1 + \epsilon)z_*)^{N+1}}{1 - (1 + \epsilon)z_*} \tag{A.13}$$

and therefore the corrections are exponentially small since $(1 + \epsilon)z_* < 1$.

To summarize we find that

$$Z_0 = \frac{1}{V_N} \int dU \, \exp\left(\sum_n \frac{z_n}{n} \mathrm{Tr} U^n \mathrm{Tr} U^{\dagger n}\right) = \prod_{n=1}^{\infty} \frac{1}{1 - z_n} - K e^{-Nc} \tag{A.14}$$

where $c = -\log(z^*) > 0$ and $K > 0$.

A.3 Correlation functions

Correlation functions Eq. (2.16)

$$\langle \prod_{i=1}^{k}(\mathrm{Tr}U^{a_i})^{b_i} \prod_{j=1}^{s}(TrU^{-c_j})^{d_j}\rangle_U = \frac{1}{Z_0}\int dU\, e^{I_0(U)} \prod_{i=1}^{k}(\mathrm{Tr}U^{a_i})^{b_i} \prod_{j=1}^{s}(TrU^{-c_j})^{d_j} \quad (A.15)$$

where a_i, b_i, c_i, d_i are positive integers of order $O(N^0)$ can now be calculated easily using the technique above. Correlation functions of the form $\langle\prod_n(\mathrm{Tr}U^{a_n}\mathrm{Tr}U^{-a_n})^{b_n}\rangle_U$ are obtained by taking derivatives on Z_0 Eq. (A.14) with respect to $\frac{z_n}{n}$

$$\langle \prod_n(\mathrm{Tr}U^{a_n}\mathrm{Tr}U^{-a_n})^{b_n}\rangle = \frac{1}{Z_0}\prod_n n^{b_n}\frac{d^{b_n}Z_0}{dz_n^{b_n}} . \quad (A.16)$$

If in Eq. (A.15) the $\{(a_i, b_i)\}$ are not matched with $\{(c_i, d_i)\}$ up to reordering, due to A.5, the correlation function is zero up to nonperturbative corrections which are of order $(z^*)^N$. For example, $\langle \mathrm{Tr}U^a\mathrm{Tr}U^a\mathrm{Tr}U^{-2a}\rangle_U$ is zero at any finite order in $\frac{1}{N^2}$ expansion unless a is zero.

The above results can be summarized by the following: the integrals can be evaluated by treating each $\mathrm{Tr}U^n$ as an independent integration variable. More explicitly, replacing

$$\frac{1}{N}\mathrm{Tr}U^n \to \phi_n, \qquad \frac{1}{N}\mathrm{Tr}U^{-n} \to \phi_{-n} = \phi_n^*, \qquad \phi_0 = 1 \quad (A.17)$$

then

$$\langle \tfrac{1}{N}\mathrm{Tr}U^{s_1}\tfrac{1}{N}\mathrm{Tr}U^{s_2}\cdots\tfrac{1}{N}\mathrm{Tr}U^{s_F}\rangle_U$$
$$= \tfrac{1}{Z_0}\int_{-\infty}^{\infty}\prod_{i=1}^{\infty}d\phi_i d\phi_i^* \ \phi_{s_1}\cdots\phi_{s_F} \ \exp\left(-N^2\sum_{n=1}^{\infty}\tfrac{1-z_n}{n}\phi_n\phi_n^*\right) +$$
$$+\text{nonperturbative in } N . \quad (A.18)$$

Appendix B

Thermodynamic properties of solution

B.1 Thermodynamic properties of Eq. (4.2)

It can be verified that a stationary point for Eq. (4.2) with $\Lambda = -6/L^2$ is given by

$$ds^2 = -(n_\sharp)^2(p(r) + h(r))dt^2 + \frac{1}{(p(r) + h_1(r))}dr^2 + \frac{r^2}{L^2}d\vec{x}^2, \tag{B.1}$$

with $p(r) = -(\frac{r^2\Lambda}{6} + \frac{m^2}{r^2}) = \frac{r^2}{L^2} - \frac{m^2}{r^2}$, and

$$h(r) = 36\left(\frac{5}{27}\alpha_1 + \frac{1}{27}\alpha_2 + \frac{1}{54}\alpha_3\right)r^2 + 2\alpha_3\frac{a^2}{r^6}. \tag{B.2}$$

The location of the horizon is now

$$R_h = r_h(1 - \frac{1}{3}(5\alpha_1 + \alpha_2 + 2\alpha_3)) \tag{B.3}$$

with $r_h^4 = m^2b^2$.

The Hawking temperature can be calculated to be

$$T_H = n_\sharp\frac{1}{4\pi}\partial_r\left(f(r) + h(r)\right)|_{R_h} = n_\sharp\frac{R_h}{L^2\pi}\left(1 + \frac{1}{3}(20\alpha_1 + 4\alpha_2 - 4\alpha_3)\right), \tag{B.4}$$

using the usual arguments. The temperature in the bulk and the boundary agree in coordinates where $n_\sharp = 1 - \frac{1}{3}(10\alpha_1 + 2\alpha_2 + \alpha_3)$.

B.2 Wald entropy formula

Instead of the procedure described in section 4.3, one could use the formula Wald derived for the entropy (see, for example, [28]). Given the action Eq. (4.2), the formula for the entropy is

$$
\begin{aligned}
S_{Wald} = 4\pi \int_{Horizon} d^3x \sqrt{h} \times \\
\times \left(1 + L^2(2\alpha_1 + \alpha_2 + 2\alpha_3)R - L^2(\alpha_2 + 4\alpha_3)h^{ij}R_{ij} + 2\alpha_3 L^2 h^{ij}h^{kl}R_{ikjl}\right),
\end{aligned} \quad \text{(B.5)}
$$

where the h_{ij} is the induced metric on the horizon and the Rieman and Ricci tensor are evaluated using the metric Eq. (B.1) with $\alpha_1, \alpha_2, \alpha_3 = 0$. From Eq. (B.5) the entropy density is

$$
s = \frac{1}{4G_N} \frac{R_h^3}{b^3} \left(1 - 8(5\alpha_1 + \alpha_2 - \alpha_3)\right)
$$

A particular case is the Gauss-Bonnet term ($\alpha_1 = 1; \alpha_2 = -4; \alpha_3 = 1$), for which the first and second coefficients vanish, and the contribution of $h^{ij}h^{kl}R_{ikjl}$ is zero. We recover therefore that adding the Gauss-Bonnet term at leading order in $\alpha_1, \alpha_2, \alpha_3$ gives no correction to the entropy if the horizon is a flat manifold ([19]).

Appendix C

Derivation of (4.38)

In this appendix we give some details for obtaining $g_1(z)$ in equation (4.38). Plugging (4.37) into the equation of motion (4.31) one finds a fairly complicated ODE for $g_1(z)$. But, by changing variable a few times, it reduces to a simpler one. Namely, defining

$$u = \sqrt{1 - 4\lambda_{GB} + 4\lambda_{GB}\frac{1}{z^4}}, \quad v = 1 - u, \qquad (C.1)$$

we get

$$(1 - v)(\partial_v(v\partial_v g_1 + 1)) + 2(v\partial_v g_1 + 1) = 0 . \qquad (C.2)$$

Here, we note that $-\ln(v)$ is a (singular) solution, as one can also show from more abstract reasoning. In fact, this led to our choice of change of variable. Now, we will solve this equation. Defining

$$h_1(u) = (u - 1)\partial_u g_1 + 1, \qquad (C.3)$$

we have

$$u\partial_u h_1 = 2h_1, \qquad (C.4)$$

which leads to

$$h_1 = c_1 u^2 \qquad (C.5)$$

105

where c_1 is an integration constant. Thus we find that

$$\partial_u g_1 = \frac{c_1 u^2 - 1}{u - 1} = u + 1 \quad \text{choosing } c_1 = 1 \ . \tag{C.6}$$

Note in order for $g_1(u)$ to be nonsingular at the horizon $u = 1$, we need to choose $c_1 = 1$ as we have done above. Thus we have

$$g_1 = \frac{1}{2} u^2 + u + c_2 \ . \tag{C.7}$$

We will choose the integration constant c_2 so that $g_1 \to 0$ as $z \to \infty$. This then leads to (4.38).

Appendix D

Calculation of η/s without field redefinition

This appendix is organized as follows: first we'll write down the equations for a perturbation on the background Eq. (B.1), using the action Eq. (4.2) and then we'll perform a calculation of η/s using the three methods outlined in the text, without doing the field redefinition Eq. (4.14).

D.1   The equations

From the action,

$$I = \frac{1}{16\pi G_N} \int d^5x \sqrt{-g}\left(R - 2\Lambda + L^2\left(\alpha_1 R^2 + \alpha_2 R_{\mu\nu}R^{\mu\nu} + \alpha_3 R^{\mu\nu\rho\sigma}R_{\mu\nu\rho\sigma}\right)\right) , \quad \text{(D.1)}$$

the equations of motion at linear level in α_i, $i = 1, 2, 3$ are

$$R_{\mu\nu} - \frac{1}{2}Rg_{\mu\nu} + \Lambda g_{\mu\nu} + \left(\alpha_1(-\frac{1}{2}R^2 g_{\mu\nu} + 2RR_{\mu\nu} + 2\nabla^2 Rg_{\mu\nu} - 2\nabla_\mu\nabla_\nu R\right) +$$

$$+ \alpha_2 \left(-\frac{1}{2}R^{\lambda\rho}R_{\lambda\rho}g_{\mu\nu} + 2R_\mu^\lambda R_{\lambda\nu} + \nabla^2 R_{\mu\nu} - \nabla^\rho\nabla_\nu R_{\mu\rho} - \nabla^\rho\nabla_\mu R_{\nu\rho} + \nabla^\rho\nabla^\sigma R_{\rho\sigma}g_{\mu\nu}\right) +$$

$$+ \alpha_3 \left(-4\nabla^\rho\nabla^\sigma R_{\mu\rho\sigma\nu} + 2R_\mu{}^{\rho\sigma\gamma}R_{\nu\rho\sigma\gamma} - \frac{1}{2}g_{\mu\nu}R^{\rho\sigma\beta\gamma}R_{\rho\sigma\beta\gamma}\right) = 0. \quad \text{(D.2)}$$

This expression can be simplified using the following identities,

$$\nabla^\rho \nabla^\sigma R_{\rho\sigma} = \frac{1}{2}\nabla^2 R$$

$$\nabla^\rho \nabla^\sigma R_{\mu\rho\sigma\nu} = \nabla^\rho(-\nabla_\rho R_{\mu\nu} + \nabla_\mu R_{\rho\nu}) = -\nabla^2 R_{\mu\nu} + \frac{1}{2}\nabla_\mu\nabla_\mu R + R_{\lambda\mu}R_\nu^\lambda - R_{\lambda\nu\rho\mu}R^{\rho\lambda}$$

$$\nabla^\rho \nabla_\mu R_{\nu\rho} + \nabla^\rho \nabla_\nu R_{\rho\mu} = \nabla_\mu\nabla_\nu R + 2R_{\lambda\mu}R_\nu^\lambda - 2R_{\lambda\nu\rho\mu}R^{\lambda\rho}.$$

Using the identities above, Eq. (D.2) can be written as

$$\begin{aligned}
R_{\mu\nu} &- \frac{1}{2}Rg_{\mu\nu} + \Lambda g_{\mu\nu} + \nabla^2 Rg_{\mu\nu}(2\alpha_1 + \frac{1}{2}\alpha_2) + \\
&+ \nabla_\mu\nabla_\mu R(-2\alpha_1 - \alpha_2 - 2\alpha_3) + \nabla^2 R_{\mu\nu}(\alpha_2 + 4\alpha_3) + \\
&+ R_\mu^\lambda R_{\lambda\mu}(-4\alpha_3) + R_{\lambda\nu\rho\mu}R^{\lambda\rho}(2\alpha_2 + 4\alpha_3) - \frac{1}{2}g_{\mu\nu}(\alpha_1 R^2 + \alpha_2 R^{\mu\nu}R_{\mu\nu} + \alpha_3 R^{\rho\sigma\beta\gamma}R_{\rho\sigma\beta\gamma}) + \\
&+ 2\alpha_1 RR_{\mu\nu} + 2\alpha_3 R_\mu{}^{\rho\sigma\lambda}R_{\nu\rho\sigma\lambda} = 0
\end{aligned} \qquad (D.3)$$

In the case of the Gauss-Bonnet term, with $\alpha_1 = \frac{\lambda_{GB}}{2} = \alpha_3, \alpha_2 = -2\lambda_{GB}$, Eq. (D.3) simplifies to be

$$\begin{aligned}
R_{\mu\nu} &- \frac{1}{2}Rg_{\mu\nu} + \Lambda g_{\mu\nu} + \left[-2\lambda_{GB}R_\mu^\lambda R_{\lambda\mu} - \frac{\lambda_{GB}}{4}g_{\mu\nu}(R^2 - 4R^{\mu\nu}R_{\mu\nu} + \right. \\
&+ R^{\rho\sigma\beta\gamma}R_{\rho\sigma\beta\gamma}) + \lambda_{GB}RR_{\mu\nu} - 2\lambda_{GB}R_{\lambda\nu\rho\mu}R^{\lambda\rho} + \lambda_{GB}R_\mu{}^{\rho\sigma\lambda}R_{\nu\rho\sigma\lambda} \left. \right] = 0 \quad (D.4)
\end{aligned}$$

As described in chapter 4, if one considers perturbation dependent only on (t, r, x_3), there are three decoupled modes propagating on the black brane background, corresponding to shear, scalar and sound channel. In the following sections we use all three of these channels to calculate η/s.

D.1.1   Kubo formula and the scalar channel

The Kubo formula relates shear viscosity over entropy density ratio to correlation functions of the stress energy tensor at finite temperature. Since the correlation function is calculated at zero spatial momentum, using any channel will give the same result, as explained above. In particular one could use the scalar channel. Expanding

now the action Eq. (D.1), and collecting all terms quadratic in the perturbation, we obtain an effective action $\tilde{I}_2$. In order to be consistent with the previous notation we can change variable to z and Fourier transform in t and $\vec{x}$. The structure of the effective action for $\phi_\omega(z) = g^{xx}h_{tr}$ will be:

$$\tilde{I}_2[\phi] = \frac{1}{16\pi G_N} \int \frac{d\omega d^3\vec{k}}{(2\pi)^4} \int_0^1 dz \big(A\phi''_\omega(z)\phi_{-\omega}(z) + B\phi'_\omega(z)\phi'_{-\omega}(z) + $$
$$+ C\phi'_\omega(z)\phi_{-\omega}(z) + D\phi_\omega(z)\phi_{-\omega}(z) + E\phi''_\omega(z)\phi''_{-\omega}(z) + F\phi''_\omega(z)\phi'_{-\omega}(z) \big). \quad \text{(D.5)}$$

In order to have a well defined variational principle, one has to add boundary terms in the action. The details are explained in [18], of which we are following the notation. Changing coordinates to $z = r/R_h$, and introducing dimensionless variables, $w = \omega L^2/(n_\sharp R_h)$, $k = qL^2/(R_h)$, the equations of motion are

$$A\phi''_\omega + C\phi'_\omega + 2D\phi_\omega - (2B\phi'_\omega + C\phi_\omega + F\phi''_\omega)' + (a\phi_\omega + 2E\phi''_\omega + F\phi'_\omega)'' = 0, \quad \text{(D.6)}$$

or explicitly

$$\phi''(z) + \frac{1 - 5z^4}{z(1 - z^4)}\phi'(z) + \frac{k^2 + (-k^2 + w^2)z^4}{(1 - z^4)^2}\phi(z) + J = 0 \quad \text{(D.7)}$$

where J is linear in the α_i. J can be expressed as $J = J_4\phi''''(z) + J_3\phi'''(z) + J_2\phi''(z) + J_1\phi'(z) + + J_0\phi(z)$, where the J_i are,

$$J_4 = z^2(1 - \frac{1}{z^4})(\alpha_2 + 4\alpha_3)$$

$$J_3 = \frac{1}{z^3}(1 + 7z^4)(\alpha_2 + 4\alpha_3)$$

$$J_2 = 0$$

$$J_1 = \frac{-1}{z^5(-1 + z^4)^2}2((5 + z^4(-1 - 45z^4 + 105z^8 + 2w^2(z^2 + z^6)))\alpha_2 +$$
$$+ 4(2 + z^4(5 - 48z^4 + 105z^8 + 2w^2(z^2 + z^6)))\alpha_3) - 4(z^2(-1 + z^4)^2(\alpha_2 + 4\alpha_3))k^2$$

$$J_0 = \frac{1}{3(-1 + z^4)^3}w^2(15\alpha_2 + 48\alpha_3 - 3w^2z^6(\alpha_2 + 4\alpha_3) + z^4(40\alpha_1 + 98\alpha_2 + 376\alpha_3) -$$
$$- z^8(40\alpha_1 + 161\alpha_2 + 616\alpha_3)) +$$
$$+ \frac{k^2}{3z^4(-1 + z^4)^2}((-3(5\alpha_2 + 2\alpha_3) + 6w^2z^6(\alpha_2 + 4\alpha_3) - 2z^4(10\alpha_1 + 23\alpha_2 + 112\alpha_3) +$$

$$+ z^8(20\alpha_1 + 157\alpha_2 + 614\alpha_3)) - \frac{(\alpha_2 + 4\alpha_3)k^4}{z^2(-1+z^4)} \tag{D.8}$$

We impose the Ansatz $\phi = (z-1)^{ic_1 + c_2(\alpha_1,\alpha_2,\alpha_3)}f(z)$, and we solve perturbatively in the α_i. The exponent is fixed expanding Eq. (D.7) close to the boundary $z = 1$ in the following way. We set $\alpha_i = 0$, expand around $z = 1$ and determine $c_1 = \pm\frac{w}{4}$, and recursive relations between derivatives of f at $z = 1$. For example, when $k = 0$, one obtains $f'(1) = -\frac{iw(w-10i)f[1]}{8(w+2i)}$ and $f''(1) = f(1)\frac{w(480i+80w+30iw^2-w^3)}{64(w^2+6iw-8)}$. Reintroducing now the α_i and expanding again at $z = 1$, we can fix the exponent. It can be verified with little effort that the exponent at linear order in the perturbation is independent of k at linear order in α_i. The final result, when $\alpha_i \neq 0, k = 0$ is (in terms of ω)

$$\phi_\omega(r) = \left(1 - \frac{1}{z^4}\right)^{-\frac{iL^2\omega}{n_\sharp 4R_h}(1-\frac{4}{3}(5\alpha_1+\alpha_2-\alpha_3))} \left(1 - \frac{3i\omega L^2}{2R_h}\frac{\alpha_3}{n_\sharp z^4} + \mathcal{O}(\omega^2)\right) \tag{D.9}$$

This solution satisfies the equations Eq. (D.2) up to order ω with incoming boundary conditions at the horizon and normalized to 1 at the boundary $z \to \infty$. Note that the exponent can be written compactly in terms of the Hawking temperature as $-i\frac{\omega}{4\pi T_H}$.

Now that we have the solution we can use Eq. (D.9) to evaluate the action on shell. The Minkowski AdS/CFT prescription tells us that if $I_{on-shell} = \frac{1}{16\pi G_N}\int d^4k/(2\pi)^4 \mathcal{F}|_{R_h}^\infty$, then $G_{xy,xy}^R(\omega, 0) = \lim_{r\to\infty} 2\mathcal{F}$. When varying the action,

$$\delta\tilde{I}_2 = \frac{1}{16\pi G_N}\int\frac{d\omega d\vec{k}}{(2\pi)^4}\left(\int_0^1 dz[EOM]\delta\phi_{-\omega} + (\mathcal{B}_1\delta\phi + \mathcal{B}_2\delta\phi')|_{R_H}^\infty\right)$$

the boundary terms are

$$\mathcal{B}_1 = -(A\phi_\omega')' + 2B\phi_\omega' + C\phi_\omega - 2(E\phi_\omega'')' + F\phi_\omega'' - (F\phi_\omega')'$$
$$\mathcal{B}_2 = A\phi_\omega + F\phi_\omega' + 2E\phi_\omega'' \tag{D.10}$$

The boundary term proportional to $\delta\phi'$ can be canceled at linear order in ϵ by a

Gibbons-Hawking term of the form

$$\mathcal{K} = -A\phi'_\omega \phi_{-\omega} - \frac{F}{2}\phi'_\omega \phi'_{-\omega} + E(p_1\phi'_\omega \phi'_{-\omega} + 2p_0\phi_\omega \phi'_{-\omega}), \tag{D.11}$$

where p_1 and p_0 are defined as the coefficients of ϕ' and ϕ respectively in Eq. (D.7).

The bulk action, Eq. (D.5) can be re-written as

$$\tilde{I}_2[\phi] = \frac{1}{16\pi G_N} \int \frac{d\omega d^3\vec{k}}{(2\pi)^4} \int_0^1 dz \left(\frac{\partial}{\partial z}\mathcal{B} + \frac{1}{2}[EOM]\phi_{-\omega} \right)$$

where ([18])

$$\mathcal{B} = -\frac{A'}{2}\phi_\omega \phi_{-\omega} + B\phi'_\omega \phi_{-\omega} + \frac{C}{2}\phi_\omega \phi_{-\omega} - E'\phi''_\omega \phi_{-\omega} +$$
$$+ E\phi''_\omega \phi'_{-\omega} - E\phi'''_\omega \phi_{-\omega} + \frac{F}{2}\phi'_\omega \phi'_{-\omega} - \frac{F'}{2}\phi'_\omega \phi_\omega \tag{D.12}$$

so that the on-shell action, after addition of the Gibbons-Hawking term, reduces to

$$\mathcal{F} = \int \frac{d\omega d\vec{k}}{(2\pi)^4}(\mathcal{K} + \mathcal{B})|_0^1. \tag{D.13}$$

Plugging in, one calculates

$$\lim_{z \to 0} 2\mathcal{F}_\omega = CT + i\omega \frac{R_h^3}{L^3}(1 - 8(5\alpha_1 + \alpha_2))$$

CT contains all contact and momentum independent terms that according to [18] must be discarded. Using Kubo's formula, this gives a value of the shear viscosity

$$\eta = \frac{1}{16\pi G_N} \frac{R_h^3}{L^3}(1 - 8(5\alpha_1 + \alpha_2)).$$

In the case of the Gauss-Bonnet term, with $\alpha_1 = c_{GB}, \alpha_2 = -4c_{GB}, \alpha_3 = c_{GB}$, the terms proportional to E in Eq. (D.12) vanish, and the value of the shear viscosity is

$$\eta_{GB} = \frac{1}{16\pi G_N} \frac{R_h^3}{L^3}(1 - 4\lambda_{GB}). \tag{D.14}$$

This gives a ratio of viscosity over entropy density equal to

$$\frac{\eta}{s} = \frac{1}{4\pi}(1 - 8\alpha_3).$$

(D.15)

For the Gauss-Bonnet term, we obtain the usual result:

$$\frac{\eta}{s} = \frac{1}{4\pi}(1 - 4\lambda_{GB})$$

(D.16)

D.1.2 Shear channel

In the shear channel Eq. (D.2) become a set of three coupled differential equations for the variables $A_0(t, r, x_3)$ and $A_z(t, r, x_3)$ (we set $h_{1r} = 0$ with a gauge transformation). Following [62] and [9] we Fourier transform in the time and x_3 direction, and we consider the gauge invariant quantity $Z(r) = qA_0(r) + \omega A_3 = -iF_{tz}$. The equation in the h_{3r} direction must be used as a constraint to decouple this equation.

Changing coordinates to $z = r/R_h$, and introducing dimensionless variables, $w = \omega L^2/(n_{\parallel}R_h)$, $k = qL^2/(R_h)$, the equation for the perturbation becomes,

$$Z''(z) + \frac{w^2z^4(1 - 5z^4) + 5k^2(-1 + z^4)^2}{z(z^4 - 1)(-w^2z^4 + k^2(-1 + z^4))}Z'(z) + \frac{w^2z^4 - k^2(z^4 - 1)}{(-1 + z^4)^2}Z(z) + J = 0$$

(D.17)

where $J = J_0Z(z) + J_1Z'(z) + J_2Z''(z) + J_3Z'''(z) + J_4Z''''(z)$ is proportional to α_i and is given by

$$J_4 = \frac{(-1 + z^4)(\alpha_2 + 4\alpha_3)}{z^2}$$

$$J_3 = \frac{2(-w^2z^4(1 + 7z^4) + k^2(3 - 10z^4 + 7z^8))(\alpha_2 + 4\alpha_3)}{z^3(-w^2z^4 + k^2(-1 + z^4))}$$

$$J_2 = 0$$

$$J_1 = \frac{2}{3z^5(-1 + z^4)^2(w^2z^4 - k^2(-1 + z^4))^2}[6k^6z^2(-1 + z^4)^4(\alpha_2 + 4\alpha_3) -$$

$$- 3w^4z^8[(5 - z^4 + 2w^2z^6 - 45z^8 + 2w^2z^{10} +$$

$$+ 105z^{12})\alpha_2 + 4(2 + 5z^4 + 2w^2z^6 - 48z^8 + 2w^2z^{10} + 105z^{12})\alpha_3] -$$

$$- 3k^4(-1 + z^4)^2[(15 + 75z^4 - 2w^2z^6 - 195z^8 + 6w^2z^{10} + 105z^{12})\alpha_2 +$$

$$+ 4(17 + 71z^4 - 2w^2z^6 - 193z^8 + 6w^2z^{10} + 105z^{12})\alpha_3] +$$

$$+2k^2w^2z^4(-1+z^4)[198\alpha_2+4z^8(5\alpha_1-89\alpha_2-361\alpha_3)+816\alpha_3+$$

$$+3w^2z^6(\alpha_2+4\alpha_3)+9w^2z^{10}(\alpha_2+4\alpha_3)+$$

$$+315z^{12}(\alpha_2+4\alpha_3)-z^4(20\alpha_1+253\alpha_2+1016\alpha_3)]]$$

$$J_0=-\frac{1}{3z^4(-1+z^4)^3(-w^2z^4+k^2(-1+z^4))}\times$$

$$\times\left[3k^6z^2(-1+z^4)^3(\alpha_2+4\alpha_3)+3k^2w^2z^4(-1+z^4)[-74\alpha_2-298\alpha_3+\right.$$

$$+3w^2z^6(\alpha_2+4\alpha_3)-4z^4(5\alpha_1+20\alpha_2+76\alpha_3)+2z^8(10\alpha_1+53\alpha_2+205\alpha_3)]-$$

$$-k^4(-1+z^4)^2[9w^2z^6(\alpha_2+4\alpha_3)-$$

$$-3(5\alpha_2+26\alpha_3)-2z^4(10\alpha_1+71\alpha_2+268\alpha_3)+z^8(20\alpha_1+157\alpha_2+614\alpha_3)]+$$

$$+w^4z^8[15\alpha_2+48\alpha_3-3w^2z^6(\alpha_2+4\alpha_3)+z^4(40\alpha_1+98\alpha_2+376\alpha_3)-$$

$$-z^8(40\alpha_1+161\alpha_2+616\alpha_3)]] \tag{D.18}$$

Solution to this equation at first order in α_i and for small k, fixed ω/k is

$$Z(z)=\left(1-\frac{1}{z^4}\right)^{-\frac{iw}{4}+\frac{1}{3}(5\alpha_1+\alpha_2-\alpha_3)}\left[1+i\frac{k^2}{4w}\left(1-2\alpha_3\left(\frac{1}{z^4}+3(1-\frac{w^2}{k^2})\right)\right)+\mathcal{O}(k^2)\right].$$

The exponent can be easily expressed in terms of the temperature, $-\frac{iw}{4}+\frac{1}{3}(5\alpha_1+\alpha_2-\alpha_3)=\frac{-i\omega}{4\pi T_H}$, and it's the same in all three channels.

The quasi-normal frequency is now obtained imposing Dirichlet boundary condition at infinity $z\to\infty$. Neglecting the term of order w^2, one obtains the condition

$$1+i\frac{k^2}{4w}(1-6\alpha_3)=0.$$

Reintroducing the original variables this is

$$\omega=-iq^2D=-iq^2\frac{n_\sharp L^2}{4R_h}(1-6\alpha_3).$$

In terms of temperature

$$D=\frac{1}{4\pi T_H}(1-8\alpha_3)$$

so now eta over s is

$$\left.\frac{\eta}{s}\right|_{shear}=\frac{1}{4\pi}(1-8\alpha_3)$$

113

D.1.3 Sound channel

The procedure to deal with the sound channel is analogous to the shear channel, apart from the fact that the algebra in this situation is much more complicated. In this case we can look for solution with ω and q of the same order. We can therefore follow the procedure of extracting the quasi-normal frequency in [9]. Using the same notation as in the shear channel $(w = \omega L^2/(n_\sharp R_h),\ k = qL^2/R_h)$, the equation is

$$
Z''(z) + Z'(z) \left(\frac{3w^2 z^4 (1 - 5z^4) + k^2(9 - 16z^4 + 15z^8)}{z(-1 + z^4)(-3w^2 z^4 + k^2(-1 + 3z^4))} \right) +
$$
$$
+ Z(z) \left(\frac{-3w^4 z^{10} + 2k^2 w^2 z^6 (-2 + 3z^4) - k^2(-1 + z^4)(-16 + k^2 z^2(-1 + 3z^4))}{z^2(-1 + z^4)^2(-3w^2 z^4 + k^2(-1 + 3z^4))} \right) +
$$
$$
+ J_{sound} = 0 \tag{D.19}
$$

The expression for J_{sound} will be contained in the next subsection. Solution to the equations of motion for small k and finite w/k is

$$
Z(z) = (1 - 1/z^4)^{ex} \left[\frac{1}{2k^2 - 3w^2} \left[-3w^2 + k^2 \left(1 + \frac{1}{z^4} - iw \left(1 - \frac{1}{z^4} \right) \right) \right] \right] +
$$
$$
+ \frac{1}{(6(2k^2 - 3W^2)^2 z^4)} \left(1 - \frac{1}{z^4} \right) \left[81 i w^5 z^4 \alpha_3 + \right.
$$
$$
+ 3k^2 w^2 \left(3(-12 - 7iw)\alpha_3 + z^4 (40\alpha_1 + 8\alpha_2 + (-20 - 63iw)\alpha_3) \right) +
$$
$$
\left. + 2k^4 (12(3 + z^4)\alpha_3 + iw(21\alpha_3 + z^4 (40\alpha_1 + 8\alpha_2 + 37\alpha_3)))) \right], \tag{D.20}
$$

The exponent ex is the same as for the shear channel, $ex = \frac{-iw}{4\pi T_H}$. One obtains a quasi-normal frequency equal to:

$$
\omega = \tilde{c}_s q - i\Gamma_{sound} q^2 =
$$
$$
= \frac{q}{\sqrt{3}} n_\sharp \left[1 + \left(\frac{10}{3}\alpha_1 + \frac{2}{3}\alpha_2 + \frac{1}{3}\alpha_3 \right) \right] - q^2 n_\sharp \frac{iL^2}{6R_h} [1 - 6\alpha_3] \tag{D.21}
$$

In the case of a conformal invariant theory, the coefficient of iq^2 in the dispersion relation is $\Gamma_{sound} = \frac{2}{3} D_s$. This result is therefore compatible with a dual gauge theory which is scale invariant and described by hydrodynamics,

$$
D_s = \frac{3}{2}\Gamma_{sound} = \frac{n_\sharp L^2}{4R_h} (1 - 6\alpha_3). \tag{D.22}
$$

After taking into account the value of $n_\sharp$, it's easy to show that the speed of sound in the gauge theory is

$$c_s = \frac{1}{\sqrt{3}},$$

(D.23)

and the diffusion coefficient agrees with what calculated in the shear channel,

$$\frac{\eta}{s}\bigg|_{sound} = \frac{\eta}{s}\bigg|_{shear} = \frac{1}{4\pi}(1 - 8\alpha_3).$$

(D.24)

D.1.4 J_{sound}

Writing $J_{sound} = J_0 Z_s(z) + J_1 Z_s'(z) + J_2 Z_s''(z) + J_3 Z_s'''(z) + J_4 Z_s''''(z)$, we obtain,

$$J_4 = \frac{1}{\left(3z^2 \left(k^2 + 3\left(-k^2 + w^2\right)z^4\right)^2\right)} \times$$

$$\times \left(\left(-1 + z^4\right)\left(27w^4 z^8(\alpha_2 + 4\alpha_3) - 18k^2 w^2 z^4 \left(-1 + 3z^4\right)(\alpha_2 + 4\alpha_3)+\right.\right.$$

$$\left.\left. + k^4 \left(32\alpha_1 + \left(19 - 18z^4 + 27z^8\right)\alpha_2 + 4\left(11 - 18z^4 + 27z^8\right)\alpha_3\right)\right)\right)$$

$$J_3 = -\frac{2}{3\left(3w^2 z^5 + k^2\left(z - 3z^5\right)\right)^3} \times$$

$$\times \left(-81w^6 z^{12}\left(1 + 7z^4\right)(\alpha_2 + 4\alpha_3) + 27k^2 w^4 z^8 \left(5 - 20z^4 + 63z^8\right)(\alpha_2 + 4\alpha_3)+\right.$$

$$+ k^6 \left(32\left(7 + 12z^4 - 3z^8\right)\alpha_1 + \left(133 + 30z^4 + 420z^8 - 702z^{12} + 567z^{16}\right)\alpha_2+\right.$$

$$\left. + 4\left(77 - 66z^4 + 444z^8 - 702z^{12} + 567z^{16}\right)\alpha_3\right) -$$

$$- 3k^4 w^2 z^4 \left(-32\left(-9 + z^4\right)\alpha_1 + \left(105 + z^4 \left(185 + 63z^4 \left(-7 + 9z^4\right)\right)\right)\alpha_2+\right.$$

$$\left.\left. + 4\left(33 + z^4 \left(193 + 63z^4 \left(-7 + 9z^4\right)\right)\right)\alpha_3\right)\right)$$

$$J_2 = 0$$

$$J_1 = \frac{2}{3(-1 + z^4)^2(3w^2 z^5 + k^2(z - 3z^5))^5} \times$$

$$\times \left(-729w^{10} z^{20}((5 + z^4(-1 - 45z^4 + 105z^8 + 2w^2(z^2 + z^6)))\alpha_2+\right.$$

$$+ 4(2 + z^4(5 - 48z^4 + 105z^8 + 2w^2(z^2 + z^6)))\alpha_3) -$$

$$- 54k^4 w^6 z^{12}(8(42 + z^4(-49 + 4w^2 z^2(-3 + 5z^4) + 15z^4(31 - 25z^4 + 3z^8)))\alpha_1+$$

$$+ (843 + z^4(-3361 + 3z^4(1550 + 2966z^4 - 6951z^8 + 4725z^{12})+$$

$$+ w^2 z^2(-63 + 5z^4(31 - 45z^4 + 81z^8))))\alpha_2+$$

$$+ 4(861 + z^4(-3791 + 3z^4(1472 + 3144z^4 - 6999z^8+$$

$$+ 4725z^{12}) + w^2 z^2(-39 + 5z^4(23 - 45z^4 + 81z^8))))\alpha_3) + 18k^6 w^4 z^8(8(-966+$$

$$+ z^4(4295 + 16w^2 z^2(5 - 17z^4 + 15z^8) + z^4(-5396 + 45z^4(122 - 62z^4 + 3z^8))))\alpha_1+$$

$$+ (-4311 + z^4(21182 + 4w^2 z^2(95 + z^4(-392 + 15z^4(40 - 36z^4 + 27z^8))) + z^4(-29333+$$

$+ 3z^4(3340 + 3z^4(6167 - 9426z^4 + 4725z^8)))))\alpha_2 + 4(-2523 + z^4(13888 + 4w^2z^2(55+$

$+ z^4(-256 + 15z^4(32 - 36z^4 + 27z^8))) + z^4(-22537 + 3z^4(1348 + 3z^4(6511 - 9420z^4+$

$+ 4725z^8)))))\alpha_3) - 3k^8w^2z^4(16(1550+$

$+ z^4(-10175 + 8w^2z^2(-17 + z^4(119 + 45z^4(-5 + 3z^4)))) +$

$+ 3z^4(9161 + z^4(-10214 + 15z^4(464 + 3z^4(-57 + z^4))))))\alpha_1 + (11755 + z^4(-78451+$

$+ 3z^4(70625 + 9z^4(-7417 - 261z^4 + 10509z^8 - 11909z^{12} + 4725z^{16})) + 2w^2z^2(-619+$

$+ z^4(4633 + 45z^4(-238 + 3z^4(86 - 57z^4 + 27z^8))))))\alpha_2+$

$+ 4(5720 + z^4(-39869 + 3z^4(37406+$

$+ 3z^4(-11255 - 7132z^4 + 33453z^8 - 35526z^{12} + 14175z^{16})) + 2w^2z^2(-347 + z^4(2729+$

$+ 45z^4(-158 + 3z^4(70 - 57z^4 + 27z^8))))))\alpha_3) - 2k^{12}(z - 4z^5 + 3z^9)^2(32(-1 + 15z^4)\alpha_1-$

$- 19\alpha_2 - 44\alpha_3 + 3z^4((89 + 27z^4(-1 + z^4))\alpha_2+$

$+ 4(49 + 27z^4(-1 + z^4))\alpha_3)) + k^{10}(32(199+$

$+ z^4(1042 + 8w^2z^2(-1 + 3z^4)(-5 + 46z^4 - 84z^8 + 45z^{12}) - 3z^4(2841 + z^4(-7028+$

$+ 5z^4(1489 - 846z^4 + 243z^8)))))\alpha_1+$

$+ 3781\alpha_2 + 8624\alpha_3 + z^4((10888 + 4w^2z^2(-1 + 3z^4)(-181+$

$+ z^4(1703 + 3z^4(-1220 + 3z^4(376 - 207z^4 + 81z^8))))+$

$+ 3z^4(-37464 + z^4(91280 + z^4(-73322+$

$+ 45z^4(-328 + 3z^4(640 - 576z^4 + 189z^8))))))\alpha_2+$

$+ 4(3113 + 4w^2z^2(-1 + 3z^4)(-101 + z^4(967+$

$+ 3z^4(-772 + 888z^4 - 621z^8 + 243z^{12}))) + 3z^4(-15995 + z^4(39379 + z^4(-21835+$

$+ 27z^4(-1501 + 3413z^4 - 2853z^8 + 945z^{12})))))\alpha_3)) + 81k^2w^8z^{16}(-3(141\alpha_2 + 616\alpha_3)+$

$+ z^4(80(-1 + z^4)^2\alpha_1 + 1204\alpha_2 + 4748\alpha_3 + z^2(12w^2(-1 + 2z^4 + 9z^8)(\alpha_2 + 4\alpha_3)+$

$+ z^2((898 - 4484z^4 + 4725z^8)\alpha_2 + 4(1049 - 4579z^4 + 4725z^8)\alpha_3)))))$

$J_0 = -\dfrac{1}{3z^6(-1 + z^4)^3(k^2 + 3(-k^2 + w^2)z^4)^5} \times$

$\times (-k^{14}z^4(-1 + z^4)^2(-1 + 3z^4)^3(32\alpha_1+$

$+ (19 - 18z^4 + 27z^8)\alpha_2 + 4(11 - 18z^4 + 27z^8)\alpha_3)-$

$- 9k^6w^4z^8(8(11328 + z^4(12w^4z^8(-3 + 5z^4)-$

$- 8(4903 + z^4(-5392 + 15z^4(142 - 24z^4 + 9z^8)))$

$+ w^2z^2(824 + z^4(-1891 + z^4(4940 + 3z^4(-338 + 75z^4(-20 + 9z^4)))))))\alpha_1+$

$+ (54048 + z^4(3w^4z^8(-163 + 815z^4 - 1485z^8 + 945z^{12}) + 32(-7567 + z^4(13366+$

$+ 9z^4(-1226 + 265z^4 + 129z^8)))+$

$+ 4w^2z^2(1406 + z^4(-5287 + z^4(5276+$

$$+ 3z^4(7018 - 14190z^4 + 7155z^8))))))\alpha_2 + 4(33048$$

$$+ z^4(3w^4z^8(-139 + 775z^4 - 1485z^8 + 945z^{12}) + 8(-22415 + 49286z^4 - 49758z^8 +$$

$$+ 15543z^{12} + 3213z^{16}) +$$

$$+ w^2z^2(4261 - 19511z^4 + 16414z^8 + 82374z^{12} - 161955z^{16} + 83025z^{20})))\alpha_3) +$$

$$+ 243w^{12}z^{26}(3w^2z^6(\alpha_2 + 4\alpha_3) - 3(5\alpha_2 + 16\alpha_3) - 2z^4(20\alpha_1 + 49\alpha_2 + 188\alpha_3) +$$

$$+ z^8(40\alpha_1 + 161\alpha_2 + 616\alpha_3)) + k^{12}z^2(1 - 4z^4 + 3z^8)(4(472 + z^4(3067 +$$

$$+ 8w^2z^2(11 - 48z^4 + 45z^8) + z^4(-8815 + 9z^4(1414 - 654z^4 - 105z^8 + 45z^{12}))))\alpha_1 +$$

$$+ 1121\alpha_2 + 2554\alpha_3 + z^4((4934 + w^2z^2(-1 + 3z^4)(-227 +$$

$$+ 609z^4 - 837z^8 + 567z^{12}) + z^4(-14405 + 27z^4(652 + 277z^4 - 958z^8 +$$

$$+ 471z^{12})))\alpha_2 + 2(4004 + 2w^2z^2(-1 + 3z^4)(-139 + 489z^4 - 837z^8 + 567z^{12}) +$$

$$+ z^4(-12527 + 27z^4(480 + 861z^4 - 1804z^8 + 921z^{12})))\alpha_3)) + 3k^8w^2z^4(16(-8256 +$$

$$+ z^4(12w^4z^8(5 - 18z^4 + 15z^8) + 4(13925 +$$

$$+ z^4(-33527 + 3z^4(10882 - 15z^4(250 - 9z^4 + 3z^8)))) +$$

$$+ 3w^2z^2(-584 + z^4(2526 + z^4(-4975 + z^4(5834 + 9z^4(-172 - 200z^4 + 75z^8)))))))\alpha_1 -$$

$$- 96(682\alpha_2 + 1391\alpha_3) + z^4((9w^4z^8(105 + z^4(-652 + 5z^4(326 - 396z^4 + 189z^8))) +$$

$$+ 64(7321 + z^4(-19486 + 3z^4(7642 - 3885z^4 + 243z^8 + 396z^{12}))) +$$

$$+ 3w^2z^2(-4847 + z^4(23182 +$$

$$+ z^4(-44805 + z^4(13060 + 9z^4(12031 - 17410z^4 + 7125z^8))))))\alpha_2 +$$

$$+ 4(3w^4z^8(235 + 3z^4(-556 + 5z^4(310 - 396z^4 + 189z^8))) +$$

$$+ 8(32236 + z^4(-96433 + 3z^4(45560 + 9z^4(-3477 + 708z^4 + 239z^8)))) +$$

$$+ 3w^2z^2(-2611 + z^4(14148 + z^4(-29175 +$$

$$+ z^4(-2656 + 9z^4(12119 - 16580z^4 + 6915z^8))))))\alpha_3)) +$$

$$+ k^{10}(-4(-6016 +$$

$$+ z^4(16w^4z^8(-1 + 3z^4)(23 - 66z^4 + 45z^8) - 128(457 - 3102z^4 + 6798z^8 -$$

$$- 6225z^{12} + 2025z^{16}) + w^2z^2(3600 + z^4(-42763 + z^4(133286 + 3z^4(-73003 +$$

$$+ 3z^4(21268 - 5253z^4 - 2970z^8 + 945z^{12}))))))))\alpha_1 + 16(893\alpha_2 + 2020\alpha_3) -$$

$$- z^4((w^4z^8(-1 + 3z^4)(1099 + 3z^4(-1736 + 3z^4(1198 + 81z^4(-16 + 7z^4)))) +$$

$$+ 2w^2z^2(3096 + z^4(-39661 + z^4(124022 + 3z^4(-57817 + 3684z^4 +$$

$$+ 98559z^8 - 111294z^{12} + 38313z^{16})))) + 16(-6253 + 3z^4(15821 +$$

$$+ z^4(-36643 + z^4(35939 + 45z^4(-289 - 21z^4 + 27z^8))))))\alpha_2 +$$

$$+ 2(2w^4z^8(-1 + 3z^4)(731 + 3z^4(-1384 + 3z^4(1118 + 81z^4(-16 + 7z^4)))) +$$

$$+ 32(-2798 + 3z^4(8001 + z^4(-20098 + z^4(22423 + 9z^4(-1214 + 99z^4 + 90z^8))))) +$$

$$+ w^2 z^2 (5493 + z^4(-77381 + z^4(253045 +$$

$$+ 3z^4(-107087 + 3z^4(-27169 + 3z^4(45035 - 47187z^4 + 16587z^8)))))))\alpha_3)) +$$

$$+ 27k^4 w^6 z^{12}(w^2 z^6(1376\alpha_1 - 1031\alpha_2 - 6010\alpha_3) +$$

$$+ 567w^4 z^{20}(\alpha_2 + 4\alpha_3) - 5088(2\alpha_2 + 9\alpha_3) + 960z^4(\alpha_1 + 55\alpha_2 + 251\alpha_3) -$$

$$- 90w^2 z^{18}(90\alpha_1 + 365\alpha_2 + 1388\alpha_3) + 45w^2 z^{22}(100\alpha_1 + 479\alpha_2 + 1846\alpha_3) -$$

$$- 192z^8(25\alpha_1 + 413\alpha_2 + 1932\alpha_3) + 4w^2 z^{14}(331\alpha_1 +$$

$$+ 2417\alpha_2 + 9007\alpha_3) + 2w^2 z^{10}(706\alpha_1 + 2417\alpha_2 + 10012\alpha_3) - 18z^{16}(160\alpha_1 +$$

$$+ (-448 + 33w^4)\alpha_2 + 4(-316 + 33w^4)\alpha_3) + z^{12}(32(210 + w^4)\alpha_1 +$$

$$+ w^4(163\alpha_2 + 620\alpha_3) + 192(149\alpha_2 + 797\alpha_3))) - 81k^2 w^8 z^{16}(240(13\alpha_2 + 58\alpha_3) +$$

$$+ z^4(20(-1 + z^4)(16 + z^4(-16 + w^2 z^2(-13 + 33z^4)))\alpha_1 - 16(445\alpha_2 + 2006\alpha_3) +$$

$$+ z^2(3w^4 z^6(-11 + 21z^4)(\alpha_2 + 4\alpha_3) + 16z^2((209 + 41z^4)\alpha_2 + 2(509 + 59z^4)\alpha_3) +$$

$$+ 2w^2((204 + 131z^4 - 1538z^8 + 1443z^{12})\alpha_2 +$$

$$+ (849 + 427z^4 - 5857z^8 + 5541z^{12})\alpha_3))))) \tag{D.25}$$

Bibliography

[1] Allan Adams, Nima Arkani-Hamed, Sergei Dubovsky, Alberto Nicolis, and Riccardo Rattazzi. Causality, analyticity and an IR obstruction to UV completion. *JHEP*, 10:014, 2006.

[2] Y. Aharonov, A. Komar, and Leonard Susskind. Superluminal behavior, causality, and instability. *Phys. Rev.*, 182:1400–1403, 1969.

[3] Ofer Aharony, Steven S. Gubser, Juan Martin Maldacena, Hirosi Ooguri, and Yaron Oz. Large N field theories, string theory and gravity. *Phys. Rept.*, 323:183–386, 2000.

[4] Ofer Aharony, Joseph Marsano, Shiraz Minwalla, Kyriakos Papadodimas, and Mark Van Raamsdonk. The Hagedorn / deconfinement phase transition in weakly coupled large N gauge theories. *Adv. Theor. Math. Phys.*, 8:603–696, 2004.

[5] Ofer Aharony, Joseph Marsano, Shiraz Minwalla, Kyriakos Papadodimas, and Mark Van Raamsdonk. A first order deconfinement transition in large N Yang-Mills theory on a small S**3. *Phys. Rev.*, D71:125018, 2005.

[6] Luis Alvarez-Gaume, Cesar Gomez, Hong Liu, and Spenta Wadia. Finite temperature effective action, AdS(5) black holes, and 1/N expansion. *Phys. Rev.*, D71:124023, 2005.

[7] Joseph J. Atick and Edward Witten. The Hagedorn Transition and the Number of Degrees of Freedom of String Theory. *Nucl. Phys.*, B310:291–334, 1988.

[8] A. A. Belavin and V. G. Knizhnik. COMPLEX GEOMETRY AND THE THEORY OF QUANTUM STRINGS. *Sov. Phys. JETP*, 64:214–228, 1986.

[9] Paolo Benincasa and Alex Buchel. Transport properties of N = 4 supersymmetric Yang-Mills theory at finite coupling. *JHEP*, 01:103, 2006.

[10] Nathan Berkovits. Quantum consistency of the superstring in AdS(5) x S**5 background. *JHEP*, 03:041, 2005.

[11] David G. Boulware and S. Deser. String Generated Gravity Models. *Phys. Rev. Lett.*, 55:2656, 1985.

[12] Raphael Bousso. The holographic principle. *Rev. Mod. Phys.*, 74:825–874, 2002.

[13] Mauro Brigante, Guido Festuccia, and Hong Liu. Inheritance principle and non-renormalization theorems at finite temperature. *Phys. Lett.*, B638:538–545, 2006.

[14] Mauro Brigante, Guido Festuccia, and Hong Liu. Hagedorn divergences and tachyon potential. *JHEP*, 06:008, 2007.

[15] Mauro Brigante, Hong Liu, Robert C. Myers, Stephen Shenker, and Sho Yaida. Viscosity Bound Violation in Higher Derivative Gravity. *Accepted by Physical Review D (D15)*, 2007.

[16] Mauro Brigante, Hong Liu, Robert C. Myers, Stephen Shenker, and Sho Yaida. The Viscosity Bound and Causality Violation. *Phys. Rev. Lett.*, 100, 2008.

[17] Alex Buchel and James T. Liu. Universality of the shear viscosity in supergravity. *Phys. Rev. Lett.*, 93:090602, 2004.

[18] Alex Buchel, James T. Liu, and Andrei O. Starinets. Coupling constant dependence of the shear viscosity in N=4 supersymmetric Yang-Mills theory. *Nucl. Phys.*, B707:56–68, 2005.

[19] Rong-Gen Cai. Gauss-Bonnet black holes in AdS spaces. *Phys. Rev.*, D65:084014, 2002.

[20] Sean M. Carroll. Spacetime and geometry: An introduction to general relativity. San Francisco, USA: Addison-Wesley (2004) 513 p.

[21] Sidney R. Coleman. 1/N. Presented at 1979 Int. School of Subnuclear Physics, Pointlike Structures Inside and Outside Hadrons, Erice, Italy, Jul 31-Aug 10, 1979.

[22] Neil R. Constable and Finn Larsen. The rolling tachyon as a matrix model. *JHEP*, 06:017, 2003.

[23] Eric D'Hoker, Daniel Z. Freedman, Samir D. Mathur, Alec Matusis, and Leonardo Rastelli. Extremal correlators in the AdS/CFT correspondence. 1999.

[24] Eric D'Hoker, Daniel Z. Freedman, and Witold Skiba. Field theory tests for correlators in the AdS/CFT correspondence. *Phys. Rev.*, D59:045008, 1999.

[25] Eric D'Hoker and D. H. Phong. The Geometry of String Perturbation Theory. *Rev. Mod. Phys.*, 60:917, 1988.

[26] Michael R. Douglas and Shamit Kachru. Flux compactification. *Rev. Mod. Phys.*, 79:733–796, 2007.

[27] K. Dusling and D. Teaney. Simulating elliptic flow with viscous hydrodynamics. 2007.

[28] Suvankar Dutta and Rajesh Gopakumar. On Euclidean and noetherian entropies in AdS space. *Phys. Rev.*, D74:044007, 2006.

[29] B. Eden, Paul S. Howe, and Peter C. West. Nilpotent invariants in N = 4 SYM. *Phys. Lett.*, B463:19–26, 1999.

[30] S. Fubini and G. Veneziano. Level structure of dual-resonance models. *Nuovo Cim.*, A64:811–840, 1969.

[31] F. Gonzalez-Rey, B. Kulik, and I. Y. Park. Non-renormalization of two point and three point correlators of N = 4 SYM in N = 1 superspace. *Phys. Lett.*, B455:164–170, 1999.

[32] D. J. Gross, M. J. Perry, and L. G. Yaffe. Instability of Flat Space at Finite Temperature. *Phys. Rev.*, D25:330–355, 1982.

[33] David J. Gross and Igor R. Klebanov. Vortices and the nonsinglet sector of the c = 1 matrix model. *Nucl. Phys.*, B354:459–474, 1991.

[34] S. S. Gubser, Igor R. Klebanov, and Alexander M. Polyakov. Gauge theory correlators from non-critical string theory. *Phys. Lett.*, B428:105–114, 1998.

[35] Steven S. Gubser, Igor R. Klebanov, and Arkady A. Tseytlin. Coupling constant dependence in the thermodynamics of N = 4 supersymmetric Yang-Mills theory. *Nucl. Phys.*, B534:202–222, 1998.

[36] R. Hagedorn. Statistical thermodynamics of strong interactions at high- energies. *Nuovo Cim. Suppl.*, 3:147–186, 1965.

[37] S. W. Hawking and Don N. Page. Thermodynamics of Black Holes in anti-De Sitter Space. *Commun. Math. Phys.*, 87:577; 1983.

[38] C. P. Herzog and D. T. Son. Schwinger-Keldysh propagators from AdS/CFT correspondence. *JHEP*, 03:046, 2003.

[39] Kerson Huang and Steven Weinberg. Ultimate temperature and the early universe. *Phys. Rev. Lett.*, 25:895–897, 1970.

[40] Kenneth A. Intriligator and Witold Skiba. Bonus symmetry and the operator product expansion of N = 4 super-Yang-Mills. *Nucl. Phys.*, B559:165–183, 1999.

[41] Ted Jacobson and Robert C. Myers. Black hole entropy and higher curvature interactions. *Phys. Rev. Lett.*, 70:3684–3687, 1993.

[42] Leo P. Kadanoff and Paul C. Martin. Hydrodynamic equations and correlation functions. *Annals of Physics*, 24:419–469, 1963.

[43] Renata Kallosh and Arvind Rajaraman. Vacua of M-theory and string theory. *Phys. Rev.*, D58:125003, 1998.

[44] Ya. I. Kogan. Vortices on the World Sheet and String's Critical Dynamics. *JETP Lett.*, 45:709–712, 1987.

[45] P. Kovtun, D. T. Son, and A. O. Starinets. Viscosity in strongly interacting quantum field theories from black hole physics. *Phys. Rev. Lett.*, 94:111601, 2005.

[46] Pavel Kovtun, Dam T. Son, and Andrei O. Starinets. Holography and hydrodynamics: Diffusion on stretched horizons. *JHEP*, 10:064, 2003.

[47] Pavel K. Kovtun and Andrei O. Starinets. Quasinormal modes and holography. *Phys. Rev.*, D72:086009, 2005.

[48] Martin Kruczenski and Albion Lawrence. Random walks and the Hagedorn transition. *JHEP*, 07:031, 2006.

[49] Sangmin Lee, Shiraz Minwalla, Mukund Rangamani, and Nathan Seiberg. Three-point functions of chiral operators in D = 4, N = 4 SYM at large N. *Adv. Theor. Math. Phys.*, 2:697–718, 1998.

[50] Hong Liu. Fine structure of Hagedorn transitions. 2004.

[51] Juan Martin Maldacena. The large N limit of superconformal field theories and supergravity. *Adv. Theor. Math. Phys.*, 2:231–252, 1998.

[52] R. R. Metsaev and A. A. Tseytlin. Type IIB superstring action in AdS(5) x S(5) background. *Nucl. Phys.*, B533:109–126, 1998.

[53] Harvey B. Meyer. A calculation of the shear viscosity in SU(3) gluodynamics. *Phys. Rev.*, D76:101701, 2007.

[54] C. W. Misner, K. S. Thorne, and J. A. Wheeler. Gravitation. San Francisco 1973, 1279p.

[55] Robert C. Myers. HIGHER DERIVATIVE GRAVITY, SURFACE TERMS AND STRING THEORY. *Phys. Rev.*, D36:392, 1987.

[56] K. H. O'Brien and C. I. Tan. Modular Invariance of Thermopartition Function and Global Phase Structure of Heterotic String. *Phys. Rev.*, D36:1184, 1987.

[57] Jacek Pawelczyk and Stefan Theisen. AdS(5) x S(5) black hole metric at O(alpha'**3). *JHEP*, 09:010, 1998.

[58] J. Polchinski. String theory. Vol. 1: An introduction to the bosonic string. Cambridge, UK: Univ. Pr. (1998) 402 p.

[59] Joseph Polchinski. Evaluation of the One Loop String Path Integral. *Commun. Math. Phys.*, 104:37, 1986.

[60] Joseph Polchinski. S-matrices from AdS spacetime. 1999.

[61] G. Policastro, D. T. Son, and A. O. Starinets. The shear viscosity of strongly coupled N = 4 supersymmetric Yang-Mills plasma. *Phys. Rev. Lett.*, 87:081601, 2001.

[62] Giuseppe Policastro, Dam T. Son, and Andrei O. Starinets. From AdS/CFT correspondence to hydrodynamics. *JHEP*, 09:043, 2002.

[63] Giuseppe Policastro, Dam T. Son, and Andrei O. Starinets. From AdS/CFT correspondence to hydrodynamics. II: Sound waves. *JHEP*, 12:054, 2002.

[64] Paul Romatschke. Fluid turbulence and eddy viscosity in relativistic heavy- ion collisions. 2007.

[65] Paul Romatschke and Ulrike Romatschke. Viscosity Information from Relativistic Nuclear Collisions: How Perfect is the Fluid Observed at RHIC? *Phys. Rev. Lett.*, 99:172301, 2007.

[66] Sunao Sakai and Atsushi Nakamura. Lattice calculation of the QGP viscosities - Present results and next project -. 2007.

[67] B. Sathiapalan. Vortices on the String World Sheet and Constraints on Toral Compactification. *Phys. Rev.*, D35:3277, 1987.

[68] Thomas Schafer. What atomic liquids can teach us about quark liquids. *Prog. Theor. Phys. Suppl.*, 168:303–311, 2007.

[69] Dam T. Son and Andrei O. Starinets. Minkowski-space correlators in AdS/CFT correspondence: Recipe and applications. *JHEP*, 09:042, 2002.

[70] Dam T. Son and Andrei O. Starinets. Viscosity, Black Holes, and Quantum Field Theory. *Ann. Rev. Nucl. Part. Sci.*, 57:95–118, 2007.

[71] Huichao Song and Ulrich W. Heinz. Suppression of elliptic flow in a minimally viscous quark- gluon plasma. *Phys. Lett.*, B658:279–283, 2008.

[72] Bo Sundborg. The Hagedorn transition, deconfinement and N = 4 SYM theory. *Nucl. Phys.*, B573:349–363, 2000.

[73] Leonard Susskind. The World as a hologram. *J. Math. Phys.*, 36:6377–6396, 1995.

[74] Leonard Susskind and Edward Witten. The holographic bound in anti-de Sitter space. 1998.

[75] Gerard 't Hooft. A PLANAR DIAGRAM THEORY FOR STRONG INTERACTIONS. *Nucl. Phys.*, B72:461, 1974.

[76] Gerard 't Hooft. Dimensional reduction in quantum gravity. 1993.

[77] Derek Teaney. Effect of shear viscosity on spectra, elliptic flow, and Hanbury Brown-Twiss radii. *Phys. Rev.*, C68:034913, 2003.

[78] Robert M. Wald. Black hole entropy is the Noether charge. *Phys. Rev.*, D48:3427–3431, 1993.

[79] Edward Witten. Anti-de Sitter space and holography. *Adv. Theor. Math. Phys.*, 2:253–291, 1998.

[80] Edward Witten. Anti-de Sitter space, thermal phase transition, and confinement in gauge theories. *Adv. Theor. Math. Phys.*, 2:505–532, 1998.

[81] Barton Zwiebach. A first course in string theory. Cambridge, UK: Univ. Pr. (2004) 558 p.

[82] Barton Zwiebach. Curvature Squared Terms and String Theories. *Phys. Lett.*, B156:315, 1985.